From Clinical Neuroscience Department
Karolinska Institutet, Stockholm, Sweden

HUMAN EMBRYONIC STEM CELLS FOR RETINAL REPAIR:

PRECLINICAL *IN VITRO* AND *IN VIVO* STUDIES FOR THE TREATMENT OF AGE-RELATED MACULAR DEGENERATION WITH HUMAN EMBRYONIC STEM CELL-DERIVED RETINAL PIGMENT EPITHELIAL CELLS

Sandra Petrus-Reurer, M.Sc.

Karolinska Institutet

Stockholm 2018

All previously published papers were reproduced with permission from the publisher.
Published by Karolinska Institutet.
Printed by Universitetsservice US-AB 2018.
Cover: *CellProfiler* output image of ZO-1 staining in human embryonic stem cell-derived retinal pigment epithelial cells cultured on human recombinant laminin-521.

ISBN 978-91-7831-156-9

HUMAN EMBRYONIC STEM CELLS FOR RETINAL REPAIR:

PRECLINICAL *IN VITRO* AND *IN VIVO* STUDIES FOR THE TREATMENT OF AGE-RELATED MACULAR DEGENERATION WITH HUMAN EMBRYONIC STEM CELL-DERIVED RETINAL PIGMENT EPITHELIAL CELLS

Thesis for Doctoral Degree (Ph.D.)

By

Sandra Petrus-Reurer

Public defence: Friday 23rd of November 2018, 10AM

Erna Möller Hall, Blickagången 16, Karolinska Institutet, Flemingsberg.

Principal Supervisor:
Prof. Anders Kvanta, Ph.D., M.D.
Karolinska Institutet/St Erik Eye Hospital
Department of Clinical Neuroscience
Division of Eye and Vision

Co-supervisor(s):
Assoc. Prof. Fredrik Lanner, Ph.D.
Karolinska Institutet
Department of Clinical Science, Intervention and Technology
Division of Obstetrics and Gynecology

Helder André, Ph.D.
Karolinska Institutet
Department of Clinical Neuroscience
Division of Eye and Vision

Sonya Stenfelt, Ph.D.
Uppsala University
Department of Neuroscience
Division of Developmental Neuroscience

Opponent:
Prof. Marius Ader, Ph.D.
Technical University Dresden
Center for Molecular and Cellular Bioengineering (CMCB)
Center for Regenerative Therapies Dresden (CRTD)

Examination Board:
Prof. Thomas Perlmann, Ph.D.
Karolinska Institutet
Department of Cell and Molecular Biology/ Ludwig Institute for Cancer Research

Assoc. Prof. Stefan Löfgren, Ph.D., M.D.
Karolinska Institutet/St Erik Eye Hospital
Department of Clinical Neuroscience
Division of Eye and Vision

Assoc. Prof. David Berglund, Ph.D., M.D.
Uppsala University
Department of Immunology, Genetics and Pathology
Division of Clinical Immunology

"Seeking means: to have a goal; but finding means: to be free, to be receptive, to have no goal"

Herman Hesse, Siddhartha

To all the supervisors that shaped me as a scientist

and to everyone

ABSTRACT

Age-related macular degeneration (AMD) is the major cause of vision loss in the industrialized countries in people above sixty years of age. The dry advanced form of the disease, also termed as geographic atrophy (GA), is characterized by the progressive death of retinal pigment epithelial cells (RPE) and consequent loss of the adjacent photoreceptor (PR) layer, leading to an impaired visual function. Since AMD has a multifactorial cause, including both genetic and epigenetic factors, a potential treatment for retinal regeneration relies on the generation of either autologous or allogeneic RPE and PR cells from human pluripotent stem cells (hPSC) *in vitro*.

The overall aim of this thesis was to develop both *in vitro* and *in vivo* methods and models to move forward a stem-cell based replacement therapy for patients suffering from dry advanced forms of AMD.

Specifically, we first developed a spontaneous, xeno-free and defined protocol to derive RPE from human embryonic stem cells (hESC-RPE) that acquired specific morphological and functional characteristics of native RPE. Additionally, we developed a large-eyed model (rabbit eye) with relevant pre-clinical imaging and surgical advantages when compared to other more commonly used rodent models. In fact, both the subretinal injections of PBS or the chemical $NaIO_3$ created a retinal degeneration phenotype very similar to the lesion present in GA patients with RPE damage and PR loss. A next logical step was to evaluate the behavior of the hESC-RPE in such models of degeneration. From these studies, we first showed that hESC-RPE can rescue the neuroretina from further damage induced at the moment of subretinal injection, and second, that hESC-RPE are not able to integrate in areas of profound retinal degeneration caused by a 7-day pre-injection of either PBS or $NaIO_3$, therefore supporting the idea of an early treatment. The use of allogeneic hESC as a transplantable source comes together with the forthcoming rejection of the donor cells. We then sought to create universal cells that lack HLA-I (hESC-RPE$^{B2M-/-}$ using CRISPR-Cas9 technology) able to evade the host adaptive immune system. Upon co-culture with T-cells under stimulatory conditions, the engineered hESC-RPE$^{B2M-/-}$ dampened CD8+ T-cell proliferation and when mixed with natural killer (NK) cells, a cytotoxic response was triggered. Furthermore, after transplantation of the hESC-RPE$^{B2M-/-}$ in the rabbit xenogeneic model, early stage rejection was reduced and the appearance of anti-human antibodies rejection associated with late rejection was delayed.

Altogether, the studies described in this thesis show evidence that allogeneic replacement therapy using subretinal injection of hESC-RPE in suspension can be a successful treatment if (i) the derived cells retain native RPE cell properties; (ii) the cells are transplanted early

enough so the subretinal milieu supports their integration; and (iii) the cells can be engineered so that they can evade the host immune system and consequent graft rejection.

SCIENTIFIC PAPERS INCLUDED IN THE THESIS

I. Bartuma, H., **Petrus-Reurer, S.,** Aronsson, M., Westman, S., André H., and Kvanta, A.[3]
In vivo imaging of subretinal bleb-induced outer retinal degeneration.
Invest. Ophthalmol. Vis. Sci. 2015; 56, 2423–2430
DOI: 10.1167/iovs.14-16208

II. Plaza Reyes, A.,[1] **Petrus-Reurer, S.,[1]** Antonsson, L., Stenfelt, S., Bartuma, H., Panula, S., Mader, T., Douagi, I., André, H., Hovatta, O.,[2] Lanner, F.,[2,3] and Kvanta, A.[2]
Xeno-free and defined human embryonic stem cell-derived retinal pigment epithelial cells functionally integrate in a large-eyed preclinical model.
Stem Cell Reports. 2016; 6:9–17
DOI: 0.1016/j.stemcr.2015.11.008

III. **Petrus-Reurer, S.,[1]** Bartuma, H.,[1] Aronsson, M., Westman, S., Fredrik, L., André H., and Kvanta, A.[3]
Integration of subretinal suspension transplants of human embryonic stem cell-derived retinal pigment epithelial cells in a large-eyed model of geographic atrophy.
Invest. Ophthalmol. Vis. Sci. 2017; 58 (2), 1314-1322
DOI: 10.1167/iovs.16-20738

IV. **Petrus-Reurer, S.**,[1] Winblad, N.,[1] Gorchs, L., Chrobok, M., Wagner, A.K., Lardner, E., Bartuma, H., Aronsson, M., Westman, S., Alici, E., Kaipe, H., Lanner, F.,[2] Kvanta, A.[2,3]
Generation and characterization of human embryonic stem cell-derived retinal pigment epithelial cells lacking major histocompatibility complex-1 and transplantation into a large-eyed preclinical model.
Manuscript

SCIENTIFIC PAPERS NOT INCLUDED IN THE THESIS

I. **Petrus-Reurer, S.,[1,3]** Bartuma, H.,[1] Aronsson, M., Westman, S., Lanner, F., Kvanta, A.
Subretinal Transplantation of Human Embryonic Stem Cell Derived Retinal Pigment Epithelial Cells into a Large-Eyed Model of Geographic Atrophy.
Journal of Visualized Experiments 2018; 131
DOI: 10.3791/56702

[1]Co-first author
[2]Co-senior author
[3]Corresponding author

CONTENTS

LIST OF ABBREVIATIONS

ABCA1	ATP-Binding Cassette A1
AMD	Age-related Macular Degeneration
APC	Antigen Presenting Cell
APOE	Apolipoprotein E
BAF	Blue-Light Fundus Autofluorescence
BCA	Bicinchoninic Acid
BEST1	Bestrophin 1
bFGF	Basic Fibroblast Growth Factor
BM	Bruch's Membrane
BMHSC	Bone Marrow Hematopoietic Stem Cells
BMP	Bone Morphogenetic Protien
BSA	Bovine Serum Albumin
BSS	Balanced Salt Solution
CCD	Charge-Coupled Device
CCL2	C-C Motif Chemokine Ligand 2
CD	Cluster of Differentiation
cDNA	Complementary Deoxyribonucleic Acid
CETP	Cholesterol Ester Transfer Protein
CFH	Complement Factor H
CFSE	Carboxyfluorescein Succinimidyl Ester
cGMP	Cyclic Guanosine Monophosphate
CIRM	California Institute for Regenerative Medicine
CMV	Cytomegalovirus
CNV	Choroidal Neovascularization
CO_2	Carbon Dioxide
CRALBP	Cellular Retinaldehyde Binding Protein
CRISPR	Clustered Regularly Interspaced Short Palindromic Repeats
cSLO	Confocal Scanning Laser Ophthalmoscope
CT	Choroidal Thickness

CX3CR1	C-X3-C Motif Chemokine Receptor 1
DAPI	4’,6-diamidino-2-phenylendole
DC	Dendritic Cell
dH_2O	Distilled Water
DKK	Dickkopf
DMEM/F12	Dulbecco's Modified Eagle Medium: Nutrient Mixture F-12
DNA	Deoxyribonucleic Acid
DNAM-1	DNAX Accessory Molecule-1
DPBS/PBS	Dulbecco’s Phosphate-Buffered Saline
EB	Embryoid Body
EDTA	Ethylenediaminetetraacetic Acid
EF1α	Elongation Factor 1-alpha
ELISA	Enzyme-Linked ImmunoSorbent Assay
ELM	External Limiting Membrane
ERG	Electroretinography
EZ	Ellipsoid Zone
FACS	Fluorescence-Activated Cell Sorting
FBS	Fetal Bovine Serum
FGF	Fibroblast Growth Factor
FITC	Fluorescein Isothiocyanate
FMO	Fluorescence Minus One
FS	Fixing Solution
GA	Geographic Atrophy
GCL	Ganglion Cell Layer
gDNA	Genomic Deoxyribonucleic Acid
GMFI	Geographic Mean Fluorescence Intensity
GMP	Good Manufacturing Practice
HE	Hematoxylin Eosin
HEK293T	Human Embryonic Kidney Cells 293 with T-Antigen
hESC	Human Embryonic Stem Cells

hESC-RPE	Human Embryonic Stem Cells-Derived Retinal Pigment Epithelial
hESC-RPE$^{B2M+/+}$	Human Embryonic Stem Cells-Derived Retinal Pigment Epithelial Wild Type
hESC-RPE$^{B2M-/-}$	Human Embryonic Stem Cells-Derived Retinal Pigment Epithelial B2M Knock Out
HLA	Human Leukocyte Antigen
hPSC	Human Pluripotent Stem Cell
HTRA1	High-Temperature Requirement A Serine Peptidase 1
HuCNS-SC	Human Central Nervous System Stem Cells
hUTSC	Human Umbilical Tissue-Derived Stem Cells
ICTRP	International Clinical Trials Registry Platform
IF	Immunofluorescence
IFN-γ	Interferon-Gamma
IGF	Insulin-Like Growth Factor
IL	Interleukin
INL	Inner Nuclear Layer
IPL	Inner Plexiform Layer
iPSC	Induced Pluripotent Stem Cells
iPSC-RPE	Induced Pluripotent Stem Cells-Derived Retinal Pigment Epithelial
IR-cSLO	Infrared-Confocal Scanning Laser Ophthalmoscopy
IS	Inner Segments
KLF	Kruppel-Like Factor
KO	Knock Out
KSR	KnockOut Serum Replacement
hrLN	Human Recombinant Laminin
LHX2	LIM Homeobox 2
LIPC	Lipase C
LPCB	London Project to Cure Blindness
MC	Multicolor
MERTK	MER receptor tyrosine kinase

MEF	Mouse Embryonic Fibroblasts
MHC	Major Histocompatibility Complex
MITF	Microphthalmia-Associated Transcription Factor
MSC	Mesechymal Stem Cell
$NaIO_3$	Sodium Iodate
Na+/K+	Sodium/Potassium
NEAA	Non-Essential Amino Acids
NFL	Nerve Fiber Layer
NK	Natural Killer
NKG2D/KLRK1	Killer Cell Lectin Like Receptor K1
NLRP3	NLR Family Pyrin Domain Containing 3
O_2	Oxygen
OCT3/4	Octamer-Binding Transcription Factor
OHT	Optokinetic Head-Tracking
OKT-3	Muromonab-CD3
OLM	Outer Limiting Membrane
ONL	Outer Nuclear Layer
OPL	Outer Plexiform Layer
ORT	Outer Retinal Thickness
OS	Outer Segments
OTX2	Orthodenticle Homeobox 2
OV	Optic Vesicle
PAX6	Paired Box Protein Pax-6
PBMC	Peripheral Blood Mononuclear Cell
PCNA	Proliferating Cell Nuclear Antigen
PD-L1/2	Programmed Death-Ligand 1/2
PEDF	Pigment Epithelium-Derived Factor
PMEL	Premelanosome Protein
PNK	Polynucleotide Kinase
POS	PR Outer Segments

PR	Photoreceptor
PVDF	Polyvinylidene Difluoride
qPCR	Quantitative Polymerase Chain Reaction
RCS	Royal College of Surgeons
RIPA	Radioimmunoprecipitation Assay Buffer
RNA	Ribonucleic Acid
RNA-seq	Ribonucleic Acid Sequencing
RP	Retinitis Pigmentosa
RPE	Retinal Pigment Epithelial Cell
RPEC	Retinal Pigment Epithelium Stem Cell
RPE65	Retinal Pigment Epithelium-Specific Protein 65kDa
RPT	Regenerative Patch Technologies
RT	Retinal Thickness
RX	Retina and Anterior Neural Fold Homeobox
SD-OCT	Spectral-Domain Optical Coherence Tomography
sgRNA	Single Guide Ribonucleic Acid
shRNA	Short Hairpin RNA
siRNA	Short Interference RNA
SIX3/6	Sine Oculis Homeobox Homolog 3/6
SOD1/2	Superoxide Dismutase 1
SOX	Sex Determining Region Y-box
ST	Subretinal Thickness
TBS	Tris-Buffered Saline
TCA	Triamcinolone
TCR	T-Cell Receptor
TEER	Transepithelial Resistance
TGF-β	Transforming Growth Factor-Beta
TIGIT	T Cell Immunoreceptor With Ig And ITIM Domains
TMD	Tissue Marking Dye
TREG	Regulatory T-Cell

TX	Transplantation
VEGF	Vascular Endothelial Growth Factor
VSX2	Visual System Homeobox 2
XF	Xeno-free
ZO-1	Zona Occuldens-1

1 INTRODUCTION

1.1 THE RETINA

The retina is part of the central nervous system and it is defined as the laminated neural component of the eye located in the inner side of the eye ball that contains the machinery to process the primary visual pathways (Purves et al., 2004). Its main function is analog to a film or a CCD in a camera: the visual field is captured by the optics of the eye that create a focused two-dimensional image on the retina, which will be translated into electrical impulses for the brain to create a visual perception.

During vertebrate embryonic development, the retina forms as an outpocketing of the ventral diencephalon neuroepithelium (neurectoderm origin) to form the optic vesicle (regulated by PAX6, RX, OTX2, SIX3/6 and LHX2 transcription factors), which undergoes invagination to form a double-layered optic cup. The distal/inner wall of the optic cup gives rise to the multilayered neural retina (guided by FGF-induction of VSX2 and SOX2 transcription factors), while the proximal/outer wall develops into the single layer of RPE (promoted by TGFβ signaling and molecules such as ActivinA). Finally, the presumptive neural retina of the optic vesicle invaginates to form the lens (of surface ectoderm origin and BMP-signaling dependent to activate PAX6 and SOX2 expression) (Fuhrmann, 2010; Heavner and Pevny, 2012).

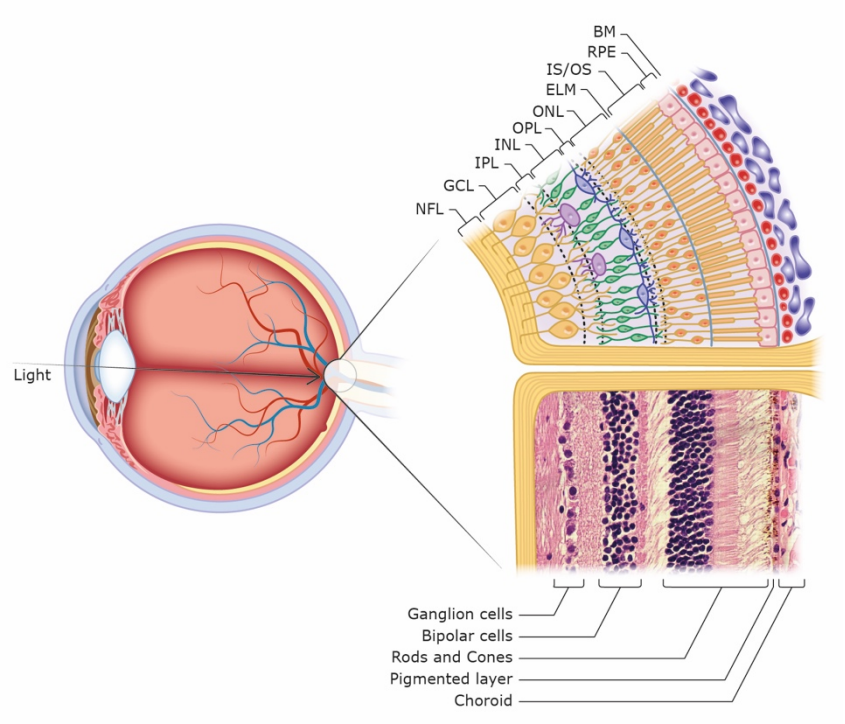

FIGURE 1. Schematic view of the structure of the eye, with magnification on the retinal layers and its correspondence with histology.
NFL (nerve fiber layer), GCL (ganglion cell layer), IPL (inner plexiform layer), INL (inner nuclear layer), OPL (outer plexiform layer), ONL (outer nuclear layer), ELM (external limiting membrane), IS/OS (inner segments/outer segments), RPE (retinal pigment epithelium), and BM (Bruch's membrane).
Note inside the drawing of the INL, the horizontal cells in blue and the amacrine cells in purple.

The adult vertebrate retina consists of ten different layers of cells including photoreceptors (PR), bipolar and ganglion cells interconnected by synapsis, in addition to an outer layer of pigmented epithelial cells (Figure 1). Specifically, from vitreous body to choroid they are: inner limiting membrane (Müller cells), nerve fiber layer (axons of ganglion cells), ganglion cell layer

(their axons become part of the optic nerve), inner plexiform layer (synapse between bipolar cell axons and ganglion and amacrine cell dendrites), inner nuclear layer (nuclei and cell bodies of amacrine, bipolar and horizontal cells), outer plexiform layer (rod and cone projections), outer nuclear layer (rods and cones cell bodies), external limiting membrane, layer of rods and cones (PR cells) and retinal pigment epithelium (RPE) layer. In short, they can then be grouped into four main processing stages laterally connected by horizontal and amacrine cells: photoreception, transmission to bipolar cells, transmission to ganglion cells and transmission along the optic nerve (Purves et al., 2004).

In an inverted retina, as the vertebrate one is, the light passes through layers of neurons and capillaries to reach the light sensing cells or PR. There are two types: rods, which mainly function in dim light and provide lower-resolution black-and-white vision (scotopic vision); and cones, responsible for the high-resolution color perception during bright daylight illumination (photopic vision). For illumination that falls in between these two levels (mesotopic vision), both rods and cones contribute to pattern information, but the specifics of how it works is still unclear. An important structure to mention is the macula, which is an oval-shaped pigmented area near the center of the retina specialized in central, high-acuity color vision. Within the macula there is the fovea centralis that contains a high density of cones that provides that high-resolution (Purves et al., 2004).

Once light reaches the PR their photopigmented membrane gets hyperpolized, contrarily to that in the dark where it remains depolarized, via a cascade triggered by 11-cis retinal to trans-retinal isomerization leading to cyclic guanosine monophosphate (cGMP) degradation and the closing of the cell sodium channels. Thus, the amount of neurotransmitter (glutamate) released in bright light is reduced and the correspondent synaptic response is transmitted to bipolar and retinal ganglion cells. These excited ganglion cells will be responsible to generate action potentials that, through the optic nerve, will reach various parts of the brain and eventually create a representation of the external light stimuli (Mannu, 2014).

Although retinal cellular composition and thickness are conserved in mammals (0.24 mm thick in mouse and in humans), eyes vary in size, refractive properties, retinal vasculature and visual photopigment (Blanch et al., 2012; Remtulla and Hallett, 1985). Additionally, all mammalian rod PR contain rhodopsin but both size and densities varies by animal size and diurnal/nocturnal behaviors. The proportion of cones and their function is highly variable and can be classified in two (short: blue/UV and medium: green wavelength for mice, rats, rabbits pigs and most New World primates), or three (allowing trichromatic color vision in Old World Monkeys and great apes) classes. Murine rodents have cones distributed throughout the retina, with dorsal-ventral differences; in rabbits and pigs cons are concentrated in a visual streak, while in diurnal primates at a fovea (same as humans) (Applebury et al., 2000; Famiglietti and Sharpe, 1995; Gerke et al., 1995; Wikler and Rakic, 1990). Regarding the

blood supply for the rabbit inner retina, it is mostly derived from the choriocapillaris (merangiotic); but in human, primate, pig, and rodent the inner retina is derived from central and cilioretinal arteries (holangiotic), and only the outer retina is supplied by the choriocapillaries. In rabbits, RPE is irregular in size and organization compared to the human regular hexagonal configuration, rod and cones are longer and thinner, and myelinated nerve fibers in the retina form nasal and temporal crescents about the optic disc (Purves et al., 2004).

1.2 THE RETINAL PIGMENT EPITHELIUM

The RPE is located between the choriocapillaris and the PR layer as depicted in Figure 1. RPE cells form a monolayer located on an extracellular basal membrane (Bruch's membrane, BM), and have a hexagonal pigmented morphology with abundant microvilli in their apical part. BM is mainly comprised of collagen type IV and laminins, primarily the isoforms LN-111, LN-332, LN-511 and LN-521, which are synthesized by the RPE and in turn adhered to BM via specific integrin interactions (Aisenbrey et al., 2006). BM has crucial structural and transport roles as being the substratum of the RPE and a vessel wall (Curcio, 2013). RPE cells are strongly attached to each other by tight junctions which makes the monolayer impermeable to the transport of water, electrolytes and larger molecules under physiological normal conditions (Campbell and Humphries, 2012). RPE cells have a fundamental role in maintaining the homeostasis of the retinal tissue, and particularly of the PR, which they are in direct contact with by providing nutrients and oxygen, and also being responsible for phagocyting the rod and cone outer segments and renewing photopigments. The RPE pigment contains melanin that absorbs stray light within the eye and also takes part in the phototransduction process (Strauss, 2005). Additionally, RPE cells secrete cytokines and growth factors in a polarized fashion (*e.g.* VEGF is produced basally towards the choroid, while PEDF or TGF-β are secreted apically towards the PR layer) contributing to a variety of functions, among which the creation of an immunosuppressive microenvironment in the subretinal space (Zamiri et al., 2006; Zhu et al., 2011). Therefore, dysfunction of the RPE involves PR degeneration and choriocapillaris atrophy leading to a visual function impairment.

1.3 AGE-RELATED MACULAR DEGENERATION

Age-related macular degeneration (AMD) is the principal cause of severe vision loss in people over 60 years of age, with an incidence of almost 500.000/year in the Western world, particularly in individuals with Caucasian ethnicity (Gehrs et al., 2006). Today, AMD is estimated to affect 170 million worldwide, a number predicted to increase to 196 million in 2020, and up to 288 million in 2040 (Wong et al., 2014), implying substantial social and financial consequences. AMD is a multifactorial disease where both genetic and environmental causes are involved in its etiology. Factors associated with damage to the RPE, the BM, or the choriocapillaris include: oxidative stress, smoking, and mutations in the

complement system (*e.g.* Factor H, components C3 and C2), or in the lipoprotein cholesterol pathway. A more exhaustive study of AMD risk factors has been reviewed by *Sobrin and Seddon* (Sobrin and Seddon, 2014).

In general terms, AMD can be classified according to the degenerative status of the retinal tissue. Early and intermediate forms of AMD are characterized by the thickening of BM and the appearance of sub-RPE deposits called drusen. The progressive accumulation of confluent drusen will lead to cumulative degenerative changes in RPE, BM, and choriocapillaris, culminating in advanced forms of the disease. These include neovascular AMD (also termed exudative or advanced "wet" AMD), which is characterized by the abnormal growth of choroidal vessels through the BM causing subretinal edema and hemorrhage (Ambati et al., 2003). Due to the abnormal angiogenesis of the vessels, this pathology is termed choroidal neovascularization (CNV). After the recognition of VEGF as a critical inducer of CNV, anti-VEGF treatment has become a gold standard making neovascular AMD a treatable condition if diagnosed in time. The second form of advanced AMD is geographic atrophy (GA) (also termed advanced "dry" AMD). As the name implies, GA is devoid of CNV and is characterized by well demarcated areas of RPE loss together with outer retinal atrophy (Ambati et al., 2003; Sunness, 1999). GA is responsible for 33% of visual loss in patients with AMD (80% among the advanced AMD cases) and is more prevalent among individuals older than 75 years old (Ferris et al., 1984).

Noninvasive retinal imaging techniques comprise spectral domain-optical coherence tomography (SD-OCT), infrared-confocal scanning laser ophtalmsocopy (IR-cSLO) and blue-light fundus autofluorescence (BAF). SD-OCT relies on the interference between the reference optical path and the path reflected back from the eye (van Velthoven et al., 2007), IR-cSLO uses 820-mm fluorescence to create an en-face fundus reflectance image of the outer retina and RPE, and BAF a 488-nm laser excitation to capture the autofluorescence emitted by fluorophores in the RPE (Delori et al., 1995; Elsner et al., 1996). Together, these multimodal methods provide detailed frontal and sagittal segmentation of the neurosensory retina and RPE, and have played an essential role as diagnostic and prognostic tools (Gobel et al., 2011) (Figure 2). For instance, SD-OCT of eyes with GA shows thinning of the outer nuclear layer, loss of the RPE, and choroidal atrophy (Forte et al., 2012; van Velthoven et al., 2007) (Figure 2C); whereas in BAF, the fundus of the diseased GA eyes depicts a clearly distinguishable fluorescent pattern characterized by demarcated patches of hypoautofluorescence in areas of RPE loss and the presence of a surrounding hyperautofluorescent rim (Delori et al., 1995; Gobel et al., 2011; Holz et al., 1999; Holz et al., 2015) (Figure 2B). The understanding of the latter pattern is yet to be clarified. Finally, other techniques such as microperimetry can be used to assess macular function of AMD affected eyes (Wu et al., 2014).

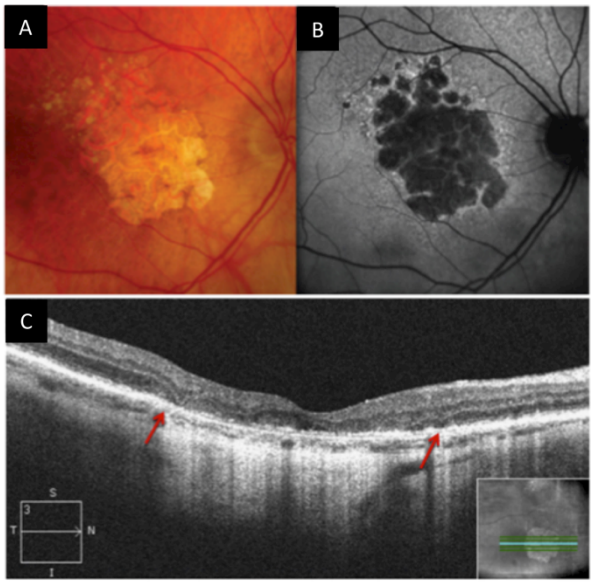

FIGURE 2. Multimodal imaging illustrating an eye with geographic atrophy.
(A) Multicolor and (B) BAF image of a patient with advanced dry AMD showing the demarcated boundaries of GA. Note in B the hypo-BAF atrophic area surrounded by a hyper-BAF rim compared to the non-atrophic zones. (C) SD-OCT image depicting loss of RPE layer (between red arrows) and thinning of the outer retinal layers that also appear atrophic. Adapted from *Nazari et al., 2015.*

Although neovascular AMD is currently treated with anti-VEGF therapies, nowadays there is no remedy available for GA. Today's strategies to face a possible therapy involve: (i) preventing RPE dysfunction or death with neuroprotective agents; (ii) maintaining for an extended time the RPE function by providing the stressed cells support (*e.g.* with specific factors, or cellular or basal membrane components), and (iii) replacing the diseased or lost RPE with a healthy RPE layer created *ex vivo*. The answer for a future treatment most likely relies on the combination of several of these strategies. In this thesis, we studied tissue replacement as a feasible approach for treatment of GA.

1.4 RPE REPLACEMENT AS TREATMENT FOR GA

As discussed above, RPE cells contribute with vital functions to the correct performance of the subretinal microenvironment, that is the reason why it is considered to be a key target for therapeutic interventions for both types of advanced AMD. However, since RPE cells do not have the ability to self-renew, some replacement attempts have been pursued either using autologous RPE harvested from the retinal periphery or using allogeneic fetal or adult RPE from cadaveric donors (Algvere et al., 1994; Phillips et al., 2003). Such transplants led to improved vision in some cases (Radtke et al., 2008) but have the disadvantage of coming from a limited source and, if autologous, they may carry predisposing genetic defects. In that sense, a more abundant and robust source is needed to provide a viable supply of healthy cells.

Such source could be provided from stem cells. Stem cells are a cell type that by definition has two properties: (i) the ability to self-renew, proliferate and give rise to the same cells maintaining their potency; and (ii) the capacity to differentiate into more specialized cell types. Depending on how restricted they are in their differential potential, they can be classified as totipotent, pluripotent, multipotent, oligopotent, or unipotent. Mainly two types

of pluripotent stem cells have been used for differentiation into RPE cells, human embryonic stem cells (hESC) and induced pluripotent stem cells (iPSC). However, multipotent cell types (or adult stem cells) such as fetal umbilical cord blood cells, hematopoietic, or mesenchymal stem cells are also being explored as therapies for retinal diseases (Fox et al., 2014; Mooney and Lamotte, 2010), yet up to date hESC or iPSC are arising as a more promising RPE source.

1.4.1 Differentiation of hESC into RPE

ESC are derived from the inner cell mass of a blastocyst embryo. These cells are considered pluripotent since they can differentiate into any cell type of the three germ-layers: ectoderm, endoderm and mesoderm (Thomson et al., 1998). Several protocols have used ES cell lines from several animals (*e.g.* monkey, mouse) to generate RPE cells (Haruta et al., 2004; Kawasaki et al., 2002; Osakada et al., 2009a). However, a xenotransplant of cells will often cause severe immunorejection. Thus, after the derivation of human stem cell lines from supernumerary human embryos, plentiful differentiation protocols to differentiate hESC into RPE cells emerged. They can be classified as spontaneous or directionally induced, both with possibilities to be xeno-free and/or defined.

Regarding spontaneous differentiation of hESC into RPE, which includes removal of basic fibroblast growth factor (bFGF) (an important factor for keeping the undifferentiated state of hESC), multiple studies have shown that RPE cells can be derived on several substrates ranging from inactivated mouse embryonic fibroblasts (MEFs)-, Matrigel-, poly-D-lysine-, or laminin-coated dishes, in addition to the use of different types of hESC culture media (*e.g.* DMEM/F12, KSR, mTeSR1, XVIVO 10) (Klimanskaya et al., 2004; Lane et al., 2014; Lund et al., 2006; Maruotti et al., 2013; Pennington et al., 2015; Plaza Reyes et al., 2016; Rowland et al., 2013; Vaajasaari et al., 2011). However, spontaneous protocols have the shortcoming of having long differentiation processes and potential less pure cultures.

hESC can also be directionally induced into hESC-RPE using several approaches comprising a two-stage induction via neural precursors (Cho et al., 2012; Choudhary et al., 2017; Zhu et al., 2013), the use of Nicotinamide and/or Activin A (Idelson et al., 2009; Leach and Clegg, 2015; Maruotti et al., 2015; Osakada et al., 2009b), or the combined used of retinal inducing factors (IGF1, Noggin, Dkk1, and bFGF together with Nicotinamide, Activin A, SU5402, and VIP) at the appropriate times to produce a faster differentiation (Buchholz et al., 2013).

Additionally, a remarkable number of protocols has emerged under the concept of trying to create clinically compliant cells, meaning an animal-free and defined product to avoid any possible microbial contamination or risk of rejection potentially brought by non-human protein into the cells during their time in culture. These xeno-free and/or defined protocols

rely on the spontaneous derivation of hESC-RPE either on recombinant matrices or using chemically defined factors/media, or both (Hongisto et al., 2017; Maruotti et al., 2013; Pennington et al., 2015; Plaza Reyes et al., 2016; Vaajasaari et al., 2011).

In all protocols, enrichment of hESC-RPE still needs to be performed either through mechanic or enzymatic procedures to remove the growing undifferentiated parts. Briefly, a standard characterization of the differentiated hESC-RPE would consist of the following steps: (i) verify the pigmented hexagonal morphology of the derived RPE cells and the apical microvilli and melanin pigments, which could be seen by conventional and electronic microscopy, respectively; (ii) analyze the presence of RPE-specific genes such as RPE65, BEST1, CRALBP, or MITF expressed as transcripts or proteins; (iii) analyze the purity of the culture by searching for genes of contaminating cell types (*e.g.* pluripotent stem cells, neural cells, fibroblasts, endothelial or non-RPE melanocyte markers) by qPCR, immunostaining or RNA single cell sequencing, in addition to tumorigenicity and biodistribution animal studies; (iv) confirm the functionality of the cells by analyzing their phagocytic capacity with FITC-labeled PR outer segments (POS) or verifying the presence of polarized channels (*e.g.* Na^+/K^+ expressed apically or BEST1 basally) via immunostaining; and (v) demonstrate the polarized secretion of growth factors such as VEGF or PEDF, and validate the presence of tight junctions through transepithelial resistance (TEER) measurements.

1.4.2 Differentiation of iPSC into RPE

The iPSC technology that emerged in 2006 has been a breakthrough capable of overcoming the possible ethical concerns and the possible rejection issues that allogeneic transplants with hESC-derived cells could entail. In an independent manner, Yamanaka and Thomson demonstrated that a terminally differentiated cell type (*e.g.* mouse fibroblasts) could be reprogrammed to an earlier state in its potency by the simple introduction of four crucial transcription factors: Oct3/4, Sox2, c-Myc, and Klf4; or Oct3/4, Sox2, Nanog, and Lin28, respectively (Takahashi and Yamanaka, 2006; Yu et al., 2007). The cells exhibited the morphology and properties of a pluripotent cell *in vitro* and *in vivo*. Such cells have been a promising source of patient-specific cells, easy to derive from an accessible source that would in theory eliminate the risk of immune rejection, thus inspiring researchers to develop iPSC-RPE as an autologous AMD treatment. Although iPSC-RPE have been derived and characterized showing a full range of the RPE features stated above (Buchholz et al., 2009; Carr et al., 2009; Hu et al., 2010; Kamao et al., 2014; Kokkinaki et al., 2011; Maruotti et al., 2013), a previous study showed that hESC-RPE seem to resemble human fetal RPE more closely than iPSC-RPE (Liao et al., 2010).

Despite the ideal therapeutic potential of the iPSC, still some concerns remain to be further explored for its optimal clinical use, such as reprogramming efficiency and safety of the cells

after the reprogramming procedure; as well as economical, time, and labor costs of the technology. Moreover, it is worth noting that iPSC derived from an AMD patient would still carry the genetic aberrancies and changes that predisposed that patient for the disease. In any case, amongst the potential clinical use, iPSC are an excellent source of cells for drug testing, investigating developmental biology, and disease modeling, as it has been shown for instance in a cell model of retinitis pigmentosa (RP) derived from RP patients that elucidated some of the possible pathogenic mechanisms of the disease (Jin et al., 2011).

1.5 ANIMAL MODELS FOR AMD

The ideal animal model to study AMD should be inexpensive, recapitulate the histological and functional changes but evolve in a rapid time course to allow more efficient studies. However, as mentioned earlier, AMD is a multifactorial and complex disease involving both genetic (*i.e.* multiple genetic polymorphisms that altogether contribute to the increased risk for AMD) and epigenetic factors. This in addition to the anatomical differences between species and the human retina hinders an accurate model of disease. Nonetheless, models of AMD have been generated in mice, rats, rabbits, pigs, and non-human primates and have contributed to unravel many important aspects about the underlying pathology of the disease (Fletcher et al., 2014; Pennesi et al., 2012; Zeiss, 2010). Despite the fact that rodents lack an anatomical macula and its PR are mainly composed of rods, they are low cost animals, they allow genetic manipulation, and the disease progression can be studied on a relatively quick time scale; advantages that are not offered by non-human primates although they possess the closest retinal anatomy to humans. Large-eyed models (*e.g.* rabbits, pigs, non-human primates) are more valuable regarding eye size and clinical relevance of the surgical procedures, which are in various ways useful for assessing the potential efficacy of a cell replacement treatment.

A very well-established preclinical animal model that mimics dry AMD/PR degeneration is the Royal College of Surgeons (RCS) rat. Specifically, they have a mutation in the MERTK gene which disrupts the RPE phagocytosis activity thus leading to outer retinal degeneration (D'Cruz et al., 2000). In addition, several other animal models have been developed following reported human mutations associated with hallmarks of early stages of the disease. These include animals with the following alterations: developing of drusen or drusen-like deposits (*e.g. Crb1*^{rd8} mutants), thickening of the BM involving lipid accumulation and defective lipid transport (*e.g.* mice under high-fat, high-glycemic-index diet, mice with alterations in cholesterol related genes such as APOE, LIPC, CETP and ABCA1 or in the lipid transport process: *CD36-null* mice) and extracellular matrix proteoglycans (*e.g.* mice overexpressing *Htra1*), immune dysregulation (*e.g.* affecting the complement system*: Cfh-null* mice and other variants, or monocyte migration to the subretinal space: *Ccl2-null, Cx3cr1-null* mice), oxidative stress (*e.g.* smoking, light exposure, and mutations in mitochondrial genes affecting the

enzyme superoxide dismutase/SOD) (for detailed references see *Fletcher et al* review (Fletcher et al., 2014)). Early to intermediate signs of macular degeneration also occur spontaneously in Cynomolgus Monkeys (*Macaca fascicularis* with early onset) and Rhesus Monkeys (*Macaca mulatta* with age-related onset but not progressive), although advanced features are rarely part of the natural history of the macular degenerative disease in these animals (Zeiss, 2010).

Modelling geographic atrophy in rodents becomes more difficult since it requires progressive deterioration of the retinal layers implying time and still multiple factors. However, alterations in chemokine pathways (*e.g. Cx3cr1/Ccl2*$^{-/-}$ mice if exposed to moderate level of light on a daily basis (Luhmann et al., 2012; Vessey et al., 2012)), defects in mitochondrial enzymes (*e.g. Sod1-null* and *Sod2* knockdown mice (Imamura et al., 2006; Justilien et al., 2007)) or in the NLRP3 inflammasome (*e.g. DICER1* knockout mice (Kaneko et al., 2011; Tarallo et al., 2012)) have been reported to induce PR and RPE cell dysfunction and loss. For mimicking CNV, laser or subretinal injury is the most commonly used method, but also subretinal VEGF gene transfer and genetic mice models of angiogenesis.

Other methods to induce retinal degeneration that in turn allow the recapitulation of more advanced stages of the AMD disease include: systemic or subretinal injections of sodium iodate and mechanical debridement of the RPE layer (Bartuma et al., 2015; Bhutto et al., 2018; Carido et al., 2014; Chowers et al., 2017; Hayashi et al., 1999; Kiilgaard et al., 2007; Leonard et al., 1997; Machalinska et al., 2010; Nork et al., 2012; Valentino et al., 1995; Yang et al., 2014). In fact, these are the most common techniques used to model retinal degeneration in large-eyed animals considering their difficulties for genetic manipulation.

1.6 SUBRETINAL HESC-RPE TRANSPLANTATION

Once an appropriately characterized hESC-RPE line has been established, a program for clinical transplantation may be considered. However, several important points need to first be addressed, including the manner in which the cells will be placed into the subretinal space, the possible rejection of the implant, and the safety of the cells in the host or patient.

1.6.1 Suspension Injections versus Monolayer-Sheet Engraftments

Regarding the transplantation format, two different strategies have been proposed: (i) introducing a cell suspension of non-polarized stem cell-derived RPE into the subretinal space; or (ii) implanting polarized sheets of stem cell-derived RPE cells with or without a supporting biomatrix.

Cell suspensions may integrate into the host subretinal space providing some beneficial effects, such as secreting growth factors and trophic molecules. The transplantation technique in large-eyed animals and humans undergoes a pars plana vitreactomy and generation of a

detachment or bleb where the cells will be then placed (Klimanskaya et al., 2004; Lund et al., 2001a; Lund et al., 2001b; Schwartz et al., 2012). In small-eyed rodents, the subretinal space is instead reached through the sclera (implying the rupture of the blood retinal barrier) without the need of performing a vitrectomy or retinotomy (Carido et al., 2014; da Cruz et al., 2007; Idelson et al., 2009; Lund et al., 2006; Vugler et al., 2008).

A concern raised with suspension transplants is the possible formation of multilayered clumps of cells that would damage the retina (Kamao et al., 2014). Another aspect to take into account is the status of the BM that in a diseased eye may not support RPE adhesion (Curcio, 2013; Sugino et al., 2011). To increase the likelihood of success, suspensions may need to be transplanted with a more supportive carrier (*e.g.* hydrogel), in an earlier disease state where the BM will be conserved enough, or the RPE cells may be manipulated to overexpress molecules such as integrins that would improve their attachment to the BM (Heller and Martin, 2014).

Transplantation of polarized hESC-RPE monolayer sheets seeded on a biomatrix is intended to mimic the native RPE and BM thereby potentially facilitating functional integration. A challenge with such membranes is to safely deliver them into the subretinal space. Several types of substrates have been used including plasma polymers, Parylene C, polyimide, and polyester membranes (Diniz et al., 2013; Kearns et al., 2012; Stanzel et al., 2014; Subrizi et al., 2012). It is crucial that these materials are inert to avoid rejections and allow diffusion of small and mid-range sized molecules. Moreover, they need to be flexible to facilitate delivery yet strong enough to preserve the cells as a monolayer. The surgery consists of conventional pars plana vitreactomy with subretinal implantation through a retinotomy that is considerably larger than for suspensions, thus increasing the risk of retinal detachment and possibly immune infiltration and graft rejection. There is also concern that these complex constructs may not be biocompatible causing retinal atrophy at the transplantation site (Ilmarinen et al., 2015; Stanzel et al., 2014). However, if successful, it has been shown that cell survival is improved when cells are transplanted as monolayer grown on sheets when compared to cell suspension injections (Diniz et al., 2013). Some of these suspension and scaffolds approaches are currently being tested in clinical safety trials (see section 1.7).

Current methods to evaluate the structural and functional integration of hESC-RPE include the use of real-time imaging techniques mentioned above (*e.g.* SD-OCT, BAF, IR-cSLO). In addition, histology and immunohistochemistry may give information on the fate of the transplanted cells as well as the surrounding retinal layers. Functionality may be tested by immunostaining for rhodopsin to demonstrate engulfment of POS, electroretinography (ERG) to determine the electrophysiologic response of the retina or by the use of behavioral tests to assess visual function (*e.g.* measures of visually-guided behaviors, optokinetic head-tracking (OHT) (Cowey and Franzini, 1979), and superior colliculus recording).

1.6.2 Immunologic Challenges of Stem Cell-Derived RPE Transplants

Upon transplantation, it is important to consider the immune properties of the stem cell-derived tissue and the environment they are intended to regenerate. Although it is well established that the eye is an immune-privileged site (Wenkel and Streilein, 2000), thus providing some protection against an immune response to the transplant, this barrier may be compromised under disease or surgical conditions. This is critical since any degree of immune response may lead to rejection of the transplanted cells. Indeed, even with a robust anti-inflammatory regimen, studies have shown progressive loss of donor cells in the subretinal space in animal models (Stanzel et al., 2014; Streilein et al., 2002).

Among the molecular mechanisms that have been suggested to be involved in subretinal immune privilege, the intrinsic properties of the RPE cells are fundamental. These include: (i) secretion of cytokines (*e.g.* TGF-β, PEDF, thrombospondin, somatostatin) with the ability to suppress both adaptive and innate immune systems (Sugita et al., 2006; Sugita et al., 2010; Sugita et al., 2009b; Zamiri et al., 2005; Zamiri et al., 2006); (ii) induction of macrophages to produce IL-10, which is known to down-regulate surface expression of the major histocompatibility complex MHC-II that in turn is the primary trigger for T-cell mediated immune responses (Zamiri et al., 2005; Zamiri et al., 2006); and (iii) secretion of TGF-β2 promoting the eye-specific regulatory T-cell (Tregs) differentiation (Hirsch et al., 2015). Tregs have an important role in suppressing effector T-cells, an action that protects tissues from aberrant immune reactivation, and have been proven to prevent immune rejection in graft-versus-host disease models (Cai et al., 2017; Hippen et al., 2011; Sakaguchi et al., 2008). On human RPE cells, Tregs are known to inhibit interferon-gamma IFN-γ-induced expression of MHC-II thus mitigating T-cell proliferation (Sugita et al., 2008; Sugita et al., 2009a).

In brief, the two main immune mechanisms triggered when the host retina receives non-autologous tissue or cells are: the innate system (cellular and humoral including complement), activated either by contaminating microbial products and endogenous proinflammatory factors released during the transplantation procedure; or stress-induced ligands that would activate natural killer (NK) cells (Figure 3A). Additionally, the adaptive response is also activated mainly triggering effector T-cells that will respond to either mismatched donor MHC antigens presented via MHC-I, or other non-self antigens presented via MHC-II of the host antigen presenting cells (APCs) (mechanisms known as direct or indirect allorecognition, respectively, Figures 3B and 3C) (Lechler et al., 2005; Murphy et al., 2011). This results in the expansion of allospecific cytotoxic (CD8+) and helper (CD4+) T-cells and the generation of alloantibodies through B-cell activation leading to graft rejection (Bradley et al., 2002). In fact, Zhang and Bok demonstrated that the expression of MHC-II on the grafted RPE cells under specific conditions promotes a progressive functional decline of the transplanted cells (Zhang and Bok, 1998), thus reinforcing the crucial role of MHC-II in long-term survival of the transplants.

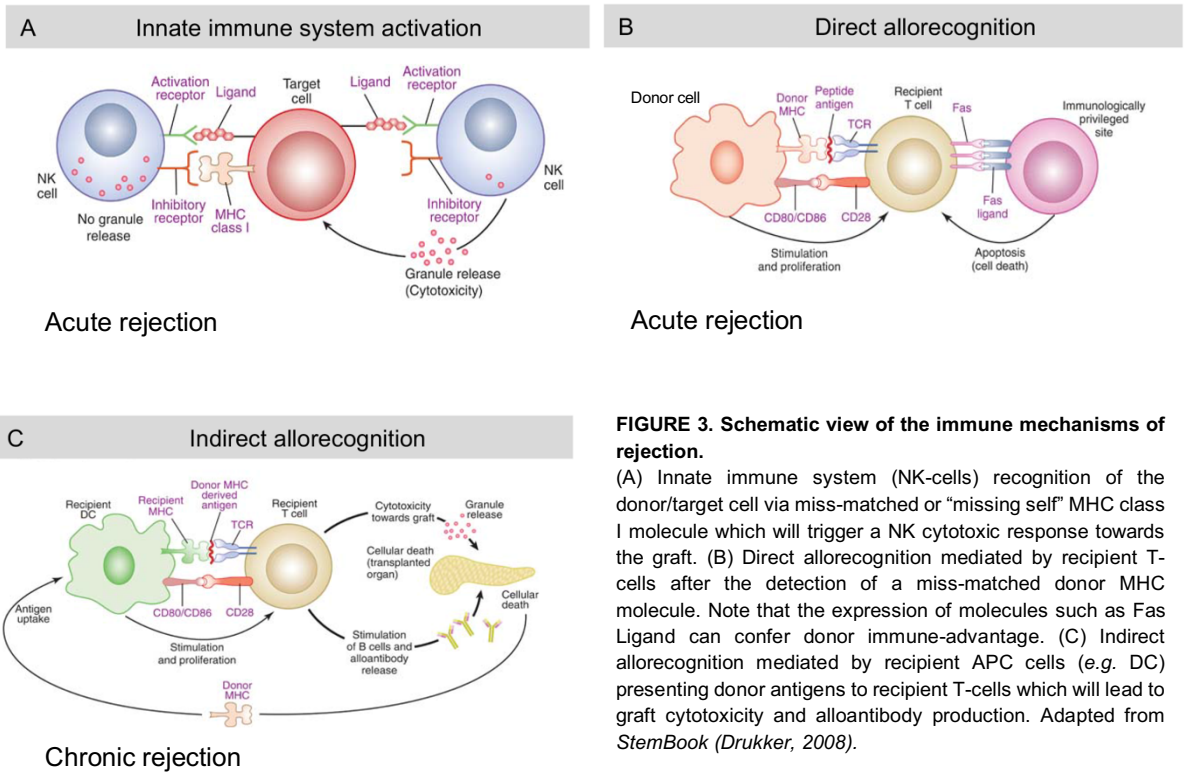

FIGURE 3. Schematic view of the immune mechanisms of rejection.
(A) Innate immune system (NK-cells) recognition of the donor/target cell via miss-matched or "missing self" MHC class I molecule which will trigger a NK cytotoxic response towards the graft. (B) Direct allorecognition mediated by recipient T-cells after the detection of a miss-matched donor MHC molecule. Note that the expression of molecules such as Fas Ligand can confer donor immune-advantage. (C) Indirect allorecognition mediated by recipient APC cells (*e.g.* DC) presenting donor antigens to recipient T-cells which will lead to graft cytotoxicity and alloantibody production. Adapted from *StemBook (Drukker, 2008).*

Consequently, it is essential to apply strategies that eliminate or minimize the risk of rejection of allogeneic stem cell-derived grafts. In addition to conventional immunosuppressive regimens in which possible toxic effects limit their efficiency (Tang and Drukker, 2011), some other approaches have been suggested: (i) mesenchymal stem cells given their immunosuppressive properties (Joe and Gregory-Evans, 2010); (ii) ES cells banking with known major histocompatibility complex antigens for matching recipients with the closest donor MHC antigen composition (Nakajima et al., 2007; Taylor et al., 2005; Thomson et al., 1998); (iii) peri-operative immunosuppression in the host after transplantation to provide the maximum protection for the limited number of cells introduced (Del Priore et al., 2003); (iv) if aiming for subretinal transplantation of RPE sheets, use of inert and biocompatible materials such as parylene or dissolvable gelatin; (v) inducing tolerance with a specific immunosuppressive drugs and dosing, or educating the recipient immune cells using donor-recipient hematopoietic chimeras or/and *ex vivo* adoptive cell therapy with donor-antigen-specific Tregs (Pasquet et al., 2011; Tang and Bluestone, 2013); and (vi) eliminating or reducing MHC (I and/or II) expression on donor cells limiting their recognition by the immune system by knock-ins with small interference RNA (siRNA) or short hairpin RNA (shRNA) (Burnett et al., 2011), or knock outs using viral or genetic engineering targeting (Abrahimi et al., 2015; Chen et al., 2015; Lu et al., 2013; Riolobos et al., 2013; Torikai et al., 2013).

1.6.3 Safety Evaluation of Transplanted hPSC-RPE Cells

To ensure a safe translation of derived RPE cells as a feasible option for patients, a standardized strategy that eliminates potential hazards associated with this type of treatment should be adopted. Prior to transplantation, stem cell-derived RPE cells should on the one hand prove to be pure or free of undifferentiated cells and pathogens and, on the other, they should show the ability to act as true RPE cells, both genetically and functionally as it has been described in previous sections.

Tumorigenicity studies are important to verify the inexistence of remnant pluripotent cells, thus demonstrating the inability of the transplanted cells to create teratomas (a tumor composed of tissues of ectodermal, mesodermal and endodermal origin) in an immunodeficient environment (*e.g.* CD-1 Nude Mouse, NU/NU Mouse, and BALB/c Nude Mouse) (Bouma et al., 2017; Kanemura et al., 2014). On the same line, DNA sequencing of the derived cells is another informative approach to further explore acquired mutations that could lead to disease or tumor formation (Bhutani et al., 2016). Preclinical animal toxicology, safety and efficacy studies are relevant to determine the potential expression of known proto-oncogenes or tumorgenesis risk. Additionally, biodistribution studies assessing the lack of migration of the cells from the transplantation site to other animal body organs are also critical. One should also be aware of the potential epigenetic modifications in the differentiated cells (especially after iPSC reprogramming), which may increase the risk of dedifferentiation drift of the derived RPE cells (Huo et al., 2014). The surgical procedure should also be carefully assessed to faithfully simulate the method to be used in humans, thus minimizing any possible further complications in this aspect.

To help such evaluations, some international guidelines to assess malignant potential of hPSC and derived products have been recently reported (Andrews et al., 2017; International Stem Cell, 2018). Finally, Good Manufacturing Practices (GMP) assuring sterility and traceability should be enforced throughout the clinical trial process (Bharti et al., 2014).

1.7 STEM CELL-DERIVED RPE CLINICAL TRIALS FOR AMD

Currently, there are at least 14 clinical trials ongoing testing stem cell-based replacement therapies registered in the International Clinical Trials Registry Platform (ICTRP) of the World Health Organization, aiming to treat advanced forms of AMD (Chichagova et al., 2018). All of these are to date in early phases, mainly assessing the safety and survival of the transplanted cells rather than efficacy. Studies include hESC-RPE, iPSC-RPE, hUTSC (human umbilical tissue-derived stem cells), BMHSC (bone marrow hematopoietic stem cells), HuCNS-SC (human central nervous system stem cells), Human-Fetal derived cells and Adipose-Derived stromal cells, with the majority of studies focusing on hESC-RPE or iPSC-RPE. Different cell

delivery methods are being tested in parallel, including subretinal suspensions or sheets as well as intravitreal injections.

The major hESC-RPE and iPSC-RPE trials include:

- *Astellas Institute for Regenerative Medicine* (Marlborough, Massachusetts, United States of America, NCT01344993) trial using subretinal hESC-RPE suspensions. They completed Phase I trial for dry AMD and Stargardt disease (18 patients). The authors reported evidence of long-term safety (5 years), graft survival, and possible biological activity of the transplanted hESC-RPE cells in AMD patients (Schwartz et al., 2012; Schwartz et al., 2015; Schwartz et al., 2016; Song et al., 2015).
- *California Project to Cure Blidness/Regenerative Patch Technologies, Ltd.* (California, United States of America, NCT02590692) trial supported by the California Institute for Regenerative Medicine (CIRM) using subretinal hESC-RPE monolayers on an ultrathin parylene scaffold. They recently completed In Phase I/II clinical trials for dry AMD trials (20 patients) and reported safety and suggested efficacy (in the short term) in some patients with severe vision loss (Kashani et al., 2018).
- *Cell Cure Neuroscience Ltd. (Hadassah Ein Kerem University Hospital, Israel, NCT02286089)* trial using subretinal hESC-RPE suspensions for dry AMD. Currently in PhaseI/II trial (15 patients).
- *London Project to Cure Blindness (LPCB)/University College London* (London, United Kingdom, NCT01691261) trial using hESC-RPE monolayers on a polyester scaffold. They recently completed Phase I clinical trial for acute wet AMD (10 patients) and reported feasibility and safety of the hESC-RPE patch transplantation (da Cruz et al., 2018).
- *RIKEN Center for Developmental Biology* (Kobe, Japan, NCT01691261) trial using iPSC-RPE monolayers on a collagen gel initially used as a temporary scaffold. This trial stands as the first clinical study using autologous iPSC-derived cells with 6 patients with wet AMD. However, the first treated patient in 2014 was reported with safety issues after transplantation and the study has then been interrupted. They have nevertheless recently reported feasibility of sheet transplantation one year post-surgery (Mandai et al., 2017).

Other studies in Phase I clinical trial aiming for advanced dry AMD worth mentioning are: *StemCells, Inc.* (Newark, California, United States of America) trial and *Janssen Research & Development, LLC* (Titusville, New Jersey, United States of America) that use suspensions of HuCNS-SC and umbilical cord blood mesenchymal stem cells, respectively. Both studies are aiming to assess the safety and preliminary efficacy of the subretinal injections.

2 AIMS OF THE STUDY

The general aim of this thesis was to develop both *in vitro* and *in vivo* methods and models to move forward a stem-cell based replacement therapy for patients suffering from the dry advanced form of AMD.

The specific aims of the four projects were:

I. To develop a xeno-free and defined protocol to derive RPE cells from hESC
II. To develop preclinical large-eyed animal models that faithfully recapitulate the GA phenotype seen in human patients
III. To assess the behaviour of the derived hESC-RPE upon transplantation in such models of degeneration
IV. To generate HLA-I knock out hESC-RPE and evaluate their immunological properties *in vitro* and in the large-eyed rabbit model

3 MATERIAL AND METHODS

3.1 ETHICS

3.1.1 Human Embryonic Stem Cells

Human embryonic stem cell (hESC) line HS980 was derived from supernumerary *in vitro* fertilized human embryos with a written consent from the donor and with the approval from the Regional Ethics Board (Dnr 2011/745-31/3). hESC were cultured under xeno-free and defined conditions according to the previously described method (Rodin et al., 2014a; Rodin et al., 2014b).

3.1.2 Animals

New Zealand white albino rabbits (provided by Lidköpings rabbit farm, Lidköping, Sweden) aged 5 months and weighing 2.5 to 4.0 kg were used at St Erik Eye Hospital (Stockholm, Sweden) after approval by the Northern Stockholm Animal Experimental Ethics Committee (Dnr N25/14). All experiments were conducted in accordance with the Statement for the Use of Animals in Ophthalmic and Vision Research.

3.2 CELL CULTURE

3.2.1 Human ESC Maintenance

hESC were maintained on hrLN-521 10 µg/mL in NutriStem hESC XF medium at 5% CO_2/5% O_2, and passaged enzymatically at a 1:10 ratio every 5-6 days.

For passaging, confluent cultures were washed with DPBS and incubated for 5 min at 37°C, 5% CO_2/5% O_2 with TrypLE Select. The enzyme was carefully removed and the cells were collected in fresh pre-warmed NutriStem hESC XF medium by gentle pipetting to obtain a single cell suspension. The cells were centrifuged at 300g for 4 min, the pellet was resuspended in fresh prewarmed NutriStem hESC XF medium and cells plated on a freshly hrLN-521 10 µg/mL coated dish. Two days after passage the medium was replaced with fresh prewarmed NutriStem hESC XF medium and changed daily.

3.2.2 Human ESC Differentiation

3.2.2.1 Suspension Embryoid Bodies

Pluripotent stem cells were cultured to confluence on hrLN-521 and manually scraped to produce embryoid bodies (EBs) using a 1000 µL pipette tip. The EBs were cultured in suspension in low attachment plates at a density of 5-7x10^4 cells/cm^2. Differentiation was performed in custom-made NutriStem hESC XF medium without bFGF and TGFβ and media

was changed twice a week. 10 µM Rho-kinase inhibitor was added to the suspension cultures only during the first 24 hours.

Following five weeks of differentiation, pigmented areas were mechanically cut out of the EBs using a scalpel. Cells were then dissociated using TrypLE Select, flushed through a 20G needle and syringe. Cells were seeded through a cell strainer (ø 40 µm) on 20 µg/mL LN-coated dishes at a cell density of 0.6-1.2x10^4 cells/cm^2 and fed three times a week with the same differentiation medium referred above.

3.2.2.2 2D Monolayer

Pluripotent stem cells were plated at a cell density of 2.4x10^4 cells/cm^2 on 20 µg/mL hrLN-111 coated dishes using NutriStem hESC XF medium. Rho-kinase inhibitor at a concentration of 10 µM was added during the first 24 hours, while cells were kept at 37°C, 5% CO_2/5% O_2. After 24 hours, hESC medium was replaced with differentiation medium NutriStem hESC XF without bFGF and TGFβ and cells were placed at 37°C, 5% CO_2. From day 6 after plating, 100 ng/mL of Activin A was added to the media. Cells were fed three times a week and kept for 4-5 weeks.

Monolayers were then trypsinized using TrypLE Select for 10 min at 37°C, 5% CO_2. The enzyme was carefully removed and the cells were collected in fresh pre-warmed differentiation medium by gentle pipetting to obtain a single cell suspension. The cells were centrifuged at 300g for 4 min, the pellet was resuspended, passed through a cell strainer (ø 40 µm), and cells were seeded on LN-coated dishes (hrLN-521 20 µg/mL) at a cell density of 7x10^4 cells/cm^2. Re-plated cells were fed three times a week during the subsequent four weeks with differentiation medium.

3.3 IMMUNE CELL CO-CULTURES

3.3.1 With PBMCs/T-Cells (T-Cell Proliferation Assay)

Day 30 (after replating) unstimulated or 2 days IFN-γ pre-stimulated (100 ng/mL) hESC-RPE cells were trypsinized as described above, irradiated (30 Gy) and plated at a cell density range of 1x10^3 (1:500) - 5.5x10^5 (1:1) cells/cm^2 (depending on the respective experiment) on hrLN-521 coated dishes (20 µg/mL) using complete RPMI medium with 10% FCS. hESC-RPE cells were left for at least 3 hours to attach to the plate. Secondly, PBMCs were isolated from buffy coats of healthy donors by a Lymphoprep density gradient. After washing with DPBS, cell numbers were assessed by counting with Türks solution, and they were then either stained with CellTrace CFSE Cell Proliferation Kit (2.5 µg/mL) or divided into two tubes for CD4+ and CD8+ isolation with commercially available CD4 and CD8-islation beads in accordance with the instructions of the manufacturers. Finally, 1 million of the labelled or unlabelled PBMCs, or isolated CD4+ or CD8+ cells were plated per well in a 24-well plate on top of the attached

unstimulated or pre-stimulated hESC-RPE; and IL-2 (1 ng or 100U), CD28 (1.25 μg/mL) or OKT-3 (25 ng/mL) molecules were added to each well if required. Co-cultures were maintained for 5 days at 37°C for further analysis.

3.3.2 With NK-Cells (Degranulation and Cytotoxicity Assay)

PBMCs were isolated as described above and consecutively NK-cells were separated with a CD56 isolation kit using autoMACs Pro Separator with the "depletes" program. Final cell numbers were assessed by Türks solution and cells were seeded out at a concentration of $1x10^6$ cells/mL in stem cell growth medium with 20% heat inactivated FBS and activated over night with 500 U/mL IL-2.

NK mediated cytotoxicity was measured in a ^{51}Cr-release assay with overnight IL-2 activated hNK-cells (effector cells) against unstimulated or 2 days IFN-γ pre-stimulated (100 ng/mL) hESC-RPE. hESC-RPE (target cells) were labelled with 70 µCi ^{51}Chromium for 1 hour at 37°C, NK-cells were then mixed with the labelled target cells at different effector:target ratios (10:1; 3:1; 1:1; 0.3:1) in a 96-well plate and incubated for 4 hours at 37°C. After, supernatants (70 µL) were transferred into 4 mL sample tubes and counted using a 2470 WIZARD2 automatic gamma counter. *Percentage of specific lysis per sample type = [(experimental - spontaneous release) / (maximum load - spontaneous release) x 100].*

3.4 CRISPR-CAS9 GENOME EDITING

CMV to EF1α promoter was exchanged into pX459 plasmid (addgene #62988) and in ampicillin-resistant TOP10 bacteria colonies, plasmid DNA was extracted using QIAprep Spin Miniprep Kit according to manufacturer's instructions. Next, PNK treated sgRNAs were directionally cloned into plasmid pX459-EF1α, STBL3 bacteria were transformed and ampiciilin-resistant colonies were picked and expanded. Plasmid DNA was extracted using QIAprep Spin Miniprep Kit according to manufacturer's instructions.

HEK293T cells (in DMEM supplemented with 10% FBS, 0.1 mM NEAA, 6 mM GlutaMAX and 1 mM Sodium Pyruvate) and hESC (HS980) were cultured to 70–80% confluency, and dissociated using TrypLE. The NEON™ Transfection System was used to electroporate 1 µg pX458_EF1α-Cas9_U6-sgRNA plasmid to a hundred thousand cells according to the manufacturer's protocol. When confluent, cells were harvested for gDNA extraction and mutation detection. After 24 hours, puromycin (0.5 µg/mL) was used for selection for extra 24 hours. For clonal expansion of hESC, once the cells reached 70–80% confluency they were dissociated, diluted and plated at a concentration of two cells per well in a 96-well plate previously coated with 15 µg/mL hrLN-521 and 1.7 µg/mL E-cadherin overnight. Single-cell

clones were cultured for further expansion and for genomic DNA extraction and Sanger sequencing of the region surrounding the edit.

Genomic DNA extraction was performed using QuickExtractTM DNA extraction solution and 1 µL of the extracted DNA was utilized for PCR amplification using Herculase II Fusion Enzyme. Mutation detection was performed using SURVEYOR Nuclease Assay according to the manufacturer's protocol. Indel percentage was calculated with the following equation: $100*1-\sqrt{((1-((b+c))/((a+b+c))))}$, where *a* symbolizes the integrated intensity of the unedited DNA fragment, and *b* and *c* represent the intensities for each cleaved fragment.

3.5 QPCR

Total RNA was isolated using the RNeasy Plus Mini Kit from Qiagen and treated with RNase-free DNase and RNaseH. Reverse transcription of RNA to cDNA was done using 1 µg of total RNA in a 20 µL reaction mixture using random hexamers and Superscript III enzyme. cDNA was preamplified using Taqman assays as primers in PCR reaction. Gene expression was quantified using Taqman assays and StepOnePlus Real-Time PCR system. Relative quantity was determined with comparative Ct (threshold cycle) method ($2^{-\Delta\Delta Ct}$).

3.6 FLOW CYTOMETRY

hESC and hESC-RPE were dissociated into single cells using TrypLE as described above. Samples were stained using the following conjugated antibodies diluted in 2% FBS and 1mM EDTA DPBS or in Brilliant Buffer. Cells were incubated with the conjugated antibodies at 4°C for 30 min and washed twice with 2% FBS and 1mM EDTA diluted in DPBS. Fluorescence minus one (FMO) controls were included for each condition to gate negative and positive cells. 7-AAD-PeCy5 or Zombie-APC-H7 NIR was added to the cells for Live/Dead stain according manufacturer instructions. Respective Geometric Mean Fluorescence Intensity (GMFI) values of the FMO controls were subtracted to obtain the final GMFI of each fluorophore. Stained cells were analyzed using a Cytoflex flow cytometer (Beckman Coulter). Analysis of the data was carried out using FlowJo v.10 software (Tree Star).

3.7 WESTERN BLOT

Total protein was extracted from cells by dissolving the collected cell pellet in cold radio-immunoprecipitation assay (RIPA) buffer and protease inhibitors on ice for 5 min. After centrifugation at 2000g for 5 min, the protein concentration from the supernatant was determined by bicinchoninic acid (BCA) Protein Assay kit with BSA standards using NanoDrop. Protein was loaded on a 4-20% Tris-Glycine Extended gel after being incubated (denatured) in 1X Laemmli sample buffer supplemented with 2-mercaptoethanol, at 95°C for 5 min. Following electrophoresis (120V for 70-80 min at room temperature), wet transfer (100V

for 60 min at room temperature) was carried out using an 0.2 µM PVDF membrane. Transferred blots were blocked using 3% BSA in 0.05% Tween-20 in DPBS prior to incubation with primary antibodies on a rotator at 4°C overnight. Secondary antibodies were incubated at room temperature for 1 hour using Alexa-680. The membrane was imaged using LI-COR Odyssey infrared imager (LI-COR).

3.8 IMMUNOFLUORESCENCE

Cells were fixed with 4% methanol free formaldehyde at room temperature for 10 min, followed by permeabilization with 0.3% Triton X-100 in DPBS for 10 min and blocking with 4% fetal bovine serum and 0.1% Tween-20 in DPBS for 1 hour both at room temperature. Primary antibodies were diluted to the specified concentrations in blocking solution, incubated overnight at 4°C. Secondary antibodies were incubated for 2 hours at room temperature and nuclei were stained with Hoechst. Images were acquired with a Zeiss LSM710-NLO point scanning confocal microscope and Olympus IX81 fluorescence microscope (Carl Zeiss Meditec). Post-acquisition analysis of the pictures was performed using ImageJ/Fiji software.

3.9 TIME-LAPSE MICROSCOPY

The Cell-IQ live imaging system (Chip-Man Technologies Ltd.) equipped with a 10x phase contrast objective, an automated stage and an integrated incubator (37°C, 5% CO_2) was used to monitor hESC-RPE behaviour. After OVs dissociation, hESC-RPE were seeded in triplicates on the different substrates: 0.1% Gelatin, hrLN-111, -332, -511, and -521 (all 20µg/mL). On day 1 after seeding, the plates were transferred to the live cell imaging equipment. Images were acquired for both the center (2x2 image grids) and the periphery (single images) of every well. Every region of interest was monitored every hour for 21 days. Cell migration (length and trajectory) was assessed for every time-lapse image stacks using NIS-Elements v.4.0 (Nikon). For each stack 10 cells were randomly chosen and manually tracked during the first 7 days of imaging.

3.10 ELISA

Supernatants from hESC-RPE or hESC-RPE and T-cell (either with CD8+ or CD4+ positive isolated PBMCs) co-cultures were collected 5 days after the cells were plated. Human VEGF, PEDF or IFN-γ secretion levels were measured with commercially available ELISA Kits in accordance with the instructions of the manufacturers. The optical density readings were measured using SpectraMax i3x Reader (MolecularDevices).

3.11 PHAGOCYTOSIS ASSAY

FITC-labelled bovine PR outer segments (POS) were isolated and kindly provided by Dr. E.F. Nandrot from Institut de la Vision, Paris (Parinot et al., 2014). hESC-RPE were cultured on Transwell membrane (0.33 cm^2) coated with hrLN-521 20 µg/mL for one month after seeding. Cells were incubated at 37°C or 4°C for 16 hours with 2.42x10^6 thawed POS/Transwell diluted in DMEM or CO_2 independent media, respectively. After incubation, cells were quenched with Trypan Blue Solution 0.2% for 10 min at room temperature, fixed with 4% methanol free formaldehyde at room temperature for 10 min and permeabilized with 0.3% Triton X-100 in DPBS for 15 min. Rhodamine phalloidin staining (20 min at room temperature) was used to visualize the cell boundaries. Nuclei were stained with Hoechst 20 min at room temperature. Images were acquired with Zeiss LSM710-NLO point scanning confocal microscope. Post-acquisition analysis of the pictures was performed using IMARIS (Bitplane).

3.12 TEER MEASUREMENTS

RPE cells were plated on Transwells (0.33 cm^2) and TEER was measured using the Millicell Electrical Resistance System volt-ohm meter (Millicell ERS-2), according to the manufacturer's instructions. Cultures were equilibrated outside the incubator at room temperature for 15-20 min before the experiment. Measurements were performed in unchanged culture media at three different positions of each well. Averages were used for further analysis. The background resistance was determined from a blank culture insert in the same media coated with the corresponding substrate but without cells, and subtracted from the respective experiment condition. Measurements are reported as resistance in ohms times the area in square centimeter ($\Omega*cm^2$).

3.13 RABBIT SERUM COLLECTION

5-10 mL of blood was extracted from rabbits prior and after subretinal injections at different time points in serum collection tubes. The tubes were left in a standing position for about 15-20 min until blood was clotted and they were then centrifuged at 20°C, 1500g for 10 min. Serum (supernatant) was quickly removed and stored at -80°C in 1 mL aliquots for further analysis.

3.14 ANTIBODY-MEDIATED ASSAY

100.000 cultured hESC-RPE were pelleted and mixed with 100 µL of serum for 30 min at room temperature. After two washes with 2% FBS and 1mM EDTA in DPBS at 300g for 5 min, secondary antibody donkey anti-rabbit was added for 20 min at 4°C and washed two extra times (300g, 5 min). Finally, 7-AAD-PeCy5 Live/Dead stain diluted in 2% FBS and 1 mM EDTA in DPBS was added to the cells. Stained cells were analyzed using a Cytoflex flow cytometer

(Beckman Beckman Coulter). Analysis of the data was carried out using FlowJo v.10 software (Tree Star).

3.15 SUBRETINAL INJECTIONS IN THE RABBIT EYE

hESC-RPE monolayers were washed with DPBS, incubated with TrypLE and dissociated to single cell suspension as described above. Cells were counted in a Neubauer hemocytometer chamber using 0.4% trypan blue, centrifuged at 300g for 4 min, and the cell pellet was resuspended in freshly filter-sterilized DPBS to a final concentration of 1000 cells/µL. The cell suspension was then aseptically aliquoted into 600 µL units and kept on ice until surgery.

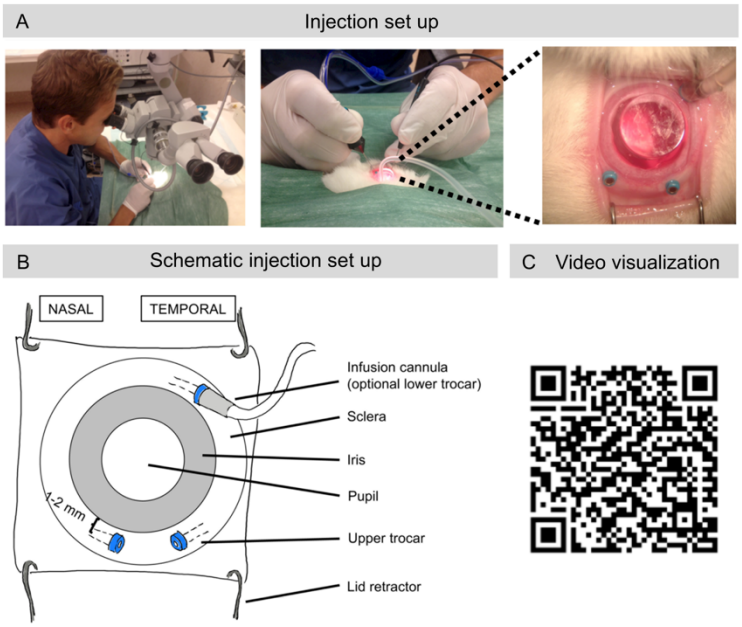

FIGURE 4. Subretinal pars plana injection set up in the rabbit eye.
(A) Pictures depicting the surgical set-up for subretinal injections. The animal is placed under the surgical microscope (left) and the surgeon holds the endoillumination probe inserted through the left trocar, and the intravitreal surgical instrument (*e.g.* subretinal injection cannula) inserted through the right trocar (middle). A flat contact lens placed on the cornea allows a magnified view of the fundus during the surgical procedure (right). (B) Close schematic view of the albino rabbit eye with the lid retractor in place and the nipple from the trocars inserted 1-2 mm deep from the limbus and at a 30-45° parallel angle, together with the trocars that facilitate the introduction of an optional infusion cannula, the endoilluminator, and the needle for injection. (C) QR code linking to a video that illustrates the different steps of the procedure. Adapted from *Petrus-Reurer et al., 2018.*

Animals were induced to general anesthesia by intramuscular administration of 35 mg/kg ketamine (Ketaminol 100 mg/mL) and 5 mg/kg xylazine (Rompun vet. 20 mg/mL), and the pupils were dilated with a mix of 0.75% cyclopentolate/2.5% phenylephrine. Microsurgeries were performed on both eyes using a 3-port 25G transvitreal pars plana technique. 25G trocars were inserted 1 mm from the limbus and an infusion cannula was connected to the lower temporal trocar (see setup in Figure 4). The cell suspension was drawn into a 1 mL syringe connected to an extension tube and a 38G polytip cannula. Without infusion or prior vitrectomy, the cannula was inserted through the upper temporal trocar. After proper tip positioning, ascertained by a focal whitening of the retina, 50 µL of cell suspension (equivalent to 50.000 cells) was injected slowly subretinally approximately 6 mm below the inferior margin of the optic nerve head, forming a uniform bleb that was clearly visible under the operating microscope. Care was taken to maintain the tip within the bleb during the injection to minimize reflux. After instrument removal light pressure was applied to the self-sealing suture-less sclerotomies. 2 mg (100 µL) of intravitreal triamcinolone (Triescence 40 mg/mL) was

administered a day prior to the surgery, and no post-surgical antibiotics were given. For the TCA cohort, intravitreal triamcinolone was re-administered every 3 months, if required.

3.16 PHALLOIDIN FLATMOUNTS

Immediately after euthanasia, the eyes were enucleated, and the injection area marked with Tissue Marking Dye (TMD). After removal of the anterior segment and vitreous, the posterior pole including the marked area was excised with a scalpel. After careful dissection of the neurosensory retina with a blunt spatula, the RPE– choroid–scleral flat-mounts were fixed in 1.5 mL fixing solution (FS) overnight at 48°C. Postfixing, the tissue was extensively washed with PBS and stained with Hoechst and rhodamine-phalloidin. Staining was performed in PBS containing 0.1% Triton X-100 for 1 hour at room temperature under slow agitation. Subsequently, samples were extensively washed with PBS and flat-mounted in between two microscope slides with fluorescent mounting medium. Deconvoluted images of the RPE layer were obtained with a fluorescence microscope (Axioskop 2 plus using the AxioVision software, Carl Zeiss).

3.17 HISTOLOGY

Immediately after euthanization by intravenous injection of 100 mg/kg pentobarbital (Allfatal vet. 100 mg/mL), the eyes were enucleated and the bleb injection area marked with green TMD. An intravitreal injection of 100 µL FS consisting of 4% buffered formaldehyde was performed. FS remained for 24-48 hours followed by embedding in paraffin. 4 µm serial sections were made through the TMD-labeled area and every 4 sections were stained with hematoxylin-eosin.

3.18 IMMUNOHISTOCHEMISTRY

Slides were deparaffinized in xylene, dehydrated in graded alcohols, and rinsed with dH_2O and Tris-buffered saline (TBS, pH 7.6). If the staining was performed using the Bond III instrument from Leica Biosystems/Leica Triolab AB the manufacturer's instructions were followed and a pH 9.0 EDTA-buffer at 100°C for 20 min was used as antigen retrival. Otherwise, 10 mM citrate buffer (trisodium citrate dehydrate, pH 6.0) with 0.05% Tween-20 at 96°C for 30 minutes was used, followed by 30 minutes in 10% normal donkey serum and 5% (w/v) protease free bovine serum albumin diluted in TBS. Primary antibodies were diluted in blocking buffer and were incubated overnight at 4°C. Secondary antibodies were diluted in blocking buffer and incubated 1 hour at room temperature; or in some cases, HRP-conjugated secondary antibodies were incubated for 30 min, followed by incubation with Tyramide Signal amplification Plus Fluorescein or Cy3 System from Perkin-Elmer. Sections were mounted with Vectashield with 4',6-diamidino-2-phenylendole (DAPI) mounting medium in a 24x50 mm

coverslip. Images were acquired with a Zeiss LSM710-NLO point scanning confocal microscope and Olympus IX81 fluorescence microscope (Carl Zeiss Meditec). Post-acquisition analysis of the pictures was performed using ImageJ/Fiji software.

3.19 MULTIMODAL RETINAL IMAGING

Anesthetized rabbits were placed in an adjustable mount. A commercial Spectralis HRA + OCT device (Heidelberg Engineering) with the Heidelberg Eye Explorer Software was used to obtain horizontal cross-sectional b-scans of hESC-RPE treated animals. The Spectralis has a real-time motion tracking system that minimizes eye motion artefacts. At least 3 cross-sectional OCT scans were obtained with simultaneous infrared- confocal scanning laser ophthalmoscope (IR-cSLO) reflectance reference images representing the upper, central and lower portion of the transplanted area. The best overall image quality was obtained when the OCT setting was on high-speed acquisition with at least 50 averaged automatic real-time images. *En-face* fundus images were obtained by IR- or multicolor cSLO (a composite of three simultaneously acquired color cSLO images). These modalities have a higher contrast level compared to conventional fundus camera photos. In addition, corresponding BAF images were captured using the Spectralis blue light-laser with an excitation wavelength of 488 nm and a barrier filter of 500 nm.

3.20 RETINAL MEASUREMENTS

To measure retinal thickness (RT) and outer retinal thickness (ORT), SD-OCT images were imported into the ImageJ software. Retinal thickness and ORT are defined as the distance from the inner retinal surface to the RPE or from the inner nuclear layer to the RPE, respectively.

For PR rescue analysis, ORT of treated regions was obtained from a section overlying at least 500 µm of continuously integrated cells (mean of 10 random measurements). ORT of non-treated control regions was obtained from the same scan 500 µm outside the bleb (mean of 5 random measurements). Relative ORT was calculated as the ratio between treated and non-treated retina. Distances were normalized to the 200 µm scale bar of the original image. All measurements were done in 14 injected eyes one month post-transplantation, or at the nearest time-point after (PAPER II).

For subretinal PBS bleb-induced analysis, the thickness of untreated and treated retina was measured 500 µm from either side of the temporal transition zone of the bleb area. All measurements were made on a horizontal OCT scan through the temporal center of the bleb, approximately 6 mm below the margin of the optic nerve head. RT and ORT distances were normalized to the 200 µm scale bar of the original image. Ten consecutive measurements on

three independent OCT scans from 9 PBS-injected eyes (one month post-transplantation) were acquired (PAPER I).

The relative IR-cSLO reflectance of subretinal blebs was estimated by using the histogram tool of the ImageJ software. The average pixel brightness was obtained by inserting a standardized circle (1 mm diameter) in the lower- right quadrant of the image immediately outside or inside of the injection area, respectively. The brightness ratio was then used as relative measure of bleb reflectance. Measurements were done in PBS- injected eyes in a time course of 28-days post-transplantation (PAPER I).

The total area of the pigmented lesions was estimated manually on IR-cSLO images using the built-in measuring tool of the Spectralis software. Integration is defined as a pigmented area >2.5 mm^2. Measurements were done in 14 injected eyes one month post-transplantation, or at the nearest time-point after (PAPER II); and in 5-14 eyes three- months post-transplantation (PAPER III), where also RPE atrophy (presence of hypo-BAF areas) was analysed either after one week and four months after initial PBS- or $NaIO_3$- treatments (PAPER III).

For subretinal/choroidal thickness measurements, SD-OCT scans were randomly made through the upper, middle and lower third of the subretinal lesions, and the scan with the largest subretinal infiltrate and simultaneous choroidal thickening was chosen for analysis. The height of the subretinal infiltrate (from the BM to the outer border of the neurosensory retina) was measured at the thickest point using ImageJ/Fiji. To obtain the value for choroidal thickening, the total thickness of the choroid was measured at the same position and subtracted from the choroidal thickness outside the bleb. Measurements were taken 7 days post-transplantation in 10-18 rabbit eyes (PAPER IV).

3.21 STATISTICS

Unpaired 2-tailed Student's *t*-test was performed comparing RT and ORT in control and PBS-treated eyes in PAPER I; and also comparing the relative ORT between eyes with integrated and with non-integrated hrLN-521-derived hESC-RPE in PAPER II.

Unpaired 2-tailed Student's *t*-test and Chi-squared test were used to compare differences in hypo-BAF areas and incidence of RPE atrophy between PBS- and $NaIO_3$- treated groups, respectively, in PAPER III; and to compare the different treatment groups in PAPER IV.
In all cases, significance was accepted at $p<0.05$.

4 RESULTS AND DISCUSSION

4.1 XENO-FREE AND DEFINED DERIVATION OF RPE FROM HESC (PAPER II)

The development of an efficient protocol to derive RPE cells from stem cells is of major importance to have a reliable, pure and unlimited source of cells to transplant. Up to date, multiple protocols showed that RPE are possible to be obtained from different cell sources (hESC, iPSC) and using different strategies (spontaneous, directionally induced, xeno-free, defined). In Paper II we describe the spontaneous, xeno-free and defined derivation protocol we developed and the characteristics of the derived hESC-RPE.

4.1.1 Methodology and hESC-RPE Characterization

4.1.1.1 Results

Confluent hESC cultured on hr-LN521 were firstly scraped to form embryonic bodies that after 3 weeks in suspension in defined and xeno-free Nutristem media without bFGF developed pigmented structures resembling optical vesicles (OVs), with an efficiency of 0.8 OVs per EB. Secondly, pigmented OVs were mechanically cut out and the dissociated single cells were plated onto different substrates including gelatin, hrLN-111, hrLN-332, hrLN-511, hrLN-521 (Figure 5). We show that hrLN-521 had the best plating efficiency and migratory properties together with hrLN-511, allowing the cells to cover the wells in a homogenous manner. Additionally, in all conditions, the plated OVs matured into pigmented hexagonal cells with a similar transcriptional profile including low expression of pluripotency associated transcripts (OCT3/4, NANOG), and strong expression of both neuroectoderm (SOX9, PAX6) and RPE-differentiation transcripts (RPE65, PMEL, BEST1). Flow cytometry analysis showed that the derived cultures had a homogenous expression of MITF and BEST1 on all LNs compared to gelatin; and immunofluorescence showed a uniform expression of CRALBP and BEST1 with clear apical polarization of ZO-1 and Na/K-ATPase. At a functional level, hESC-RPE cultures showed polarized secretion of VEGF and PEDF as well as active phagocytosis of POS and tight junction integrity that got stronger over time determined by TEER measurements. For the latter, cultures on gelatin and hrLN-332 did not manage to reach that confluent stage.

4.1.1.2 Discussion

The establishment of a methodology that eliminates any undefined and animal-based products possibly contained in the differentiation process of hESC-RPE (*e.g.* media, substrate) is fundamental to avoid microbial contamination and presence of non-human proteins. In fact, a not defined final product could contribute to a faster rejection of the transplanted cells by the recipient immune system, which would mean the end of such replacement therapy. However, a recent 4-year report of a clinical trial leaded by *Schwartz et al* that used a batch of cells derived from hESC expanded on mouse feeders and further grown on gelatin and in non-

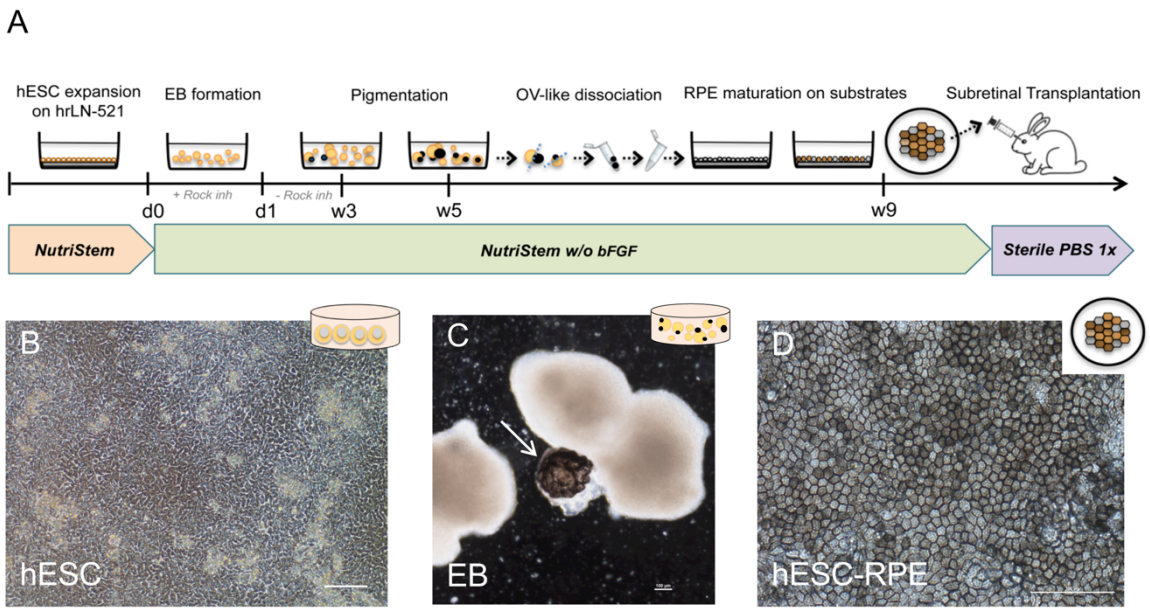

FIGURE 5. Xeno-Free and Defined RPE Differentiation of hESC-RPE.
(A) Scheme of the hESC-RPE differentiation protocol. Confluent hESC cultures are scraped and cultured in low-attachment plates to form EBs with Rock inhibitor during the first 24 hours. OV-like structures appear following week 3. At week 5, OVs are cut out with a scalpel and dissociated into single cells that are plated on hr-LN521 and cultured until homogeneous pigmentation is reached (week 9). Single-cell suspension of RPE cells are used for subretinal injection in the rabbit eye. (B) Representative picture of hESC. (C) Representative image of embryonic bodies and pigmented optic vesicles (arrow) after 3 weeks in suspension culture. (D) Representative picture of the derived hESC-RPE after 9 weeks in culture. Note the compacted monolayer of cobblestone pigmented cells. Adapted from *Plaza Reyes et al., 2016.* Scale bars: 100 µm.

defined media, showed no rejection or any other adverse effects of the transplanted allogeneic cells, although the patients were under a strong immunosuppressive regime (Schwartz et al., 2016). In any case, a cleaner product could reduce the dose of immunosuppressant drugs given to the transplanted patients.

Considering that our protocol relies on spontaneous differentiation and a more growth factor-directed approach would avoid batch to batch variation, the efficiency in obtaining pigmented OVs is remarkably high compared to other xeno-free and spontaneous protocols (Lane et al., 2014; Maruotti et al., 2013; Pennington et al., 2015), and in line with other more defined approaches (Choudhary et al., 2017; Hongisto et al., 2017; Idelson et al., 2009; Maruotti et al., 2015; Osakada et al., 2009b). In addition to the manual dissection of pigmented OVs, our results show that the use of biologically relevant cell substrates is important for obtaining a homogenous mature and pigmented culture of hESC-RPE. In fact, the chosen laminins are all present in the BM, meaning that cells with properties resembling the native RPE cells expressing specific integrin subunits (*e.g.* α3, α6 and β1) will preferentially be selected over other cell types present in the OV in LN substrates compared to gelatin, therefore increasing the purity of the final product. Previous studies showed that LN511 and LN521 support the highest degree of migration (Aisenbrey et al., 2006), which could explain the observed advantage of hrLN-521 over the rest of the tested substrates. Of interest, the appearance of RPE cell pigmentation was induced by hrLN111 in a faster manner than with any of the other analyzed matrices, as also suggested previously (Rowland et al., 2013). Furthermore, it is

important to highlight that the expansion of cells in suboptimal conditions (*e.g.* gelatin, with 8% seeding efficiency compared to hrLN-521 with 69%) have the inherent risk of selecting for growth-promoting genetic abnormalities. In fact, single cell flow cytometry analysis of MITF and BEST1 revealed significant heterogeneity in gelatin (47/70% MITF/BEST1 positive cells) compared to the rest of the LN cultures (around 90/95% MITF/BEST1-positive cells). Finally, having a source of cells with the potential to mature and acquire functional characteristics similar to the native RPE (including morphology, RPE-specific marker expression, monolayer integrity, polarized growth factor secretion and phagocytic activity) implies that upon transplantation they might have better chances to integrate and restore the role of the damaged native cells.

4.2 ESTABLISHMENT OF PRECLINICAL LARGE-EYED ANIMAL MODELS FOR GA (PAPERS I AND III)

Up to date, genetic mouse models and RCS rats are the most commonly used models aiming to study advanced dry AMD (D'Cruz et al., 2000; Pennesi et al., 2012). These models usually exhibit a specific defective aspect involved in the pathology of complex nature, therefore implying that the field is lacking a model that faithfully recapitulates the phenotype of the human disease. Additionally, the use of rodent eyes is limiting in terms of imaging and surgical techniques, which differ from the clinical setup. Although pig or non-human primate eyes are closer to the human physiology and clinical approach, they require higher maintenance costs to be kept in reasonable numbers for the same time-span as other smaller animals. In Papers I and III we describe two models of retinal degeneration using the rabbit eye intending to develop a more suitable preclinical model for GA that is affordable and has the advantages of a large-eyed model of disease.

4.2.1 Injection/PBS-Induced Degeneration Model (PAPER I)

4.2.1.1 Results

Following the human surgical retinal approach, a transvitreal pars plana technique was used to generate subretinal blebs of PBS or BSS in albino or pigmented rabbits. In addition, the same multimodal imaging (including SD-OCT, IR-cSLO and BAF) used in a clinical setup served to analyze the retinal phenotype. SD-OCT revealed 11 hyper- and hypo-reflective bands in the rabbit retina with clear delineation analogy to the human retina (Figure 6). In addition, the subretinal injection-induced outer retinal degeneration over the course of 28 days showing a demarked circular area in the bleb region with a hyporeflective margin and a hyperreflective center on MC and IR-cSLO, as well as thinning of the neurosensory retinal layers going from the outer nuclear cell layer to the outermost RPE/Bruch's layer. In fact, the subretinal injection significantly reduced both total retinal and outer retinal thickness when compared to control eyes. This degenerative effect was persistent upon 12 weeks after

induction of the subretinal blebs, showed by IR-cSLO, SD-OCT and HE stainings. Furthermore, subretinal layers including RPE/Bruch's also appeared to be affected as BAF revealed a "salt-and pepper-like" (hyper and hypofluorescent) pattern, and phalloidin-stained RPE flatmounts were indicative of a disturbed hexagonal RPE mosaic (Figure 7A).

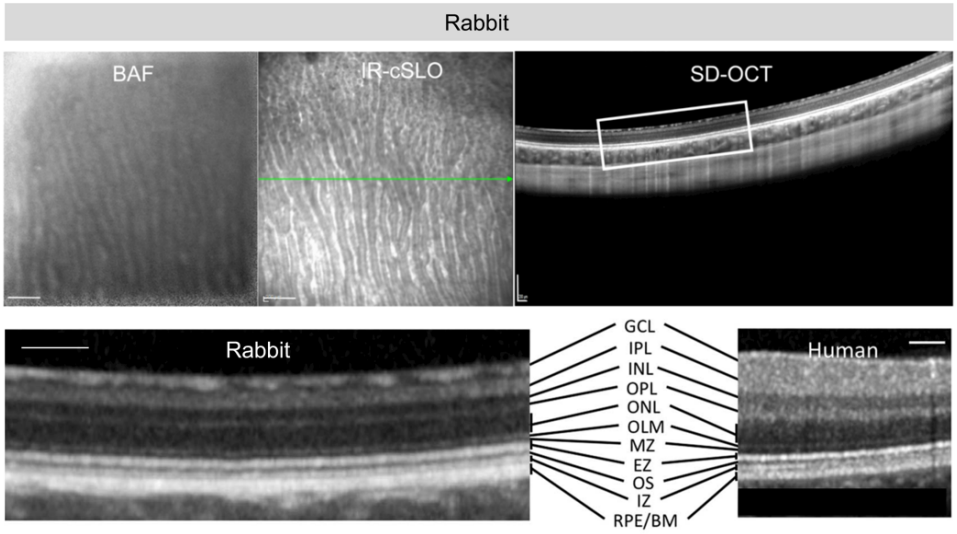

FIGURE 6. Normal albino rabbit retina *in vivo* multi-modal imaging.
In vivo BAF, IR-cSLO, and SD-OCT images representing a normal albino rabbit retina. A magnification (white box) of the SD-OCT b-scans shows 11 distinct hyper- and hyporeflective retinal layers with similar retinal delineation to the human (lower SD-OCT images): GCL (ganglion cell layer), IPL (inner plexiform layer), INL (inner nuclear layer), OPL (outer plexiform layer), ONL (outer nuclear layer), OLM (outer limiting membrane), EZ (ellipsoid zone), OS (outer segments), RPE (retinal pigment epithelium), and BM (Bruch's membrane). Adapted from *Bartuma et al., 2015.* Scale bars: 1 mm (BAF and IR-cSLO), 200 µm (SD-OCT), 100 µm (SD-OCT Rabbit, Human).

4.2.1.2 Discussion

The large-eyed rabbit is a well-established ocular model with accumulated data on anatomy and physiology over the past centuries (Hughes, 1972). Moreover, rabbits are easy to handle and breed, and are economic (*e.g.* purchase, housing and maintaining) and readily available compared to other large-eyed mammal models. For all these reasons, rabbit eyes have been an instrumental model for the evaluation of the effects of new medical eye technologies and surgical procedures that are currently in practice (Prince, 1964). Here we report for the first time that multimodal imaging can be used in rabbits showing that their retinal anatomy is comparable to the human one. This multimodal imaging tool provides detailed morphologic information noninvasively and in real-time, therefore becoming a key instrument to study retinal degeneration or to optimize and monitor new treatments targeting the subretinal space. Specifically, we first show that the subretinal injection of PBS induces retinal damage in the large-eyed rabbit eye; and second, that this damage can be captured by the imaging modalities to show different aspects of retinal degeneration resembling human advanced dry AMD. These changes include: a gradual loss of the PR layers by time dependent thinning of the layers (SD-OCT) and demarked hyperreflection (IR-CSLO), and changes in the RPE layer indicated by hypo-BAF in the areas of injection.

Despite lagomorphs being phylogenetically closer to humans than rodents, they possess a merangiotic retina and a visual streak in contrast to a holangiotic retina and a fovea present in primates (Blanch et al., 2012), thus meaning that that most of the blood supply of the inner rabbit retina is derived from the choriocapilaries. This morphological difference in vascularization could explain the neurosensitive retina degeneration phenotype seen in PBS-injected rabbit eyes, which actually allowed for modelling of early stages of GA. In fact, bleb injection generates a retinal detachment that maintains the neuroretina without vascular support until the bleb resolves (which can take up to 2 days). This time without proper oxygen and nutrients could be a major factor causing the degeneration of the PR cells. However, the RPE layer do have a vascular supply right underneath the supportive BM. Therefore, the most plausible explanation behind the detected perturbed RPE layer (showed by hypoBAF and flatmounts) could be due to the mechanical pressure of the injection itself that would damage and even wipe out the native RPE cells, therefore causing their degeneration. Toxicity and injected volume could be two additional variables influencing in the retinal damage. However, PBS or BSS are physiologic salt solutions routinely used in eye care and should be non-toxic to the rabbit retina. We used a volume of 50 μL, which relative to the rabbit eye size is similar to the 100 μL volume used in macaque and to the 100-150 μL in current clinical cell therapy trials, which could result in more pronounced damage compared to larger volumes. Related to this and worth considering in the clinical situation is the injection-associated retinal damage for subretinal administration that could then have a direct detrimental effect on the already diseased PR and RPE layers.

Overall, and despite the anatomical differences between rabbits and humans, the described model of injecting PBS in a merangiotic retina recapitulated some relevant features seen in human GA, including hypo-BAF and thinning of the outer retinal layers. However, a model with a more consistent damage in the RPE layer deserved additional exploration.

4.2.2 Chemically/$NaIO_3$-Induced Degeneration Model (PAPER III)

4.2.2.1 Results

In this study we further demonstrated that subretinal injections of PBS could induce a long-term GA-like phenotype that consisted of two areas of damage seen by SD-OCT, histology and RPE65 immunofluorescence: an outer damage with hyper-BAF area with PR loss yet intact RPE layer, and an inner area of more profound damage shown by hypo-BAF and corresponding atrophic PR and RPE layers. In fact, PR loss and hyper-BAF were observed in all treated eyes, whereas the presence of hypo-BAF areas were rare. Therefore, in order to more specifically target the RPE, we injected $NaIO_3$ subretinally in a dose-dependent manner. These injections showed that a dose of 0.1 mM caused changes similar to PBS alone (hyper-BAF), whereas higher doses (1 and 10 mM) caused large areas of RPE degeneration (hypo-

BAF) accompanied by a progressive loss of both the outer neuroretinal layer and the RPE/Bruch's/choriocapillary complex demonstrated by SD-OCT, histology and RPE65 immunofluorescence (Figure 7B). Doses of 10 mM caused further inner plexiform layer degeneration. In short, 1 mM $NaIO_3$-injected eyes had a significantly higher frequency of areas with RPE loss than in PBS-injected eyes, therefore arising as a more consistent approach to induce degeneration of the neuroretina/RPE/choroid complex in the large-eyed model that also resembled clinical GA.

4.2.2.2 Discussion

The proposed $NaIO_3$ model shows highly reproducible irreversible PR and RPE degeneration upon subretinal injection. As mentioned in the previous discussion, the mechanisms underlying neuroretinal and RPE cell loss are of different nature. The generation of a temporal subertinal bleb that induces retinal hypoxia in a merangiotic setup might be enough to cause PR death. However, since RPE do not detach from the choroidal support, the most likely explanation relies on the mechanical disruption induced by the injection itself, which is supported by the PBS model showing RPE loss in a limited fashion. Also, some recent reports showed that death mechanisms are different between PR and RPE, the former through apoptosis and the latter through necroptosis (Hanus et al., 2016), which could determine the different sensitivity of the cells to mechanical or chemical insults. Additionally, our data suggests that RPE loss accentuates neuroretinal death since the neurosensory retina present in hypo-BAF areas was more atrophic than in the hyper-BAF regions.

The local administration of $NaIO_3$ to induce retinal degeneration differs from conventional approaches that use a systemic route. Local subretinal injections are advantageous in the sense of having an adjacent healthy retina to compare to, in addition to studying an animal that is not under other possible systemic adverse effects of the chemical substance. Regardless of the administration route, several studies in rabbit, rodent and pig models confirmed the outer neuroretinal degeneration and RPE/Bruch's damage that we also describe (Grignolo et al., 1966; Mones et al., 2016; Wang et al., 2014; Yang et al., 2014).

Relevant to our model, and that genetically modified animals may lack, is the progressive structural PR and RPE damage showed by increasing hypo-BAF through time, in addition to PR thinning showed by histology and SD-OCT. This progressive model of disease can open a window to study the progression of the pathology under the same physiological conditions. However, the exact extend to which the injection/chemically-induced GA damage in the rabbit model corresponds to the GA damage caused by aging factors in humans remains to be assessed. For such evaluation, the aging variable should be incorporated to the model by for instance causing oxidative stress in the RPE cell layer with a 670 mm-laser light. Regardless, we demonstrate that the two models presented in this section induce many of the

characteristic changes of GA that current animal models fail to emulate, including degeneration of outer neuroretinal layer degeneration, RPE/Bruch's complex and choroidal layers showed by well-defined hyperreflecrtive IR-cSLO areas, thinning of the PR layer on SD-OCT and loss of RPE on BAF (Figure 7). Overall, PBS-induced changes were milder, mimicking an earlier disease phenotype; whereas $NaIO_3$-induced changes related closer to end-stage GA with more extensive choroidal atrophy, and PR and RPE loss.

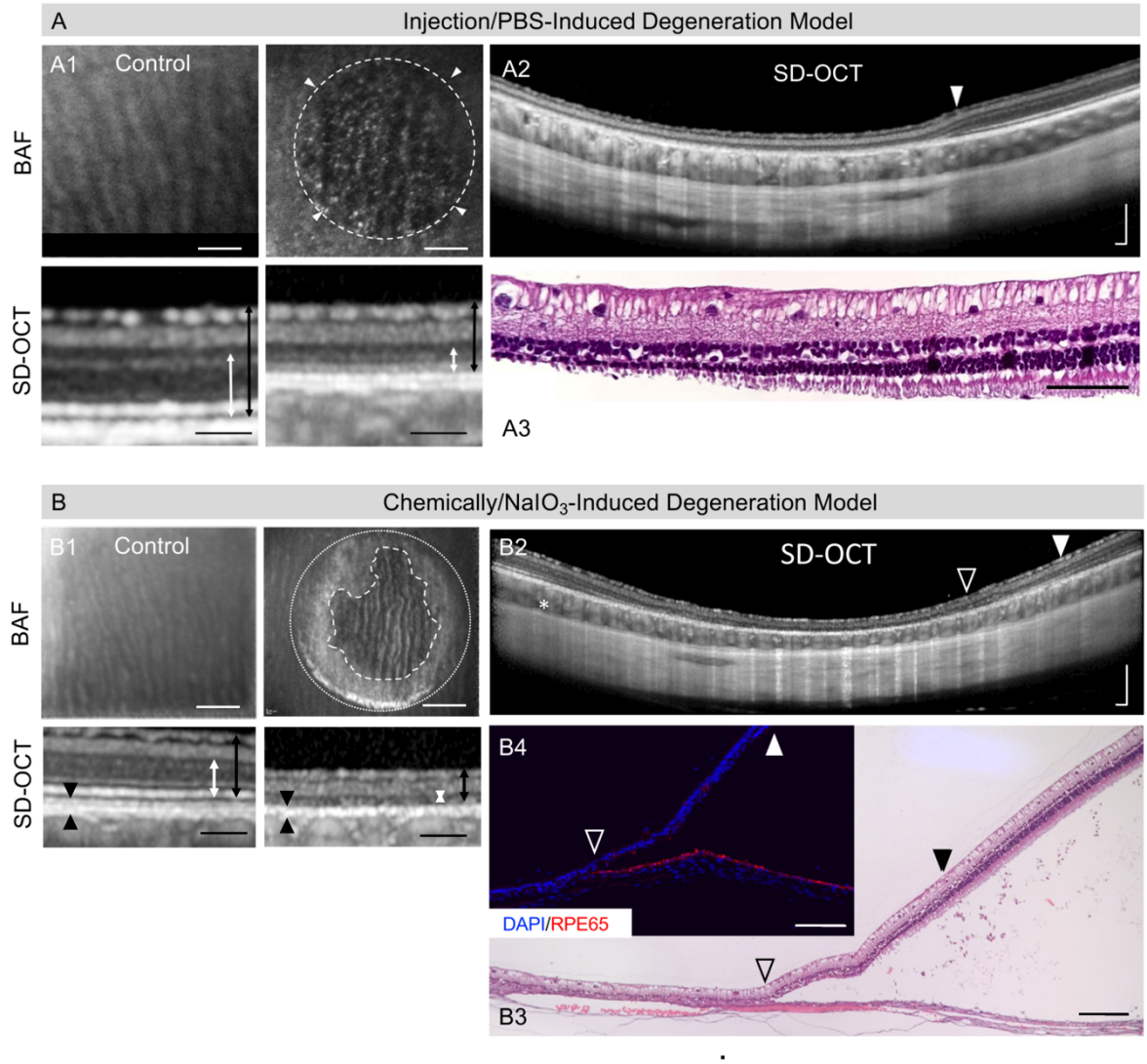

FIGURE 7. Summary of the GA-like phenotypes upon subretinal injection of PBS or $NaIO_3$.
(A) Subretinal injection of PBS induced PR degeneration and RPE disturbance demonstrated by thinning of the neuroretinal layers in SD-OCT (A1 and A2), and hyper- and hypoflurescent dots in BAF (A1, dashed line) four weeks after injection. Arrows in A1 indicate total (black, from inner retinal surface to RPE/BM) and outer retinal (white, from INL to RPE/BM) thickness. Non-injected control retina is shown for comparison. (A3) Corresponding HE-stained histologic sections show gradual reduction of the ONL in the area of the subretinal bleb. The RPE, choroid, and sclera were lost during tissue processing and are not shown. (B) Subretinal injection of 1 mM $NaIO_3$ induces PR and RPE loss demonstrated by thinning of the neuroretinal layers in SD-OCT (B1 and B2) and the RPE/Bruch's/choriocapillaris layer (B1, closed arrowheads), and hypo-BAF areas (B1, dashed line) surrounded by hyper-BAF in the bleb area (dotted line) three months after injection. Non-injected control retina is shown for comparison. HE-stained (B3) and RPE65 immunostaining (B4) of histologic sections show gradual neuroretinal atrophy, fusion with the underlaying layer and loss of the native RPE corresponding to areas of hypo-BAF. Note choroidal atrophy (B2, asterisk). The bleb margin (closed arrowhead) and border of RPE loss (open arrowhead) is marked in B2-B4. Adapted from *Bartuma et al., 2015*; and *Petrus-Reurer et al., 2017.* Scale bars: (A1, B1 BAF) 1mm; (A1 SD-OCT) 100 µm; (B1 SD-OCT, A2, B2) 200 µm; (A3, B3, B4) 100 µm.

Altogether, PBS/$NaIO_3$ blebs in the rabbit eye induce damage that faithfully captures most of the pathology of clinical GA, therefore arising as a relevant preclinical model for investigating the restoring capacity of hESC-RPE.

4.3 ASSESSMENT OF HESC-RPE INTEGRATION IN DEGENERATION MODELS FOR GA

Transplantation of RPE cells derived from PSC as replacement therapy for advanced AMD aims to stop the progression of the disease and hopes for vision restoration. Currently, different approaches have been tested, either using iPSC or hESC-derived cells transplanted in mice, rats, pigs or non-human primate models of disease in sheets or in suspension with transcleral or transvitreal injection techniques. In Papers II and III, we describe the outcome of the transplanted hESC-RPE cells in suspension using a transvitreal pars plana technique, firstly in the injection-induced degeneration model (Paper II) and, secondly, after 7-days pretreatment either by injection or chemically-induced methods (Paper III).

4.3.1 hESC-RPE Transplantation in the Injection-Induced Non-Pretreated Model (PAPER II)

4.3.1.1 Results

Albino rabbits were chosen to facilitate the tracking of the pigmented hESC-RPE on a transparent retinal background using multimodal imaging. Suspensions of hESC-RPE cells were transplanted into the subretinal space and after 1, 8 and 34-weeks histology and immunofluorescent stainings demonstrated that a monolayer of donor cells of human origin (NuMA positive) integrated in the host RPE layer overlaid by well-preserved PR. At eight weeks after transplantation, cells became heavily pigmented and acquired basolateral expression of BEST1. Remarkably, after 34-weeks donor cells were positive for the specific RPE marker RPE65 and showed cytoplasmic rhodopsin suggestive of maintained phagocytic activity. Additionally, eyes transplanted with hESC-RPE cells had significantly more preserved ONL and POS layers (seen in SD-OCT and histology) when compared to injected eyes that lacked or had minimal hESC-RPE integration (similar to PBS treatment alone), therefore rescuing their outer retinal thickness upon injection-induced damage. Finally, the transplantation of either hESC or fibroblasts formed transient cell aggregates that did not protect from the PR loss.

4.3.1.2 Discussion

Half of the transplanted human donor grafts in suspension after subretinal injections in the rabbit eye model showed hESC-RPE integrated patches of at least 2.5 mm^2, which is considered an excellent outcome for xeno-transplantation. The specific mechanism of PR

rescue by the integrated hESC-RPE (protective effect) is not clear and would most likely differ from the human setting due to the species-anatomical differences. However, a plausible hypothesis in the rabbit model could be that upon retinal detachment due to the subretinal bleb, integrated hESC-RPE provide the necessary support when the retina reattaches; whereas if not present and the native RPE cells have been denuded or are unhealthy, the hypoxic-survivor PR are left without the cells that would support and connect them to the choriocapillary bed, therefore leading to their degeneration.

Failure of integration frequently correlated with signs of immunoreaction, including cell infiltration, retinal atrophy and donor cell loss. Thus, xeno-graft rejection indeed might be the most probable explanation for the variability between animals and between eyes of the same animal, which will then require a more optimized immunosuppressive protocol. Actually, the use of a transvitreal approach to inject the donor cells compared to a transcleral surgery (used mostly in rodent injections) that would disrupt the blood-retinal barrier should reduce the risk of triggering an inflammatory response. Another factor that could contribute to a better integration could be the native state of the injected cells with certain adhesion or survival properties. In fact, a previous study showed that an intermediate state of differentiation (week 4 after passaging and differentiation of RPE stem cell-derived RPE cells from donor eyes) had the best integration and vision rescue outcome in the RCS rat model (Davis et al., 2017), which could correlate with our day 30 cells after OV dissociation. However, further experiments injecting hESC-RPE at different maturity stages in our model could shed some light in this matter. Interestingly, hESC-RPE de-pigment and de-mature upon trypsinzation (thus making the exact differentiation state of the injected cells unclear) possibly via an epithelial-to-mesenchymal transition, which should make them more migratory and maybe better equipped for integration. Then, re-acquisition of tight junctions and maturation/pigmentation –including down-regulation of activating molecules (*e.g.* HLA-II) or secretion of immunosuppressive factors (*e.g.* TGFβ or PEDF), is crucial to avoid immunoreaction and to increase survival of the integrated cells. Additionally, a not completely denuded native RPE cell layer could also affect integration of the donor cells to the host BM. For this reason, transplantation of hESC-RPE in pretreated animals with either injection or chemically-induced retinal degeneration merited further evaluation and will be discussed in the next section.

Interesting to note is the number of cells used for transplantation, which for the rabbits was 50.000 cells/50 μL compared to the high concentrations injected in rodents, typically 50.000 cells/1 μL in a three-times smaller eye. This made our surgical approach more controlled and with less chances of having multilayering and clumping of cells. In fact, some studies in rodents have shown that PR rescue was neither RPE-specific nor correlated with an intact donor cell layer (Pinilla et al., 2009).

Finally, the transplantation of hESC-RPE in the injection-induced large-eyed model could be performed with a surgical technique and instrumentation that was identical to a clinical setting, and could be monitored through time with high-resolution imaging techniques. In addition, and despite possible rejection of the xeno-transplant, we showed that hESC-RPE could integrate forming monolayers ten-times the size of a conventional RPE sheet for up to eight months, maintaining functionalities of native RPE cells and with ability to rescue PR from injection-induced degeneration in a specific and sensitive manner, where both non-RPE and non-integrated RPE cells were ineffective. The correlation of the hESC-RPE integration in the rabbit versus a human setting is unclear, and can only be tested with human subjects and allogeneic cells.

4.3.2 hESC-RPE Transplantation in the Injection/PBS- or Chemically/$NaIO_3$-Induced Pretreated Models (PAPER III)

4.3.2.1 Results

Firstly, hESC-RPE transplantation in non-pretreated naive eyes formed extensive pigmented subretinal monolayers correctly placed in between PR and Burch's membrane and not overlaying with native RPE cells. Notably, after 3 months, hESC-RPE cells were not found in areas of outer retinal degeneration and native RPE loss but instead in adjacent areas overlaid with well-preserved PR. Secondly, a pretreatment model for GA was induced by subretinal injections of either PBS or $NaIO_3$ 7-days prior to hESC-RPE transplantation at the same site where the initial bleb was located. For the PBS pretreated eyes, SD-OCT and BAF images taken before transplantation confirmed loss of PR layers. After 3 months, hESC-RPE were not found integrated but occasional pigmented dots or hyperreflective patches indicative of donor cells could be detected by cSLO, SD-OCT, histology and RPE65 immunostaining. For the 1 mM $NaIO_3$ pretreated eyes, SD-OCT and BAF before reinjection confirmed loss of PR layers as well as presence of hyper- and hypo-BAF. However, after 3 months, no trace of hESC-RPE was observed by either cSLO or SD-OCT (see summary in Table 1). Overall, these results suggest that hESC-RPE in suspension cannot integrate in areas of pre-induced retinal damage but instead in areas with a well-conserved outer neuroretina/RPE complex.

TABLE 1. Summary of the integration outcome of the transplanted hESC-RPE into the injection-induced (PBS) or chemically-induced ($NaIO_3$) GA-like damage models.
Adapted from *Petrus-Reurer et al., 2017.*

[a] Pigmented area > 2.5 mm^2
[b] 0.0 mm2 < pigmented area < 2.5 mm^2
[c] Pigmented area = 0.0 mm^2
[d] Area of hypo-BAF detected before transplantation. NA, not applicable

Treatment	Eyes Included (n)	Integration (n)[a]	Trace[b]	No Integration[c]	RPE Atrophy (n)[d]
None	14	5	6	3	NA
PBS	5	0	2	3	1
$NaIO_3$	5	0	0	5	5

4.3.2.2 Discussion

Transplantation of hESC-RPE in the injection-induced model formed extensive functional monolayers. However, in some instances integrated hESC-RPE cells were only found in the boundaries of a more pronounced damage overlaid with a well-preserved PR layer. This observation suggests that donor cells should be able to integrate if several variables come together: (i) native RPE cells are denuded (due to injection or chemical toxicity) to create space for the donor cells; (ii) mechanical pressure of the injection does not affect the BM so the cells have a matrix to attach to; and (iii) immune infiltration remains controlled by the immunosuppressive dose so the grafted cells are not rejected. Therefore, if any of these conditions is not fulfilled, integration in a xeno-model fails. Actually, the fact that denudation of the native RPE layer (especially with the $NaIO_3$ pretreatment) did not improve hESC-RPE integration into the host tissue as other studies have shown (Carido et al., 2014) is puzzling. Possible explanations include: rejection of the cells before they reached the integration side, or/and severe damage in the RPE/Bruch's complex due to injection or/and $NaIO_3$ toxicity, which would have impeded donor cell attachment. To be able to rule out one or the other, new experiments with a more controlled host immune system will need to be performed (*e.g.* different doses or types of immunosuppressant or use of immune-evasive cells). Interestingly, in the PBS pretreatment model we showed that RPE atrophy was significantly less present than in $NaIO_3$ pretreated eyes, and that some traces of hESC-RPE cells could still be found integrated. Putative explanations of the poor yet traceable integration in the PBS pretreatment model compared to $NaIO_3$ could be that: (i) native RPE were denuded but not sufficiently by the subretinal injection of PBS (in fact donor hESC-RPE were surrounded by native RPE positive for RPE65); (ii) the RPE/Bruch's complex was affected by the injection itself in the PBS model but still to a milder degree than in $NaIO_3$ treated eyes (injection in addition to chemical exposure); or/and (iii) the immune reaction might have been present in both cases but at a different rejection phase, so total clearance of the injected cells in the PBS pretreated model was not yet reached. In summary, in this study, the notably low-null rate of hESC-RPE integration could be a consequence of the unique features of the rabbit eye, the nature of the induced degeneration (PBS or $NaIO_3$) or the immunosuppressive regime. Despite that, we observed that hESC-RPE in suspension could integrate properly only if the subretinal milieu is sufficiently preserved, regardless of the initial status of the neuroretina; and again, the neuroretina was conserved if the RPE layer was not impaired.

In addition, it should be considered that pretreated areas were injected twice therefore increasing the risk of mechanical disruption of the outer blood-retina barrier that could trigger an immune response. This observation is critical to consider when transplanting hESC-RPE into pathologic eyes lacking a properly functional blood-retina barrier, since they will probably be more susceptible to immune reactivity. This double injection also causes a second round of neuroretinal detachment from the blood supply (in addition to the induced or chemical

damage generated with the pretreatment injection) as discussed above, thus adding an extra layer of challenge to the transplantation success.

Having all this in mind, if successful repopulation of hESC-RPE is to be achieved in areas of extensive outer neuroretina/RPE/Bruch's atrophy, the implementation of sheets of polarized hESC-RPE with or without supportive biomatrix or the use of hydrogels that could help RPE attachment in a damaged Bruch's should be considered. However, it will be important to optimize the sheet technology, as surgical difficulties and potential immunological response to the transplant leading to outer retinal atrophy in large-eyed animals have been reported (Ilmarinen et al., 2015; Stanzel et al., 2014).

Finally, our preclinical data suggests that suspension transplants of hESC-RPE may have the capacity to functionally repopulate the area outside the GA but not the GA area itself, as shown also by Schwartz et al in preliminary data from the first clinical trial on hESC-RPE in GA patients (Schwartz et al., 2016). Therefore, for the suspension approach to be functionally effective (*i.e.* stopping the progression of the disease and maintaining the remaining PR alive), it will be crucial to choose patients diagnosed in an early stage of the disease with a relatively conserved outer retina.

4.4 GENERATION AND IMMUNOLOGICAL EVALUATION OF HLA-I KNOCK OUT HESC-RPE (PAPER IV)

Avoiding the rejection of a transplanted graft by the host immune system is essential for the success of any allogeneic stem-cell based replacement therapy. Several immune escape approaches have been suggested, such as the use of iPSC cells, PSC-banking of HLA-homozygous superdonors or the establishment of a universal line lacking the HLA molecules that would identify the donor cells as foreign. In Paper IV we first describe the generation of a HLA-I knock out (KO) hESC line that is further differentiated into hESC-RPE and, second, we evaluate its immunological properties *in vitro* after co-culture with T- and NK- cells, and *in vivo* after subretinal transplantation in the large-eyed rabbit model.

4.4.1 *In Vitro* Characterization of hESC-RPE$^{B2M+/+}$ and hESC-RPE$^{B2M-/-}$

4.4.1.1 Results

The B2M locus was targeted using CRISPR-Cas9 technology with a sgRNA cutting efficiency of approximately 40%. IF, WB and flow cytometry confirmed that the B2M-targeting generated a dysfunctional HLA-I protein that was not able to be presented to the cell surface but was still present intracellularly. Engineered hESC were further differentiated into hESC-RPE that maintained pigmentation, morphology and immunosuppressive characteristics of native RPE cells but also lacked the extracellular expression of HLA-I. Interestingly, 20- or 50-times less hESC-RPE cells than PBMCs in a stimulatory environment (2 day 100ng/mL IFN-γ pre-

stimulation of hESC-RPE, and IL-2+CD28 added to the co-cultures) was sufficient to generate a 4-fold increase in CD8+ T-cell proliferation compared to PBMCs only. Subsequently, co-culture of hESC-RPE with isolated CD8+ or CD4+ T-cells at selected ratios showed a clear reduction in the levels of IFN-γ (as measure of T-cell activation) especially secreted by CD8+ T-cells when hESC-RPE$^{B2M-/-}$ were present. Analysis of specific T-cell ligands in both hESC and hESC-RPE genotypes showed that PD-L1 was highly expressed in all lines by either unstimulated or 2/5-days IFN-γ stimulated cells. In addition, about 5% of the hESC-RPE cells were able to express co-stimulatory ligand CD80 if stimulation was present. When co-cultured with freshly isolated NK-cells, chromium assay revealed that hESC-RPE$^{B2M-/-}$ were more susceptible to NK killing than hESC-RPE$^{B2M+/+}$ and that 2-days 100ng/mL IFN-γ pre-stimulation of hESC-RPE notably reduced the cytotoxicity levels in both lines. Additionally, we also tested if the maturity of the hESC-RPE cells could have an effect in NK killing, and both hESC and younger hESC-RPE$^{B2M+/+}$ (d14-d20) were more targeted than more mature hESC-RPE$^{B2M+/+}$ (d25-d33). Further analysis on the NK-cell ligands showed that all HLA molecules were downregulated in unstimulated or 2/5 days IFN-γ stimulated hESC-RPE$^{B2M-/-}$. PCNA (upregulated during cell stress and recognized by the activating NK-cell receptor NKp30) and MICAB (upregulated during proliferation and recognized by the activating NK-cell receptor NKG2D) were poorly detected in both hESC-RPE lines, but the latter was especially up-regulated on 5-days stimulated hESC cultures. CD112 (a ligand for the activating receptor DNAM-1 and the inhibitory receptor TIGIT) was highly expressed in all cell types and conditions, and CD155 (another ligand for DNAM-1, TIGIT and CD96, ascribed with both activating and inhibitory functions) was upregulated in higher levels in 2/5-days IFN-γ stimulated hESC and hESC-RPE$^{B2M+/+}$ compared to hESC-RPE$^{B2M-/-}$.

4.4.1.2 Discussion

The use of CRISPR-Cas9 technology has recently emerged as an efficient and easy approach to create targeted point mutations in specific genes of interest that due to inaccurate DNA repair lead to a defective protein. In fact, targeting the B2M locus using this technology is the way we generated the HLA-I KO hESC line described in this study. However, one of the limitations of this method is the potential off-target sequences that might emerge from unspecific guide-binding. Although in our case, neither hESC nor hESC-RPE showed impaired native characteristics, a more detailed analysis of the mutations present in the engineered sequences needs to be assessed by whole-genome DNA sequencing.

The observed immunosuppressive capacity of hESC-RPE could be due to the secretion of PEDF, TGFβ3 or IL-10, or the expression of CD95 or PD-L1 ligands (Idelson et al., 2018; Sugita et al., 2010; Sugita et al., 2009b; Usui et al., 2008; Wenkel and Streilein, 2000; Zamiri et al., 2006), the latter also suggested by our data. However, it is worth considering that in the

pathologic retina (*e.g.* altered blood-retina barrier, BM or/and the RPE), this immunosuppressive capacity might be altered promoting a more immune-susceptible subretinal space. Thus, the use of an optimized dose of immunosuppressants or a less immunogenic graft would be desirable for an allogeneic transplant.

In vitro co-cultures of T-cells and hESC-RPE in a specific RPE:immune cell ratio, together with inflammatory/stimulatory molecules such as IFN-γ or IL-2, showed that the lack of HLA-I (hESC-RPE$^{B2M-/-}$) reduced CD8+ T-cell activation measured by IFN-γ production; therefore confirming that foreign antigens presented via HLA-I molecules could trigger cytotoxic T-cells and acute graft rejection. Of interest is the fact that approximately 5% of the hESC-RPE cell population under IFN-γ stimulation up-regulated the co-stimulatory ligand CD80, implying that T-cell mediated immune reaction could be triggered without APCs.

When co-cultured with NK-cells, our data showed that the "missing self" phenotype of the hESC-RPE$^{B2M-/-}$ more potently triggers an innate cytotoxic NK response than the mismatched HLA-I present in hESC-RPE$^{B2M+/+}$. This killing could be mediated by the CD112 ligand for the activating receptor DNAM-1 which appeared highly up-regulated, as has been previously demonstrated (Cerboni et al., 2014; Dressel et al., 2010; Kruse et al., 2015). Interestingly, 2-days IFN-γ stimulation decreased the cytotoxicity levels in both lines, which could be due to the up- or down-regulation of certain inhibitory ligands that would block the NK action. A potential candidate that we have not evaluated is HLA-E, which has been incorporated into hESC by other groups to avoid innate immune system-mediated rejection (Gornalusse et al., 2017; Sugita et al., 2018). Another candidate could be CD155 since it was found to be down-regulated in hESC-RPE$^{B2M-/-}$ compared to hESC-RPE$^{B2M+/+}$ under stimulatory conditions. In line with other studies that propose both activating and inhibitory functions of this ligand (binding to either the activating receptor DNAM-1 or the inhibitory receptors TIGIT and CD96 (Bottino et al., 2003; Chan et al., 2014; Georgiev et al., 2018; Levin et al., 2011; Stengel et al., 2012; Tahara-Hanaoka et al., 2004)), our data suggests a potential dual role of CD155 also inhibiting NK cytotoxicity. Further investigations with KO lines for CD155 would be required to identify its specific effects.

Another critical observation of our results is that the maturation stage of the cells influences the NK cytotoxic activity, since hESC and younger hESC-RPE$^{B2M+/+}$ (below day 20) were more killed than older hESC-RPE (above day 25). This could be related to the consolidation of a more mature RPE phenotype (*e.g.* secretion of growth factors and stabilization of tight junctions), which could also involve up-regulation of NK inhibitory ligands in more mature cells, or down-regulation of activating NK ligands in younger cells. Further studies on the specific ligands expressed in each time point should provide some insight on this maturation-dependent differences in cytotoxicity. This may have critical implications in future

transplantation studies since younger cells may integrate better but also become rejected more easily.

Several considerations to bear in mind with the use of hESC-RPE$^{B2M-/-}$ cells include: whether the lack of HLA-I molecules will make them unrecognizable by the host immune system with increased risk of tumor formation or infections. Therefore, a fail-safe/suicidal cassette system integration enabling the elimination of the engineered cells upon administration of a specific drug should be considered. Additionally, the presence of sugars, minor antigens that do not require HLA molecule presentation or pieces of dead grafted cells could also be a source of recognition by APCs that could start an immune reaction. In this case, low doses of immunosuppressants will still be needed.

In summary, our data shows that hESC-RPE$^{B2M-/-}$ have the potential to partially escape the adaptive immune system, especially when CD8+ T-cells are involved. However, cells lacking both HLA-I and HLA-II molecules would avoid both CD4+ and CD8+ T-cell recognition. In this case, the innate immune system (including NK-cells) may still be activated, thus requiring the integration of specific NK inhibitory ligands such as HLA-E, as discussed above.

4.4.2 Transplantation of hESC-RPE$^{B2M+/+}$ and hESC-RPE$^{B2M-/-}$ in a Xenograft Model

4.4.2.1 Results

Cell infiltration from subretinal hESC-RPE$^{B2M+/+}$ transplants in non-immunosuppressed and TCA-treated animals was analyzed by real-time multimodal imaging through time. Grafts under TCA displayed homogenous monolayer integration evidenced by IR-cSLO and SD-OCT. However, in most cases at later time points, SD-OCT revealed a pronounced mass in the subretinal space displacing the pigmented donor cell layer accompanied by a thickening of the choroid, and eventually leading to an atrophic retina and choroid. Histological analysis confirmed a dense packed subretinal infiltrate with mononuclear and inflammatory cells. Further tissue stainings of the infiltrated areas revealed that rabbit immune cells from both the innate (NK-cells: CD56+, macrophages: RAM11+) and the adaptive (T-cells: CD3+) immune system were present at different rejection stages compared to non-rejected eyes. Interestingly, HLA-I was expressed in grafted cells also in later stages with deteriorated cell integrity, and HLA-II only appeared positive in cases of pronounced rejection. Rejection was shown in all non-immunosuppressed eyes within one week post-transplantation; whereas in TCA-treated animals, subretinal infiltration was seen rarely after one week, only in half of the transplanted eyes after one month, and in most of the eyes after three months.

Subretinal injections of hESC-RPE$^{B2M-/-}$ in non-immunosuppressed animals showed no signs of rejection in almost half of the transplanted eyes after one week, also in accordance with

both choroidal and subretinal thickness measurements at that time point that showed significant decrease compared to hESC-RPE$^{B2M+/+}$. The addition of TCA did not further reduce rejection in hESC-RPE$^{B2M-/-}$ transplanted eyes after 90 days. We also analyzed the amount of anti-human antibodies present in rabbit serums collected at different time-points before and after injection. Without TCA treatment, anti-human antibodies were already detected one week after hESC-RPE$^{B2M+/+}$ transplantation, whereas in hESC-RPE$^{B2M/-}$ transplanted animals, they appeared after two weeks in two-fold lower amounts compared to hESC-RPE$^{B2M+/+}$. With TCA treatment, anti-human antibody levels were not detected after one week, and they were present in low amounts (compared to hESC-RPE$^{B2M+/+}$ without TCA) after two weeks. Anti-human antibodies were detected in all the conditions analyzed after one and three months.

4.4.2.2 Discussion

A first aspect to be considered in our study is the use of a xenogeneic rabbit model, which resulted in rapid rejection of the grafted human cells, especially if immunosuppression was not administered. However, in a comparable clinical setting, the donor cells would be allogeneic and rejection would be expected to be less prominent. Thus, any reduction in rejection identified in the xenogeneic model should also be expected to translate into the human allogeneic setting.

Without immunosuppression, hESC-RPE$^{B2M+/+}$ donor cells triggered rapid rejection, whereas TCA delayed and in some cases impeded rejection. The rejection stages presented in this study for hESC-RPE$^{B2M+/+}$ cells are categorized depending on the level of retinal infiltration and atrophy, which do not necessarily correlate with time since local factors might be involved. In fact, immune reaction is highly dependent on the degree of damage of the BM and the blood-retinal barrier that would allow the host immune system to infiltrate in the grafted area, with determinant consequences for donor cell integration, as discussed in previous sections. Our data shows that the type of infiltrating cells present in these eyes belong to both innate and adaptive immune systems in all stages of rejection, which might be explained by the host-donor species difference. Evaluation of the specific type of T-cells present (CD8+ or CD4+ or both) in the infiltrations deserves further exploration since a reduction in CD8+ T-cells would be expected after hESC-RPE$^{B2M-/-}$ transplantation.

Transplantation of hESC-RPE$^{B2M-/-}$ showed a reduced acute inflammation in both the subretinal and choroidal spaces, and delayed the appearance of anti-graft (human) antibodies compared to hESC-RPE$^{B2M+/+}$. This suggests that early immune reaction might be triggered by HLA-I antigens recognized by the host innate (NK-cell) and adaptive (CD8+ T-cell) immune system. Interestingly, the addition of TCA immunosuppression did not further reduce rejection of hESC-RPE$^{B2M-/-}$ transplanted eyes and rejection was still observed through time, which may

be due to antibodies produced against human cells via indirect allorecognition by APC (macrophages, dendritic cells, lymphocytes B) through mismatched HLA-II if up-regulated, or the presence of minor antigens or other cell surface proteins/sugars. Any of these events will lead to CD4+ T-cell activation, B-cell maturation and antibody production contributing to delayed graft rejection.

In brief, although it is clear that hESC-RPE can induce both adaptive and innate immunoresponses *in vitro* and *in vivo*, the lack of HLA-I molecule showed a reduced and delayed immune response to the xenograft which may translate into better survival of a human allograft (see summary in Table 2). This would in turn reduce the need for immunosuppressive drugs. Altogether, hESC-RPE$^{B2M-/-}$ are the first step towards universal donor cells for cell replacement therapy in AMD and related conditions.

TABLE 2. Summary of the *in vitro* and *in vivo* techniques used and results obtained to study the immunogenic properties of hESC-RPE$^{B2M-/-}$ and hESC-RPE$^{B2M+/+}$.

	METHOD	RESULT
		hESC-RPE$^{B2M-/-}$ vs hESC-RPE$^{B2M+/+}$
IN VITRO	T-CELL PROLIFERATION (CFSE, IFN-ɣ ELISA) T-CELL LIGANDS (Flow Cytometry)	- Reduced CD8+T-cell Proliferation (1:20, 1:50 hESC-RPE:T-Cell +IL-2+CD28) - No pronounced difference in immunosuppressive ability (1:1 and 1:2 hESC-RPE:PBMC +OKT-3) - Up-regulation of PD-L1 with and without IFN-ɣ hESC-RPE stimulation for both lines
	NK-CELL CYTOTOXICITY (^{51}Chromium) NK-CELL LIGANDS (Flow Cytometry)	- Increased NK-Cytotoxicity - Decreased NK-Cytotoxicity with IFN-ɣ hESC-RPE pretreatment for both lines - Up-regulation of CD112 with and without IFN-ɣ hESC-RPE stimulation for both lines; down-regulation of CD155 with IFN-ɣ hESC-RPE stimulation
IN VIVO	SD-OCT (Subretinal/Choroidal Thickness)	Without TCA: - Decreased ST/CT at day 7 post-tx - Day 7: 100% rejection post-tx for hESC-RPE$^{B2M+/+}$ - Day 7: 50%, day 30: 75%, day 90: 100% rejection post-tx for hESC-RPE$^{B2M-/-}$ With TCA, for both lines: - Unchanged ST/CT at day 7 post-tx - Day 7: 0-10%, day 30: 50%, day 90: 100% rejection post-tx
	IF STAINING (NK-cells, Macrophages, T-cells)	All present in all stages of rejection
	ANTI-HUMAN ANTIBODY DETECTION (Flow Cytometry)	Without TCA: - Day 7 post-tx onwards for hESC-RPE$^{B2M+/+}$ - Day 14 post-tx onwards for hESC-RPE$^{B2M-/-}$ With TCA, for both lines : - Day 14 post-tx onwards

5 CONCLUSIONS

In this thesis we established a xeno-free and defined protocol to derive RPE cells from hESC. In addition, we took advantage of the surgical and retinal high-resolution imaging techniques that the large-eyed rabbit eye offers to develop a preclinical model of GA that faithfully emulates the pathological characteristics of clinical GA. We also assessed the integration capacity of the derived hESC-RPE into such models of disease. Finally, we developed a CRISPR-Cas9 based immune escaping strategy to avoid rejection of the grafted donor hESC-RPE cells into the host retinal tissue.

The main findings of these studies are:

- The spontaneous xeno-free and defined protocol allowed the efficient derivation of hESC-RPE cells that exhibited characteristics of native RPE cells, including morphology, pigmentation, marker expresssion, monolayer integrity and polarization together with phagocytic activity.
- hrLN-521 not only elimininated the need for undefined or xeno-derived matrix components but also emerged as a more supportive culture substrate for the derivation of hESC-RPE.
- The large-eyed rabbit model allowed the use of noninvasive high-resolution and real-time imaging techniques in addition to surgical techniques identical to a clinical setting.
- Subretinal injections of PBS or $NaIO_3$ in the rabbit eye induced damage that faitfully captured most of the pathology of clinical GA: PBS-injection (injection-induced) mimicked an earlier disease phenotype with loss of PR layers on SD-OCT and hyper- and hypo-BAF of the RPE; $NaIO_3$-injection (chemically-induced) mimicked end-stage GA with choroidal atrophy, more extensive loss of outer retinal layers and hypo-BAF areas of RPE loss.
- Suspension transplants of hESC-RPE using a minimally invasive surgical procedure in the large-eyed disease model achieved high-yield functional long term hESC-RPE integration with PR preservation in the injection-induced non-pretreated model.
- In the PBS/$NaIO_3$ pretreated model, suspension transplants of hESC-RPE did not integrate in areas of profound GA damage but did integrate only if the subretinal milieu was sufficiently preserved.
- hESC-RPE lacking HLA-I could be generated by targeting the B2M locus using CRISPR-Cas9 technology.
- Both hESC-RPE$^{B2M+/+}$ and hESC-RPE$^{B2M-/-}$ had an immunosuppressive ability but under specific ratio and stimulatory conditions they both triggered T-cell proliferation.
- Under stimulatory conditions, hESC-RPE$^{B2M-/-}$ significantly reduced CD8+ T-cell activation and consequent IFN-γ production; and upon mixing with NK-cells hESC-

RPE$^{B2M-/-}$ triggered a higher cytotoxic response than hESC-RPE$^{B2M+/+}$, which was reduced for both cells types if pretreated with IFN-γ for 2 days.

- Mature hESC-RPE$^{B2M+/+}$ (above 25-days) exhibited less NK cytotoxic effect than hESC or younger hESC-RPE$^{B2M+/+}$ (below 20-days).
- In the large-eyed model, transplantation of hESC-RPE$^{B2M+/+}$ without TCA showed rejection within one week with infiltrates from both the innate and adaptive immune systems at all stages of rejection; whereas transplantation of hESC-RPE$^{B2M-/-}$ showed a reduced acute early inflammation in the grafted areas and surrounding vascular bed and a belated appearance of a anti-human antibodies, overall delaying the rejection appeareance over time.
- The addition of TCA immunosuppression did not further reduce rejection of hESC-RPE$^{B2M-/-}$ transplanted eyes over time.

6 FUTURE PRESPECTIVES AND CHALLENGES

In the past ten years, stem cell-based treatments for the advanced forms of AMD have translated into preclinical and clinical studies at a vertiginous speed. However, in order to grant a safe and efficient therapy, the evaluation of the challenges entailed to bring these therapies into the bedside is of critical importance.

Briefly, such concerns and obstacles can be summarized in the following points (Nazari et al., 2015) (Figure 8): (i) development of sources of RPE and retinal progenitors that are low cost, reliable, robust enough, and able to be expanded and commercialized; (ii) optimization of the methods to deliver stem cell derived-RPE into the subretinal space in an efficient manner; (iii) long-term survival and function of the implanted cells; (iv) long-term safety of the procedure and the cells, assuring the inexistence of any type of tumor formation at any time after transplantation; (v) methods to minimize the risk of immune rejection of the transplanted cells; (vi) election of the optimal timing for transplantation considering risk-benefit for the patient; (vii) assessment if the replacement therapies slow the progression of the retinal degeneration or factually improve vision by integrating into the host retina and restoring retinal function.

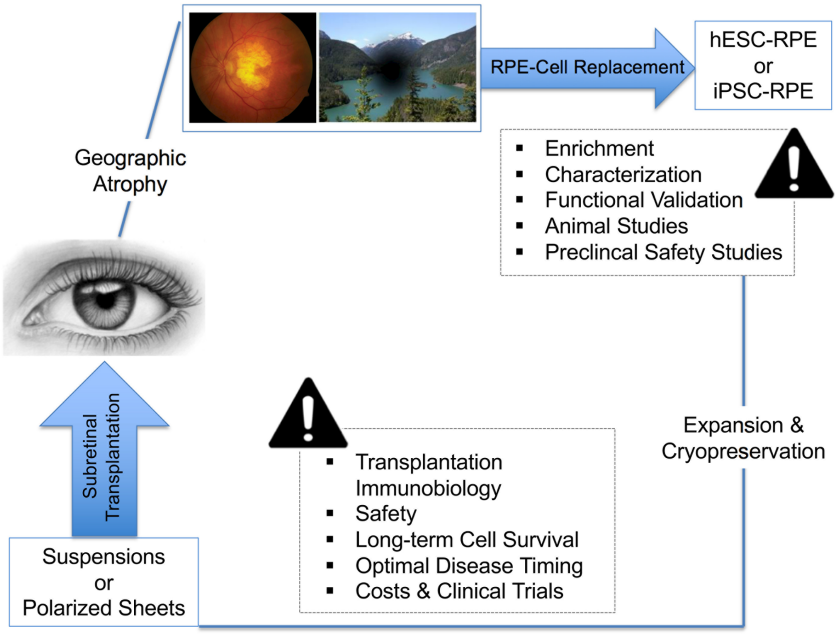

FIGURE 8. Diagram that recapitulates the main steps towards a stem-cell based therapy for the treatment of GA. The panels highlighted with an exclamation mark summarize possible concerns and challenges of the stem cell-based treatments.

The studies described in this thesis work aimed to acquire novel knowledge in several of the before mentioned aspects to transit to the bed side in the most efficient and safe manner. Firstly, we describe the derivation of functional RPE cells from hESC utilizing a spontaneous xeno-free and defined protocol which should avoid any immune reaction due to non-human proteins; however, a more directed approach would improve the batch to batch variability and would make it more suitable to scale up. Of note, progress in the mobilization of adult tissue-specific retinal stem cells or the reprogramming of Müller glial cells into a retinal neuronal fate

in vivo would simplify the technical complexities of the approaches that are currently in clinical stage (Coles et al., 2004; Zhao et al., 2014). Additionally, the derived cells should be tested for acquired pathogenic mutations by whole-genome DNA sequencing, and also tumorigenicity and biodistribution studies should be carried out in the appropriate animal models (International Stem Cell, 2018). In fact, these studies have been pursued already in our lab showing that the derived cells appeared safe in all the performed tests. Moreover, the use of specific cell surface markers differentially expressed in hESC-RPE could serve as a quality control of the purity of the final product, but also as an enrichment method for hESC-RPE upon RPE induction (Choudhary and Whiting, 2016).

Secondly, we describe the development of two large-eyed models that recapitulate the characteristics of clinical GA, in earlier or later stages, by multimodal retinal imaging and histology. The relevance of this model relies, firstly, on the localized generation of RPE damage that accentuates neuretinal loss due to the merangiotic retina of the rabbit, and secondly, on the preclinical imaging methods used for its evaluation. However, a limitation could reside on the fact that the described models might not be able to recapitulate progressive degeneration due to age. For this purpose, a photooxidative-damage model induced by the 670 mm-laser light could mimic an aging phenotype in RPE cells that could be worth considering as a practically feasible comparison to our models of disease. Also, and despite the high costs, the use of non-human primates with a closer retinal physiology with modelled GA (chemically-induced with for instance $NaIO_3$ since it is the most suitable for a holangiotic retina) would represent the most similar phenotype to the human pathology.

Thirdly, we show that suspension transplants of hESC-RPE can integrate and form uniform monolayers in between PR and choriocapillaries up to eight months if rejection is under control, therefore reinforcing that suspension transplants could allow long-term survival of functional cells. However, we reported no integration in areas of pronounced GA damage with altered RPE/Bruch's complex. A possible solution will then be the use of sheets or injectable hydrogels that could on the one hand facilitate RPE cell integration in a damaged Bruch's, and on the other, assemble the lost retinal elements and nerve connections to resume visual function. Although sheets come with the inherent risk of surgical complications and putative immune reaction of the transplant, thus requiring further optimization of the implantation technology, they might then be a better approach for treatment of late stage GA. However, for early stages with a well-preserved subretinal milieu, suspension transplants may be the best option. If the cells in suspension manage to integrate in monolayer and mature they (i) could suppress the host immune system by the secretion of immunosuppressive factors and the expression of certain inhibitory ligand; and (ii) they should be able to cover up to ten times the surface of a sheet with a minimally invasive procedure. The use of hydrogels is an option that deserves further investigation since some studies have shown their potential in combining the

advantages of both sheet and suspensions approaches (Ballios et al., 2015; Ballios et al., 2010). At this stage, gene therapy may serve to introduce therapeutic genes or factors that could also potentiate survival, integration, protection or function of the transplanted cells (Gamm et al., 2007).

Finally, the control of the host immune system is key for the success of the transplantation so that the graft does not get rejected acutely in the host tissue. In this respect, the use of iPSC should be a safe but expensive way to go. Other strategies include: induction of graft tolerance by the host immune system *ex vivo*, hPSC banking to maximize donor and host HLA matching or the production of universal lines of hPSC that would be able to escape the immune system. Following this last approach, we generated hESC-RPE lacking HLA-I and upon evaluation of their immunological properties they showed to be less immunogenic towards the adaptive immune system and presented evidence of a reduced rejection reaction in the xenogeneic rabbit model. However, an improved approach would need to be developed at least by (i) adding another escaping layer on the adaptive immune system with an HLA-II knock out; (ii) avoiding the cytotoxic effect of NK-cells by for instance integrating the HLA-E inhibitory ligand; and (iii) the addition of a fail-safe construct that would eliminate the unrecognizable health-threating engineered cells being infectious or tumorigenic. Additionally, the use of optimized humanized models (*e.g.* mice, rabbit, pig) would be the most plausible way to test with reasonable costs and numbers the immunoreactivity of the cells in an allogeneic *in vivo* context.

To conclude, the overall aim of the therapy suggested in this thesis work is the use of hESC-RPE cells injected in suspension for the treatment of patients in early stages of GA that could serve to slow the progression of the retinal degeneration and preserve as long as possible the existent neuretinal layers so that visual functional will not be impaired further. To factually restore retinal function and improve vision in late stages of disease, co-transplantation of not only RPE but also other neuroretinal cells or progenitors with a biocompatible carrier that would facilitate its integration and restoration of the lost neural connections would be required. Some years of interdisciplinary research are ahead, aiming to elucidate the specific cues to make this last approach a tangible reality for millions of patients suffering from retinal blindness.

7 POPULAR SCIENCE SUMMARY

Age-related macular degeneration (AMD) is one of the most common cause of visual loss associated with age in the Western countries, accounting for more than eight million people affected worldwide. The disease is mainly characterized by the degeneration of one of the constituent layers of the retina known as retinal pigment epithelial cells (RPE). RPE carry out important functions to maintain the proper functioning of photoreceptor (PR) cells, which are in charge of transmitting the visual stimuli to the brain. Therefore, if RPE are damaged, PR are in turn also impaired. The advanced form of AMD in which RPE cells die because of unknown specific causes has no available treatment today.

A possible way around it is to replace the lost RPE layer with almost identical cells generated in a dish from pluripotent stem cells, *i.e.* cells with the potentially to become any cell type of the body. The establishment of such regenerative approach is actually what this thesis is focused on.

We first developed a methodology to get RPE cells from pluripotent cells derived from human embryos in a well-defined manner and with no components of animal origin that could cause an immune rejection when transplanted into the human eye. Secondly, we developed an animal model (rabbit eye) of disease that recapitulates the main features seen clinically in human patients, including both RPE and PR damage. Additionally, this model allowed us to use the same surgical and retinal imaging techniques as used in the clinics, therefore facilitating the translation of the proposed treatment to the bedside. Thirdly, we demonstrated that treating patients in an early stage of the disease with reasonably preserved retinas is crucial for the transplanted cells to integrate in the host tissue, and stop the progression of the degeneration by preserving the remaining PR. Finally, we developed a strategy for the donor cells to escape the immune system by hiding some of the molecules that identify them as foreign. We then demonstrated that these modified cells can escape some parts of the adaptive immune (T-cells) but not the innate (NK-cells) system, therefore implying that further genetic modifications will need to be implemented in the cells to fully avoid their immune recognition. When we transplanted the engineered cells into the rabbit eye model, and despite the species difference, the early immune reaction of the host was reduced, and the presence of anti-human antibodies in the rabbit blood was delayed.

Altogether these studies show that the treatment of advanced stages of AMD using stem cell derived RPE cells can be a tangible possibility if: (i) the derived cells retain properties of the native RPE cells; (ii) the cells are transplanted in early stages of the disease with a considerably well-conserved retina; and (iii) the cells can be engineered so that they can evade the host immune system and consequent graft rejection. Although further investigations will need to be carried out to finally bring this therapy in the most efficient, safe and

immunocompatible manner, we hope that these studies shed some light on important preclinical aspects so that patients suffering from retinal blindness can soon benefit from a stem-cell based treatment modality.

8 ACKNOWLEDGEMENTS

Reached this point I truly wish that all our team efforts and contributions are valuable to the field and will help facilitating the transition to the clinics for the better quality of life of patients that suffer from age-related macular degeneration.

And a last thing but still very important that I am missing to say is **"BIG THANKS"** to all the people that helped, inspired and supported me during these four years of PhD. It has been an intense period that went by in the blink of an eye, but has been filled up with all sorts of experiences and knowledge. From here, I would like to thank everyone that has shared any moment along this path with me.

Firstly, I would like to strength the role of both main supervisor **Anders Kvanta** and co-supervisor **Fredrik Lanner** in this journey. You have been and are very important pillars and invaluable sources of know-how in many different situations and practical matters; as well as examples of great motivation and inspiration. It has been a pleasure to be the hands-on bridge between you both and learn from your different expertise and ways of doing science. I always felt glad to perceive the sincere communication that there is in between you which made this bridging a very easy task for me, and that allowed things to move forward in the most reasonable and efficient manner. Thanks Anders for your guidance, enthusiasm and your motivation to do good work; and also for the constant feedback and availability wherever and whenever it was needed. Thanks Fredrik for your open-door policy, approachability and valuable discussions that made my science objective and critical. Thanks to both for your trust in my opinions and my work, and for encouraging me to think independently, which is one of the most valuable things I take with me from this experience. I am very grateful that I could get the luxurious opportunity to belong to your two labs and I wish you, your family and both the Kvanta and Lanner labs the best for the future to come.

Thanks to my co-supervisor **Helder André** for all the scientific discussions, feedback and mentoring that this journey involved. Thanks for your fast and concrete answers that solved problems in no time. Talking with you has always been very comforting and I really value the co-supervisor friendship we now have. Wish you all the best with your scientific career.

Thanks to my co-supervisor **Sonya Stenfelt** to put this supervisor constellation together and for all the help to get me registered as PhD from the distance, which allowed a right-away and smooth start as soon as I landed to Stockholm. Hope you found your path outside the academia and I wish it will be a fruitful experience.

Thanks to my mentor, **Ana Teixeira** for the meetings we had along this way, which have always been very encouraging and inspiring.

I would also like to use this space to thank all the supervisors prior to my PhD time that had a profound influence on my choices and scientific development. **Malu Calle** de la Universitat de Vic (Barcelona, Espanya), tu vas ser la meva primera mentora i el teu suport va ser el motor inicial del que som ara com a investigadora. Moltes gràcies per la confiança i per la rigorositat de fer ciència que em vas inculcar. **Núria Malats**, va ser un període breu al CNIO (Madrid, Espanya) però intens en el que vaig palpar els valors del dia a dia d'un científic. Va ser el teu tarannà i la teva manera de fer que em va inspirar a seguir desengranant la meva curiositat fent recerca. **Mario Fernández Fraga**, IUOPA (Oviedo, España) muchas gracias por tu apoyo durante los seis meses que estuve en tu grupo. Tu entusiasmo y ganas de hacer y las de tu equipo consolidaron mi apuesta por seguir adelante mi carrera científica, de lo que estoy muy agradecida. **Stefan Schulte-Merker** and **Bas Ponsioen** back then at the Hubrecht Institute (Utrecht, the NL), I would always be grateful for all the knowledge I learnt in your lab, not only about the vascular and lymphatic system but also about zebrafish and microscopy, and for the enthusiasm and excitement you both had for science. **Christine Mummery** and **Valeria Orlova** at the LUMC (Leiden, the NL), thanks Christine for all the support you offered during my stay in your lab, and thanks Valeria for the knowledge you taught me in many scientific aspects and for your passion for science, which made me realize that the constant hard work and uncountable hours spent trying to find out a small piece of a big puzzle are simply rewarded by doing it.

I would also like to thank my colleagues in the two labs I belong to in both Huddinge/Flemingsberg campus and in Sankt Erik Eye Hospital. In this 4 years I worked in a very dynamic environment, but the combination of all of you made this PhD experience even more valuable. You are all great fellows and researchers with whom I could discuss science but also have great fun in and outside the lab :)

From St Eriks: **Monica Aronsson** and **Diana Rydholm**, for your always positive and charming attitude with us and with the rabbits, which I am sure they do sense, and that undoubtedly contributes to a research of high-quality. **Hammurabi Bartuma**, for your always cheerful mood and enthusiasm to do and move things forward, even if late hours and despite the clinic and family overload. I really enjoyed working with you and also all the ARVO moments together. **Parviz Mammadzada**, you were the St Erik PhD of reference, thanks for all the tips and all the fun times shared around. **Flavia Plastino**, you will be my RPE fellow, I wish you all the best in this period, learn and enjoy as much as you can. **Emma Lardner** and **Sofie Westman**, for your always positive attitude and your will to help with the tissue stainings or the SD-OCT scans despite the extra-work hours. **Yesenia Ortega**, por tu vitalidad, tu simpatía y entusiasmo por aprender.

From Huddinge/Flemingsberg: **Outi Hovatta,** thanks for being as you are and for sharing all your vast scientific experience and knowledge with us. Thanks for initiating this RPE project

and to connect Fredrik and Anders to push it forward. **Liselotte Antonsson** and **Mona Hedenskog**, for all the help sorting out any (constant) lab problem that emerged. Thanks Liselotte for sharing your knowledge and feelings about hESC and I wish you all the best in your new job. To **Siqin Wu** and his new team, **Paschalis Efstathopoulos** and **Nariman Gharari**, for all the back-and-forth-fun times in CL1, the scientific discussions and your awesome way of pronouncing my name: “SandRRRRa”. **Heather Main**, thanks for all the discussions on the RPE monolayer protocol and the developmental biology of the eye field. The hESC-RPE GMP are now in your hands, and wishing you will get them there very soon ;) **Pankaj Kumar**, for being the one picking up on all sorts of bioinformatics analysis of the RPE project, and being involved in it from the very beginning even though you I’m sure you would have never imagined to end up in the eye business. **JP Shell** for sharing some of your lab expertise and for all the scientific discussions and fun stories around the lunch table. **Nicolás Ortega**, Nicolasetee, gracias por todas las bromas, las risas y los buenos momentos compartidos dentro y fuera del lab! **Nerges Winblad**, thanks for all the discussions shared about CRISPR and about immunology, and for all the good work with the insane WB and clone businesses, that both my soul and prayers were all in for those knock outs to (NOT) show up. **Cheng Zhao**, for your always will to help in a patient and nice manner. **Sophie Petropoulos**, love your drive and motivation, thanks for all the inspiring talks about science and Canada land, and wish you all the best as a group leader which I have no doubt that will lead to amazing science. **Sarita Panula**, for all the knowledge shared, advice about experiments and organizational skills that helped the lab run almost like a charm. You were truly the reference PhD student in the lab for all your multiple high-performance skills and I wish you all the best in your new GMP challenge! Thanks to former lab members: **Theresa Mader**, **Jie Hao**, **Sebastian Hildebrand**, **Geeta Ravindran**, **Philipp Schenk** for all the shared moments in the lab while I was running around.

Thanks to **Pauliina Damdimopoulou** and to her lab members **Astrud Tuck**, **Richelle Duque Björnvang** for all the fun with celebrations and around the lunch table. And **Leni Wagner**, for all those hand in hand lunchies, fikas, dinners and scientific discussions: from tissue stainings/ImageJ, FACS/FJ to single cell RNA sequencing, from eye to ovaries, from CD markers to DDX4, from mesenchymal to granulosa cells and from oocytes to RPE cells, at any time and place. Thanks for the help you always offered when you saw me in a higher speed than usual, and for all the shared moments in and outside the lab that would take me another thesis to list up. Still pending in our list is to work side by side under the same project (de-frosting the -80°C doesn’t count :P), but some day, in or outside academia we will make it happen. Thanks for being how you are. Thanks for your f r i e n d s h i p.

Thanks to the RPE team, **Sara Padrell** y **Álvaro Plaza** por sobrevivir esos periodos intensivos de experimentos (sortings, qPCRs, FACSes, validations, teratomas, countingssss, etc) y los

never-ending CD/monolayer paper meetings con Fredrik. Gràcies Sara per la teva disponibilitat i el bon tarannà que transmets. Gracias Álvaro por las discusiones, por tu paciencia y por guiarme en los inicios del RPE project. Esa primera publicación fue un proceso intenso pero evidenció que nos entendemos y trabajamos codo con codo de la manera más eficiente y precisa. Gracias por tu saber estar, por tu amistad y por todos los momentos vividos fuera del lab, que en cuatro años ha habido muchos de memorables :)

Thanks to the collaborators for your time, your discussions and your knowledge. Without them parts of this thesis would not have been easy at all to pursue: **Helen Kaipe** and **Evren Alici,** for your availability and great discussions about experiments and puzzling results. **Laia Gorchs** per tots els moments compartits a altes hores de la tarda amb els T-cell experiments que per una o altra raó acabaven esdevenint hiper-complexes… però sí, sempre ens quedarà el sushi! **Michael Chrobok** and **Arnika Wagner** thanks for all the scientific discussions, for your positive attitude and always will to help out; and Michael for carrying out those never-last-crazy chromium experiments. **Camilla Mohlin** for your enthusiasm and help whenever a complement question came up. Looking forward to that porcine neuroretinal explants-RPE co-culture paper!

Thanks to some KI facilities and their coordinators **Iyadh Douagi, Stefan Mienke** (FACS facility in HERM), **Sylvie Le Guyader** and **Gabriela Imreh** (Microscopy facility in BioNut) for answering patiently to my panic questions in my early days with your instruments, and for sharing all sorts of tips and knowledge to make the best out of them.

Thanks to CNS and St Eriks officers **Mia Pettersson/Susanne Jonson/Maria Persson**, **Tina Melander/Josefine Jarvas**, **Eva Holmgaard/Kseniya Hartvigsson** and **Catharina Kuylenstierna** for always trying to help with some paperwork struggle. Also thanks to you **Galina Drozdova** for being my CLINTEC administrator although me not belonging to it, and your help sorting any paperwork/logistic problem efficiently. Thanks for all the other fun moments we spent together (also with **Alex Lundberg**) outside the office-lab space despite our packed and uncoordinated lives :)

Thanks to **Tango Restaurang** crew for the great spirits, and to its manager **Nan-Chung Huang** for your always positive mood and readiness; and of course, for feeding me many days of this PhD!

During this journey I also engaged in some organizational teams that I truly enjoyed being part of (despite the usual moments of craziness on top of the scientific life). Thanks to the all the organizing members of the **Winter/Ski Conference 2016, 2017, 2018** for the team effort resulting in a highly valued and unique conference in KI that allow PhDs to share their scientific projects and experiences in a ski setting. Thanks to **Magali Merrien**, for being my other hand pioneering the **Huddinge Pubs** aiming to entertain the southerner KIs. It was a pleasure to

share it with you and was cool to realize how harmonic our party ideas were. Thanks also for all the fun times spent together in different formats and around different Stockholm hoods.

Thanks to all the friends I was lucky to have here in Stockholm, in and outside KI. Thanks for each one of the moments of joy we spent together in all sorts of setups: dinners, lunchies, brunchies, parties, pubs, concerts, trips, excursions, fikas, BBQs, corridor/flatshares, conferences, sports,… during these four years, and that sometimes just popped up last minute out of a random text on a Friday or Saturday night :P Without them, any of this scientific progress would have happened that smoothly. But let's keep them up, because I am sure there are many more awesome times waiting to come!

Mauricio Somarribas, el Mauricet, que conozco desde casi el minuto cero en que llegué a Estocolmo. Gracias por todos los planes improvisados, por tu música y por tu amistad a lo largo del camino. **Valentina Carannante,** Vale, gracias por tu amistad, por tu tacto y por todas las risas y conversaciones compartidas. Aprovecha esta etapa en KI para potenciar tu talento científico del que rebosas. **Tatiana Álvarez**, Tati, l'ànima lliure de KI, m'encanta la teva dedicació i capacitat de fer bona feina, keep it up que les dues sabem que d'això en falta. Gràcies per tots els moments compartits anytime i malgrat estar fins els topes. **Yildiz Kelahmetoglu,** thanks for all the chipi-squid shared moments especially at the beginning of our paths here, that were many. In the end our ways diverged a bit but I know you are there if I need. Keep up that drive that makes you move mountains. **Jorge Correia**, chipi's other half, thanks for your always good mood, sarcastic jokes and scientific motivation that will bring you far. **Magda Kurek**, thanks for being Magda, and for all the time we spent throughout. I'm grateful for your hated-back-and-forth trips to Huddinge because they made you come south so our friendship could emerge :) And **Kuba Lewicki**, thanks for all the fun times together, and your enthusiasm about SciComm! I'm sure one way or another your scientific creativity will shine. And super thanks for accepting being my toastmaster! **Rafa González**, gracias por tu salero, estima y tu buen humor, la diversión está asegurada al salir de cena o copas contigo. El viaje a Hawaii nos marcó y siempre nos quedará como un recuerdo único (¡También por el infinito trayecto!). Te deseo mucha suerte en esta nueva etapa en tierra sueca :) **Burcu Bestas**, thanks for all our corridor chats while you were listening to horror movies, for all the reversed times that now I'm going through, for the guitar moments, and for your open heart and friendship. And thanks **Cihan Selvi** for the good vibes every time I've been around you both. **Vladimir Pabón** and **Olof Gissberg**, for all the corridor times and those unforgettable "Beer and Whiskey" festivals. **Ksenia Goroshchuk**, for those lab-to-lab moments that made the everyday frenetic live more enjoyable. **Gianvitto Arpino**, Gianvittinoooo, thanks for your energy and vitality, not having you around the KI events these days is always a bit of a shock but your move was for good and I'm happy for you (Sandraaa, Sandraaa!). **Alberto Jover**, mi mañico prefe, muchas gracias por tu autenticidad y por tu cariño. Desde el principio tuvimos

una conexión especial. No cambies que vales mucho. **Aida Rodríguez**, de Asturias a Suecia y tiro porque me toca. Gracias por tu buena actitud y por esos momentos guachis de MF/Biomedicum pubs o de fiestas caseras. Thanks **Lucio Monaco**, for being a super fan of my choir events and for the fun times around. **Gonçalo Brito**, the first man I knew even before I moved to Stockholm, the CMB pub master, the ski conference promoter, and the Vecura-Huddinge mate. Thanks for your openness, your charm and for introducing me many of the CMB people I know these days. **Simona Hankeová**, for our moves and laughter, and for our lovely retina commons. **Pedro Veliça**, for the fun pubs, the innebandy games together with **Deirdre E. Flanagan**, and for making science, finally, Pedromics-ally understandable. Wish you both the best with the little one that just became part of your lives. **David Grommisch** and **Matheus Dyczynski**, thanks for all those beers and random chats about live, and David for the fun spent together, the scientific talks, THE badminton match and the squash that some day will come. **Alena Salašová**, Alča, thanks for your honesty and for being as you are, and for all the cool times spent around together**. Susanne Neumann**, I'm proud to say that despite all the difficulties, we managed a couple of things together that were great fun, but that was not enough, we should fix our agendas soon! Thanks for your openness, your positive mood and your good spirits that moves crowds. **Irene González** and **Vincent Millischer**, thanks for the shared dinners around Stockholm. Irene gracias por tu buen hacer, por siempre estar ahí y por tu amable hospitalidad. **Ana Amaral**, thanks for your spontaneity and creative being, and thanks for always being opened for any fun or cultural activity that is around :) **Agustín Solá**, gracias por estar siempre dispuesto a poner una mano, por tu buen carácter y por seguir animando NEO con los Dead Cell Society pubs. My Årsta girls, **Tina Jacob**, for all the fun times, for your honesty, hard working and awesome leading skills. Was great to work hand in hand with you for the last ski conference. Wish you all the best with these exciting times that are about to come in your life. And **Erle Refsum**, my dearest neighbour, for accepting all my spontaneous plans, for your charm and easiness. It was always super nice to hang out with you. **Christine Zimmer**, **Angelina Schwarz** and **Magali Merrien**, the ethics girl gang, for all the awesomely-planned-dinners and enjoyable times together. **João P. Alves**, thanks for nice chats and those very useful thesis tips. **Laia Mira**, pel teu bon humor i gràcie valenciana que portes arreu. **Luisa Bone**, tú fuiste una de las últimas incorporaciones y me encontraste en pre-defence period total. ¡Gracias por todos los momentos improvisados que me sacaban de esa locura! **Giuseppe Santopolo**, **Shahul Hameed**, **Anastasia Magaoulopoulou**, **Lucía Peña**, **Néstor Aramis**, **Sharesta Kohenkohen**, **Silke Sohn**, **Parisa Rabiei Far**, **Mihaela Zabulica**, **Renata Vernaitė**, **Axel Leppert, Médoune Sarr, Ana Marín** and **Robin Pronk** for all the fun pub and conference times together. **Rosa Sotile**, for all the lovely time full of laughter we had in Stockholm but also in NYC! **Anja Mezger**, for our tennis matches and great shared moments, wish you all the best now with your new family member. **Maria Alsina** i **Jordi Planas**, gràcies per tots els moments catalans compartits entre soparets, cantates i

BBQs en els meus inicis del doctorat. **Clara Márquina** y **Sera Álvarez**, gracias por todas las risas compartidas entre impro shows y cenitas. ¡Os deseo lo mejor en Aussie land! **Philipp Schenk** and **Julia Karte**, you came in the very last bits of this PhD but it truly was a breath of fresh air. Thanks for all the shared moments squashing, pizzaing, cake baking, slack-lining… it was awesome to have you here, but yess, München is my next obligatory stop! **Jess Yi Aile Gong**, it was a short flatshare but a very enjoyable one. Thanks for those chats and cool shared times. **Marta Duran** and **Jon Barreneitxea**, my Jägargatan gang, gracias por todas las cenas compartidas y por todos los momentos de diversión callejeando por Estocolmo a cualquier hora como buenos newbees que fuimos. **Clara Kammüller**, who would have guessed that after our Utrecht time we will both end up in Stockholm and on top living in the same building? It was super awesome to have you here and to share those runs, dinners and fun events in Swedish land with you. **Maria Grazia Cozzupoli**, the first girl I met when I stepped in St Erik lab four years back, thanks for that first month that was enough to set up a very tight mutual bond. **Celia Monteagudo**, **Marta Requena** y **Sergio Campos**, gracias por las conversaciones y por todos los buenos momentos compartidos en esos meses de fría oscuridad sueca. **Luciano di Stefano**, Luchiis, por tu sencillez y por esas risas y bailoteos entre divas divinas. **Nina Kaukua**, still missing you in Stockholm, but thanks for the fun shared and for all the PhD tips. **Pedro Moutinho**, Pedriitooooo, for your positive vibe, your craziness and your cool way of seeing the world. **Tiago Braga**, Tiaginhooo, thanks for your always good vibes and your participation to any social or musical events that I have been part of. **Hara Alonso**, por tu arte y por nuestras profundas conversaciones de camino a casa después de noches intensas en Fylkingen. **Lisa Nilsson**, my choir soul mate, thanks for your charm and for all the shared fun moments in and outside the choir. **Johanna Axelsson**, **Rosario Llenas**, **Violeta de Lama**, **Ana Andermo, Sara Oppenheimer** thanks for the nice times spent together in different events and places around Stockholm. Your individual energy is uncountable. The Egipcian gang: **Karim Elgammal**, **Mahmoud Ahmed Ismail**, **Shady Mansour**, for your always great mood and awesome house parties filled up with cool people (and shisha!).

And from my around periods in Vic, Madrid, Oviedo and The Netherlands: **Maria Vila**, **Laura Plancheria**, **Jenny Caner**, **Miriam Gutiérrez**, **Dani Amado** per tots els retrobaments UVic que reviuen els moments uni i resituen les nostres arrels biotecs. **Marta Garrote**, pels bons moments dins i fora del conservatori, perquè estic segura que la teva perseverància i perspicàcia et portarà molt lluny com a metgessa. **Jane Kim**, **Marta Brandt** and **Sarah Gutkind**, the girls of the CNIO time, thanks for keeping up the friendship after almost ten years of those awesome two months in Madrid. **María Suárez**, mi Mariniiiiis, ¡Qué haría yo sin nuestras dosis! Gracias por todos los momentos compartidos y por ser como eres, porque cada vez que nuestros caminos se entrecruzan saltan chispas de la felicidad que rebosamos. **Anna Oliveras**, per la teva autenticitat i per la vocació com a científica que portes a dins. I

pels nostres moments asturinanicos entre sidres que sempre ens quedaran en el record. **Covi Huidobro**, por tu hospitalidad, generosidad y buen carácter. Tu constancia y hacer científico como doctoranda fue todo un modelo a seguir y que todavía sigo teniendo presente :)

The Zwolle team: **Olga Szczodry**, **Erica de Zan**, **David Díaz**, **Camilla Tomasetta**, **Niklas Stausberg**, for all the fun times in and outside Utrecht that were and are about to come, for our gang times with "the follow rivers" and for all the craziness that made that year a very special one. **Sandra Segura**, la meva floreta de l'Hubrecht, per tots els bons moments utrechtians i per un lligam que perdura de la mà del nostre progrés científic. **Miriam Stumpf** y **Virginia Rodríguez**, por vuestra amistad y todos los "girl's moments" en Utrecht, Leiden o Amsterdam. Miriam, gracias por tu confianza, y por tu manera de ser comprensible y abierta. Vir, gracias por tu genuidad, por las risas, por tu complicidad. Y mil gracias por mandarme ese link con una posición de PhD en medicina regenerativa ofrecida por Karolinska que marcaría los próximos cuatro años de mi vida. **Giulia Meneghello**, mi plusitaaaa, gracias por tu alegría y vitalidad que te hacen única. Gracias por todos los momentos compartidos entre couch surfers en Leiden y por todos los que vinieron después fuera de NL. Ay, ¡La de aventuras pendientes que tenemos, plusi! **Ilaria My**, my first LUMC soul mate, thanks for the hand in hand hard work shared in that noisy corridor space, and for all the awesome times we spent together out of the lab. Your stay was just for a couple of months but enough to know that our friendship will last way longer. **Cathelijne van den Berg**, Caaat, thanks for all the great times in and outside the lab in Leiden. You were my PhD referent when I was still a master student and I always valued your hard work and passion. Gracias por todas las conversaciones, helados, tapas, paseos en bici... Bedankt voor je echte vriendschap. **Klara Blom**, gracias por tu hospitalidad y por todos los pío-momentos divertidos que pasamos en casa. **Sofia Gomes**, por las risas y tu entusiasmo, ¡Y por las auroras que nos quedan! **Pelin Gül**, for your crazy energy and drive to do things, and for all our guitar moments. Gràcies **Martina Jutglar**, **Cèlia Rovira**, **Marta Mestres** and **Sandra Juárez**, les meves catalanes de Leiden i Utrecht per totes les rialles i moments compartits en els que intentàvem arreglar el món i més. Gràcies per ser com sou, perquè sou úniques i fantàstiques. **Tània Martiáñez** y **Marco Anink**, **Juan Guadix** y **Carol Rivas**, **Román González** y **Espe Muñoz**, gracias por todas esas birras y bistecs (Tània!) y por cuidar a la peque del grupo como nadie. Gracias Tània, Juan y Román por vuestra inspiración y buen ejemplo científico.

Thanks to **ALL** once again for still being part of my life challenging friendship throughout the speed of time!

I com no, els incondicionals de Menorca, de Lô: **Moni Pons** per sempre ser-hi a pesar d'estar enfora i per tots es nostrus "ara o mais". **Vane Gornés** per sa teva alegria i es teu cor obert, i perquè mai, mai ens llevin es nostrus moments de gavell. **Nere Ziarreta** y **Sara Fernández** por ser como sóis, por vuestra amistad que no pasa a pesar de los años y porque sé que si

necesito estáis ahí y sin falta. **Maria Mascaró**, per tots es bons compartits des que érem ben petites, per es teu bon fer i per s'interès que sempre has tingut sobre el que he anat fent recerca. I es **Cuxitos** meus, per tots es moments compartits cada vegada que sa vigatana, sa madrilenya, s'asturiana, s'holandesa o sa sueca d'arrel alaurenca aterrava a sa roqueta. **Lucas Carreras**, **Quim Ameller**, **Sebas Pons**, **Josep López** i **Enric Barber**, per tots es bons moments per Lô per ses festes o per Nadal, i Lucas, per totes ses posades al dia entre cafè i cafè en ses que intentam aclarir el món i ses nostres vides científiques. Gràcies **Lina Olives**, per ses xerradetes i per tot es recolzament i ànim que sempre m'has donat. I gràcies **Marga Pons**, per sa teva il·lusió cada vegada que te xerr de sa meva feina i per una amistat que creix amb els anys.

Moltes gràcies de tot cor a sa **família Petrus-Reurer**, als que hi són i als que ja no hi són, per tot es suport i per tota s'estima. Gràcies pares **Margaret** i **Tolo** i abuela **Catalina** per tot el que m'hau ensenyat i donat; i per sempre ser-hi, telèfon en mà, passi el que passi i salvant qualsevol distància. Gràcies per haver-me inculcat els valors que em fan ser com som, i també els de sa feina i de s'esforç que m'han fet arribar fins aquí. Perquè sí, en certa manera sa sort se la crea un mateix. Gràcies per haver-me deixat volar tan amunt com ses meves ales han volgut.

"Success is a journey, not a destination". And indeed, after this particular stretch, I couldn't agree more. But, undoubtedly, the journey continues.

9 REFERENCES

Abrahimi, P., Chang, W.G., Kluger, M.S., Qyang, Y., Tellides, G., Saltzman, W.M., and Pober, J.S. (2015). Efficient gene disruption in cultured primary human endothelial cells by CRISPR/Cas9. Circ Res *117*, 121-128.

Aisenbrey, S., Zhang, M., Bacher, D., Yee, J., Brunken, W.J., and Hunter, D.D. (2006). Retinal pigment epithelial cells synthesize laminins, including laminin 5, and adhere to them through alpha3- and alpha6-containing integrins. Invest Ophthalmol Vis Sci *47*, 5537-5544.

Algvere, P.V., Berglin, L., Gouras, P., and Sheng, Y. (1994). Transplantation of fetal retinal pigment epithelium in age-related macular degeneration with subfoveal neovascularization. Graefes Arch Clin Exp Ophthalmol *232*, 707-716.

Ambati, J., Ambati, B.K., Yoo, S.H., Ianchulev, S., and Adamis, A.P. (2003). Age-related macular degeneration: etiology, pathogenesis, and therapeutic strategies. Surv Ophthalmol *48*, 257-293.

Andrews, P.W., Ben-David, U., Benvenisty, N., Coffey, P., Eggan, K., Knowles, B.B., Nagy, A., Pera, M., Reubinoff, B., Rugg-Gunn, P.J., and Stacey, G.N. (2017). Assessing the Safety of Human Pluripotent Stem Cells and Their Derivatives for Clinical Applications. Stem Cell Reports *9*, 1-4.

Applebury, M.L., Antoch, M.P., Baxter, L.C., Chun, L.L., Falk, J.D., Farhangfar, F., Kage, K., Krzystolik, M.G., Lyass, L.A., and Robbins, J.T. (2000). The murine cone photoreceptor: a single cone type expresses both S and M opsins with retinal spatial patterning. Neuron *27*, 513-523.

Ballios, B.G., Cooke, M.J., Donaldson, L., Coles, B.L., Morshead, C.M., van der Kooy, D., and Shoichet, M.S. (2015). A Hyaluronan-Based Injectable Hydrogel Improves the Survival and Integration of Stem Cell Progeny following Transplantation. Stem Cell Reports *4*, 1031-1045.

Ballios, B.G., Cooke, M.J., van der Kooy, D., and Shoichet, M.S. (2010). A hydrogel-based stem cell delivery system to treat retinal degenerative diseases. Biomaterials *31*, 2555-2564.

Bartuma, H., Petrus-Reurer, S., Aronsson, M., Westman, S., Andre, H., and Kvanta, A. (2015). In Vivo Imaging of Subretinal Bleb-Induced Outer Retinal Degeneration in the Rabbit. Invest Ophthalmol Vis Sci *56*, 2423-2430.

Bharti, K., Rao, M., Hull, S.C., Stroncek, D., Brooks, B.P., Feigal, E., van Meurs, J.C., Huang, C.A., and Miller, S.S. (2014). Developing cellular therapies for retinal degenerative diseases. Invest Ophthalmol Vis Sci *55*, 1191-1202.

Bhutani, K., Nazor, K.L., Williams, R., Tran, H., Dai, H., Dzakula, Z., Cho, E.H., Pang, A.W., Rao, M., Cao, H., Schork, N.J., and Loring, J.F. (2016). Whole-genome mutational burden analysis of three pluripotency induction methods. Nat Commun *7*, 10536.

Bhutto, I.A., Ogura, S., Baldeosingh, R., McLeod, D.S., Lutty, G.A., and Edwards, M.M. (2018). An Acute Injury Model for the Phenotypic Characteristics of Geographic Atrophy. Invest Ophthalmol Vis Sci *59*, AMD143-AMD151.

Blanch, R.J., Ahmed, Z., Berry, M., Scott, R.A., and Logan, A. (2012). Animal models of retinal injury. Invest Ophthalmol Vis Sci *53*, 2913-2920.

Bottino, C., Castriconi, R., Pende, D., Rivera, P., Nanni, M., Carnemolla, B., Cantoni, C., Grassi, J., Marcenaro, S., Reymond, N., Vitale, M., Moretta, L., Lopez, M., and Moretta, A. (2003). Identification of PVR (CD155) and Nectin-2 (CD112) as cell surface ligands for the human DNAM-1 (CD226) activating molecule. J Exp Med *198*, 557-567.

Bouma, M.J., van Iterson, M., Janssen, B., Mummery, C.L., Salvatori, D.C.F., and Freund, C. (2017). Differentiation-Defective Human Induced Pluripotent Stem Cells Reveal Strengths and Limitations of the Teratoma Assay and In Vitro Pluripotency Assays. Stem Cell Reports *8*, 1340-1353.

Bradley, J.A., Bolton, E.M., and Pedersen, R.A. (2002). Stem cell medicine encounters the immune system. Nat Rev Immunol *2*, 859-871.

Buchholz, D.E., Hikita, S.T., Rowland, T.J., Friedrich, A.M., Hinman, C.R., Johnson, L.V., and Clegg, D.O. (2009). Derivation of functional retinal pigmented epithelium from induced pluripotent stem cells. Stem Cells *27*, 2427-2434.

Buchholz, D.E., Pennington, B.O., Croze, R.H., Hinman, C.R., Coffey, P.J., and Clegg, D.O. (2013). Rapid and efficient directed differentiation of human pluripotent stem cells into retinal pigmented epithelium. Stem Cells Transl Med *2*, 384-393.

Burnett, J.C., Rossi, J.J., and Tiemann, K. (2011). Current progress of siRNA/shRNA therapeutics in clinical trials. Biotechnol J *6*, 1130-1146.

Cai, S., Hou, J., Fujino, M., Zhang, Q., Ichimaru, N., Takahara, S., Araki, R., Lu, L., Chen, J.M., Zhuang, J., Zhu, P., and Li, X.K. (2017). iPSC-Derived Regulatory Dendritic Cells Inhibit Allograft Rejection by Generating Alloantigen-Specific Regulatory T Cells. Stem Cell Reports *8*, 1174-1189.

Campbell, M., and Humphries, P. (2012). The blood-retina barrier: tight junctions and barrier modulation. Adv Exp Med Biol *763*, 70-84.

Carido, M., Zhu, Y., Postel, K., Benkner, B., Cimalla, P., Karl, M.O., Kurth, T., Paquet-Durand, F., Koch, E., Munch, T.A., Tanaka, E.M., and Ader, M. (2014). Characterization of a mouse model with complete RPE loss and its use for RPE cell transplantation. Invest Ophthalmol Vis Sci *55*, 5431-5444.

Carr, A.J., Vugler, A., Lawrence, J., Chen, L.L., Ahmado, A., Chen, F.K., Semo, M., Gias, C., da Cruz, L., Moore, H.D., Walsh, J., and Coffey, P.J. (2009). Molecular characterization and functional analysis of phagocytosis by human embryonic stem cell-derived RPE cells using a novel human retinal assay. Mol Vis *15*, 283-295.

Cerboni, C., Fionda, C., Soriani, A., Zingoni, A., Doria, M., Cippitelli, M., and Santoni, A. (2014). The DNA Damage Response: A Common Pathway in the Regulation of NKG2D and DNAM-1 Ligand Expression in Normal, Infected, and Cancer Cells. Front Immunol *4*, 508.

Chan, C.J., Martinet, L., Gilfillan, S., Souza-Fonseca-Guimaraes, F., Chow, M.T., Town, L., Ritchie, D.S., Colonna, M., Andrews, D.M., and Smyth, M.J. (2014). The receptors CD96 and CD226 oppose each other in the regulation of natural killer cell functions. Nat Immunol *15*, 431-438.

Chen, H., Li, Y., Lin, X., Cui, D., Cui, C., Li, H., and Xiao, L. (2015). Functional disruption of human leukocyte antigen II in human embryonic stem cell. Biol Res *48*, 59.

Chichagova, V., Hallam, D., Collin, J., Zerti, D., Dorgau, B., Felemban, M., Lako, M., and Steel, D.H. (2018). Cellular regeneration strategies for macular degeneration: past, present and future. Eye (Lond) *32*, 946-971.

Cho, M.S., Kim, S.J., Ku, S.Y., Park, J.H., Lee, H., Yoo, D.H., Park, U.C., Song, S.A., Choi, Y.M., and Yu, H.G. (2012). Generation of retinal pigment epithelial cells from human embryonic stem cell-derived spherical neural masses. Stem Cell Res *9*, 101-109.

Choudhary, P., Booth, H., Gutteridge, A., Surmacz, B., Louca, I., Steer, J., Kerby, J., and Whiting, P.J. (2017). Directing Differentiation of Pluripotent Stem Cells Toward Retinal Pigment Epithelium Lineage. STEM CELLS Translational Medicine *6*, 490-501.

Choudhary, P., and Whiting, P.J. (2016). A strategy to ensure safety of stem cell-derived retinal pigment epithelium cells. Stem Cell Res Ther *7*, 127.

Chowers, G., Cohen, M., Marks-Ohana, D., Stika, S., Eijzenberg, A., Banin, E., and Obolensky, A. (2017). Course of Sodium Iodate-Induced Retinal Degeneration in Albino and Pigmented Mice. Invest Ophthalmol Vis Sci *58*, 2239-2249.

Coles, B.L., Angenieux, B., Inoue, T., Del Rio-Tsonis, K., Spence, J.R., McInnes, R.R., Arsenijevic, Y., and van der Kooy, D. (2004). Facile isolation and the characterization of human retinal stem cells. Proc Natl Acad Sci U S A *101*, 15772-15777.

Cowey, A., and Franzini, C. (1979). The retinal origin of uncrossed optic nerve fibres in rats and their role in visual discrimination. Exp Brain Res *35*, 443-455.

Curcio, C.A.J., M. (2013). Structure, Function, and Pathology of Bruch's Membrane. Anatomy and Physiology *Section 1. Chapter 20*, 465-481.

D'Cruz, P.M., Yasumura, D., Weir, J., Matthes, M.T., Abderrahim, H., LaVail, M.M., and Vollrath, D. (2000). Mutation of the receptor tyrosine kinase gene Mertk in the retinal dystrophic RCS rat. Hum Mol Genet *9*, 645-651.

da Cruz, L., Chen, F.K., Ahmado, A., Greenwood, J., and Coffey, P. (2007). RPE transplantation and its role in retinal disease. Prog Retin Eye Res *26*, 598-635.

da Cruz, L., Fynes, K., Georgiadis, O., Kerby, J., Luo, Y.H., Ahmado, A., Vernon, A., Daniels, J.T., Nommiste, B., Hasan, S.M., Gooljar, S.B., Carr, A.F., Vugler, A., Ramsden, C.M., Bictash, M., Fenster, M., Steer, J., Harbinson, T., Wilbrey, A., Tufail, A., Feng, G., Whitlock, M., Robson, A.G., Holder, G.E., Sagoo, M.S., Loudon, P.T., Whiting, P., and Coffey, P.J. (2018). Phase 1 clinical study of an embryonic stem cell-derived retinal pigment epithelium patch in age-related macular degeneration. Nat Biotechnol *36*, 328-337.

Davis, R.J., Alam, N.M., Zhao, C., Muller, C., Saini, J.S., Blenkinsop, T.A., Mazzoni, F., Campbell, M., Borden, S.M., Charniga, C.J., Lederman, P.L., Aguilar, V., Naimark, M., Fiske, M., Boles, N., Temple, S., Finnemann, S.C., Prusky, G.T., and Stern, J.H. (2017). The Developmental Stage of Adult Human Stem Cell-Derived Retinal Pigment Epithelium Cells Influences Transplant Efficacy for Vision Rescue. Stem Cell Reports *9*, 42-49.

Del Priore, L.V., Ishida, O., Johnson, E.W., Sheng, Y., Jacoby, D.B., Geng, L., Tezel, T.H., and Kaplan, H.J. (2003). Triple immune suppression increases short-term survival of porcine fetal retinal pigment epithelium xenografts. Invest Ophthalmol Vis Sci *44*, 4044-4053.

Delori, F.C., Dorey, C.K., Staurenghi, G., Arend, O., Goger, D.G., and Weiter, J.J. (1995). In vivo fluorescence of the ocular fundus exhibits retinal pigment epithelium lipofuscin characteristics. Invest Ophthalmol Vis Sci *36*, 718-729.

Diniz, B., Thomas, P., Thomas, B., Ribeiro, R., Hu, Y., Brant, R., Ahuja, A., Zhu, D., Liu, L., Koss, M., Maia, M., Chader, G., Hinton, D.R., and Humayun, M.S. (2013). Subretinal implantation of retinal pigment epithelial cells derived from human embryonic stem cells: improved survival when implanted as a monolayer. Invest Ophthalmol Vis Sci *54*, 5087-5096.

Dressel, R., Nolte, J., Elsner, L., Novota, P., Guan, K., Streckfuss-Bomeke, K., Hasenfuss, G., Jaenisch, R., and Engel, W. (2010). Pluripotent stem cells are highly susceptible targets for syngeneic, allogeneic, and xenogeneic natural killer cells. FASEB J *24*, 2164-2177.

Drukker, M. (2008). StemBook [Internet]. Immunological considerations for cell therapy using human embryonic stem cell derivatives (Cambridge, MA, USA: Harvard Stem Cell Institute).

Elsner, A.E., Burns, S.A., Weiter, J.J., and Delori, F.C. (1996). Infrared imaging of sub-retinal structures in the human ocular fundus. Vision Res *36*, 191-205.

Famiglietti, E.V., and Sharpe, S.J. (1995). Regional topography of rod and immunocytochemically characterized "blue" and "green" cone photoreceptors in rabbit retina. Vis Neurosci *12*, 1151-1175.

Ferris, F.L., 3rd, Fine, S.L., and Hyman, L. (1984). Age-related macular degeneration and blindness due to neovascular maculopathy. Arch Ophthalmol *102*, 1640-1642.

Fletcher, E.L., Jobling, A.I., Greferath, U., Mills, S.A., Waugh, M., Ho, T., de Iongh, R.U., Phipps, J.A., and Vessey, K.A. (2014). Studying age-related macular degeneration using animal models. Optom Vis Sci *91*, 878-886.

Forte, R., Querques, G., Querques, L., Massamba, N., Le Tien, V., and Souied, E.H. (2012). Multimodal imaging of dry age-related macular degeneration. Acta Ophthalmol *90*, e281-287.

Fox, I.J., Daley, G.Q., Goldman, S.A., Huard, J., Kamp, T.J., and Trucco, M. (2014). Stem cell therapy. Use of differentiated pluripotent stem cells as replacement therapy for treating disease. Science *345*, 1247391.

Fuhrmann, S. (2010). Eye morphogenesis and patterning of the optic vesicle. Curr Top Dev Biol *93*, 61-84.

Gamm, D.M., Wang, S., Lu, B., Girman, S., Holmes, T., Bischoff, N., Shearer, R.L., Sauve, Y., Capowski, E., Svendsen, C.N., and Lund, R.D. (2007). Protection of visual functions by human neural progenitors in a rat model of retinal disease. PLoS One *2*, e338.

Gehrs, K.M., Anderson, D.H., Johnson, L.V., and Hageman, G.S. (2006). Age-related macular degeneration--emerging pathogenetic and therapeutic concepts. Ann Med *38*, 450-471.

Georgiev, H., Ravens, I., Papadogianni, G., and Bernhardt, G. (2018). Coming of Age: CD96 Emerges as Modulator of Immune Responses. Front Immunol *9*, 1072.

Gerke, C.G., Hao, Y., and Wong, F. (1995). Topography of rods and cones in the retina of the domestic pig. Hong Kong Med J *1*, 302-308.

Gobel, A.P., Fleckenstein, M., Schmitz-Valckenberg, S., Brinkmann, C.K., and Holz, F.G. (2011). Imaging geographic atrophy in age-related macular degeneration. Ophthalmologica *226*, 182-190.

Gornalusse, G.G., Hirata, R.K., Funk, S.E., Riolobos, L., Lopes, V.S., Manske, G., Prunkard, D., Colunga, A.G., Hanafi, L.A., Clegg, D.O., Turtle, C., and Russell, D.W. (2017). HLA-E-expressing pluripotent stem cells escape allogeneic responses and lysis by NK cells. Nat Biotechnol *35*, 765-772.

Grignolo, A., Orzalesi, N., and Calabria, G.A. (1966). Studies on the fine structure and the rhodopsin cycle of the rabbit retina in experimental degeneration induced by sodium iodate. Exp Eye Res *5*, 86-97.

Hanus, J., Anderson, C., Sarraf, D., Ma, J., and Wang, S. (2016). Retinal pigment epithelial cell necroptosis in response to sodium iodate. Cell Death Discov *2*, 16054.

Haruta, M., Sasai, Y., Kawasaki, H., Amemiya, K., Ooto, S., Kitada, M., Suemori, H., Nakatsuji, N., Ide, C., Honda, Y., and Takahashi, M. (2004). In vitro and in vivo characterization of pigment epithelial cells differentiated from primate embryonic stem cells. Invest Ophthalmol Vis Sci *45*, 1020-1025.

Hayashi, A., Majji, A.B., Fujioka, S., Kim, H.C., Fukushima, I., and de Juan, E., Jr. (1999). Surgically induced degeneration and regeneration of the choriocapillaris in rabbit. Graefes Arch Clin Exp Ophthalmol *237*, 668-677.

Heavner, W., and Pevny, L. (2012). Eye development and retinogenesis. Cold Spring Harb Perspect Biol *4*.

Heller, J.P., and Martin, K.R. (2014). Enhancing RPE Cell-Based Therapy Outcomes for AMD: The Role of Bruch's Membrane. Transl Vis Sci Technol *3*, 11.

Hippen, K.L., Riley, J.L., June, C.H., and Blazar, B.R. (2011). Clinical perspectives for regulatory T cells in transplantation tolerance. Semin Immunol *23*, 462-468.

Hirsch, L., Nazari, H., Sreekumar, P.G., Kannan, R., Dustin, L., Zhu, D., Barron, E., and Hinton, D.R. (2015). TGF-beta2 secretion from RPE decreases with polarization and becomes apically oriented. Cytokine *71*, 394-396.

Holz, F.G., Bellmann, C., Margaritidis, M., Schutt, F., Otto, T.P., and Volcker, H.E. (1999). Patterns of increased in vivo fundus autofluorescence in the junctional zone of geographic atrophy of the retinal pigment epithelium associated with age-related macular degeneration. Graefes Arch Clin Exp Ophthalmol *237*, 145-152.

Holz, F.G., Steinberg, J.S., Gobel, A., Fleckenstein, M., and Schmitz-Valckenberg, S. (2015). Fundus autofluorescence imaging in dry AMD: 2014 Jules Gonin lecture of the Retina Research Foundation. Graefes Arch Clin Exp Ophthalmol *253*, 7-16.

Hongisto, H., Ilmarinen, T., Vattulainen, M., Mikhailova, A., and Skottman, H. (2017). Xeno- and feeder-free differentiation of human pluripotent stem cells to two distinct ocular epithelial cell types using simple modifications of one method. Stem Cell Res Ther *8*, 291.

Hu, Q., Friedrich, A.M., Johnson, L.V., and Clegg, D.O. (2010). Memory in induced pluripotent stem cells: reprogrammed human retinal-pigmented epithelial cells show tendency for spontaneous redifferentiation. Stem Cells *28*, 1981-1991.

Hughes, A. (1972). A schematic eye for the rabbit. Vision Res *12*, 123-138.

Huo, J.S., Baylin, S.B., and Zambidis, E.T. (2014). Cancer-like epigenetic derangements of human pluripotent stem cells and their impact on applications in regeneration and repair. Curr Opin Genet Dev *28*, 43-49.

Idelson, M., Alper, R., Obolensky, A., Ben-Shushan, E., Hemo, I., Yachimovich-Cohen, N., Khaner, H., Smith, Y., Wiser, O., Gropp, M., Cohen, M.A., Even-Ram, S., Berman-Zaken, Y., Matzrafi, L., Rechavi, G., Banin, E., and Reubinoff, B. (2009). Directed differentiation of human embryonic stem cells into functional retinal pigment epithelium cells. Cell Stem Cell *5*, 396-408.

Idelson, M., Alper, R., Obolensky, A., Yachimovich-Cohen, N., Rachmilewitz, J., Ejzenberg, A., Beider, E., Banin, E., and Reubinoff, B. (2018). Immunological Properties of Human Embryonic Stem Cell-Derived Retinal Pigment Epithelial Cells. Stem Cell Reports *11*, 681-695.

Ilmarinen, T., Hiidenmaa, H., Koobi, P., Nymark, S., Sorkio, A., Wang, J.H., Stanzel, B.V., Thieltges, F., Alajuuma, P., Oksala, O., Kataja, M., Uusitalo, H., and Skottman, H. (2015). Ultrathin Polyimide Membrane as Cell Carrier for Subretinal Transplantation of Human Embryonic Stem Cell Derived Retinal Pigment Epithelium. PLoS One *10*, e0143669.

Imamura, Y., Noda, S., Hashizume, K., Shinoda, K., Yamaguchi, M., Uchiyama, S., Shimizu, T., Mizushima, Y., Shirasawa, T., and Tsubota, K. (2006). Drusen, choroidal neovascularization, and retinal pigment epithelium dysfunction in SOD1-deficient mice: a model of age-related macular degeneration. Proc Natl Acad Sci U S A *103*, 11282-11287.

International Stem Cell, I. (2018). Assessment of established techniques to determine developmental and malignant potential of human pluripotent stem cells. Nat Commun *9*, 1925.

Jin, Z.B., Okamoto, S., Osakada, F., Homma, K., Assawachananont, J., Hirami, Y., Iwata, T., and Takahashi, M. (2011). Modeling retinal degeneration using patient-specific induced pluripotent stem cells. PLoS One *6*, e17084.

Joe, A.W., and Gregory-Evans, K. (2010). Mesenchymal stem cells and potential applications in treating ocular disease. Curr Eye Res *35*, 941-952.

Justilien, V., Pang, J.J., Renganathan, K., Zhan, X., Crabb, J.W., Kim, S.R., Sparrow, J.R., Hauswirth, W.W., and Lewin, A.S. (2007). SOD2 knockdown mouse model of early AMD. Invest Ophthalmol Vis Sci *48*, 4407-4420.

Kamao, H., Mandai, M., Okamoto, S., Sakai, N., Suga, A., Sugita, S., Kiryu, J., and Takahashi, M. (2014). Characterization of human induced pluripotent stem cell-derived retinal pigment epithelium cell sheets aiming for clinical application. Stem Cell Reports *2*, 205-218.

Kaneko, H., Dridi, S., Tarallo, V., Gelfand, B.D., Fowler, B.J., Cho, W.G., Kleinman, M.E., Ponicsan, S.L., Hauswirth, W.W., Chiodo, V.A., Kariko, K., Yoo, J.W., Lee, D.K., Hadziahmetovic, M., Song, Y., Misra, S., Chaudhuri, G., Buaas, F.W., Braun, R.E., Hinton, D.R., Zhang, Q., Grossniklaus, H.E., Provis, J.M., Madigan, M.C., Milam,

A.H., Justice, N.L., Albuquerque, R.J., Blandford, A.D., Bogdanovich, S., Hirano, Y., Witta, J., Fuchs, E., Littman, D.R., Ambati, B.K., Rudin, C.M., Chong, M.M., Provost, P., Kugel, J.F., Goodrich, J.A., Dunaief, J.L., Baffi, J.Z., and Ambati, J. (2011). DICER1 deficit induces Alu RNA toxicity in age-related macular degeneration. Nature *471*, 325-330.

Kanemura, H., Go, M.J., Shikamura, M., Nishishita, N., Sakai, N., Kamao, H., Mandai, M., Morinaga, C., Takahashi, M., and Kawamata, S. (2014). Tumorigenicity studies of induced pluripotent stem cell (iPSC)-derived retinal pigment epithelium (RPE) for the treatment of age-related macular degeneration. PLoS One *9*, e85336.

Kashani, A.H., Lebkowski, J.S., Rahhal, F.M., Avery, R.L., Salehi-Had, H., Dang, W., Lin, C.M., Mitra, D., Zhu, D., Thomas, B.B., Hikita, S.T., Pennington, B.O., Johnson, L.V., Clegg, D.O., Hinton, D.R., and Humayun, M.S. (2018). A bioengineered retinal pigment epithelial monolayer for advanced, dry age-related macular degeneration. Sci Transl Med *10*.

Kawasaki, H., Suemori, H., Mizuseki, K., Watanabe, K., Urano, F., Ichinose, H., Haruta, M., Takahashi, M., Yoshikawa, K., Nishikawa, S., Nakatsuji, N., and Sasai, Y. (2002). Generation of dopaminergic neurons and pigmented epithelia from primate ES cells by stromal cell-derived inducing activity. Proc Natl Acad Sci U S A *99*, 1580-1585.

Kearns, V., Mistry, A., Mason, S., Krishna, Y., Sheridan, C., Short, R., and Williams, R.L. (2012). Plasma polymer coatings to aid retinal pigment epithelial growth for transplantation in the treatment of age related macular degeneration. J Mater Sci Mater Med *23*, 2013-2021.

Kiilgaard, J.F., Prause, J.U., Prause, M., Scherfig, E., Nissen, M.H., and la Cour, M. (2007). Subretinal posterior pole injury induces selective proliferation of RPE cells in the periphery in in vivo studies in pigs. Invest Ophthalmol Vis Sci *48*, 355-360.

Klimanskaya, I., Hipp, J., Rezai, K.A., West, M., Atala, A., and Lanza, R. (2004). Derivation and comparative assessment of retinal pigment epithelium from human embryonic stem cells using transcriptomics. Cloning Stem Cells *6*, 217-245.

Kokkinaki, M., Sahibzada, N., and Golestaneh, N. (2011). Human induced pluripotent stem-derived retinal pigment epithelium (RPE) cells exhibit ion transport, membrane potential, polarized vascular endothelial growth factor secretion, and gene expression pattern similar to native RPE. Stem Cells *29*, 825-835.

Kruse, V., Hamann, C., Monecke, S., Cyganek, L., Elsner, L., Hubscher, D., Walter, L., Streckfuss-Bomeke, K., Guan, K., and Dressel, R. (2015). Human Induced Pluripotent Stem Cells Are Targets for Allogeneic and Autologous Natural Killer (NK) Cells and Killing Is Partly Mediated by the Activating NK Receptor DNAM-1. PLoS One *10*, e0125544.

Lane, A., Philip, L.R., Ruban, L., Fynes, K., Smart, M., Carr, A., Mason, C., and Coffey, P. (2014). Engineering efficient retinal pigment epithelium differentiation from human pluripotent stem cells. Stem Cells Transl Med *3*, 1295-1304.

Leach, L.L., and Clegg, D.O. (2015). Concise Review: Making Stem Cells Retinal: Methods for Deriving Retinal Pigment Epithelium and Implications for Patients With Ocular Disease. Stem Cells *33*, 2363-2373.

Lechler, R.I., Sykes, M., Thomson, A.W., and Turka, L.A. (2005). Organ transplantation--how much of the promise has been realized? Nat Med *11*, 605-613.

Leonard, D.S., Zhang, X.G., Panozzo, G., Sugino, I.K., and Zarbin, M.A. (1997). Clinicopathologic correlation of localized retinal pigment epithelium debridement. Invest Ophthalmol Vis Sci *38*, 1094-1109.

Levin, S.D., Taft, D.W., Brandt, C.S., Bucher, C., Howard, E.D., Chadwick, E.M., Johnston, J., Hammond, A., Bontadelli, K., Ardourel, D., Hebb, L., Wolf, A., Bukowski, T.R., Rixon, M.W., Kuijper, J.L., Ostrander, C.D., West, J.W., Bilsborough, J., Fox, B., Gao, Z., Xu, W., Ramsdell, F., Blazar, B.R., and Lewis, K.E. (2011). Vstm3 is a member of the CD28 family and an important modulator of T-cell function. Eur J Immunol *41*, 902-915.

Liao, J.L., Yu, J., Huang, K., Hu, J., Diemer, T., Ma, Z., Dvash, T., Yang, X.J., Travis, G.H., Williams, D.S., Bok, D., and Fan, G. (2010). Molecular signature of primary retinal pigment epithelium and stem-cell-derived RPE cells. Hum Mol Genet *19*, 4229-4238.

Lu, P., Chen, J., He, L., Ren, J., Chen, H., Rao, L., Zhuang, Q., Li, H., Li, L., Bao, L., He, J., Zhang, W., Zhu, F., Cui, C., and Xiao, L. (2013). Generating hypoimmunogenic human embryonic stem cells by the disruption of beta 2-microglobulin. Stem Cell Rev *9*, 806-813.

Luhmann, U.F., Lange, C.A., Robbie, S., Munro, P.M., Cowing, J.A., Armer, H.E., Luong, V., Carvalho, L.S., MacLaren, R.E., Fitzke, F.W., Bainbridge, J.W., and Ali, R.R. (2012). Differential modulation of retinal degeneration by Ccl2 and Cx3cr1 chemokine signalling. PLoS One *7*, e35551.

Lund, R.D., Adamson, P., Sauve, Y., Keegan, D.J., Girman, S.V., Wang, S., Winton, H., Kanuga, N., Kwan, A.S., Beauchene, L., Zerbib, A., Hetherington, L., Couraud, P.O., Coffey, P., and Greenwood, J. (2001a). Subretinal transplantation of genetically modified human cell lines attenuates loss of visual function in dystrophic rats. Proc Natl Acad Sci U S A *98*, 9942-9947.

Lund, R.D., Kwan, A.S., Keegan, D.J., Sauve, Y., Coffey, P.J., and Lawrence, J.M. (2001b). Cell transplantation as a treatment for retinal disease. Prog Retin Eye Res *20*, 415-449.

Lund, R.D., Wang, S., Klimanskaya, I., Holmes, T., Ramos-Kelsey, R., Lu, B., Girman, S., Bischoff, N., Sauve, Y., and Lanza, R. (2006). Human embryonic stem cell-derived cells rescue visual function in dystrophic RCS rats. Cloning Stem Cells *8*, 189-199.

Machalinska, A., Lubinski, W., Klos, P., Kawa, M., Baumert, B., Penkala, K., Grzegrzolka, R., Karczewicz, D., Wiszniewska, B., and Machalinski, B. (2010). Sodium iodate selectively injuries the posterior pole of the retina in a dose-dependent manner: morphological and electrophysiological study. Neurochem Res *35*, 1819-1827.

Mandai, M., Watanabe, A., Kurimoto, Y., Hirami, Y., Morinaga, C., Daimon, T., Fujihara, M., Akimaru, H., Sakai, N., Shibata, Y., Terada, M., Nomiya, Y., Tanishima, S., Nakamura, M., Kamao, H., Sugita, S., Onishi, A., Ito, T., Fujita, K., Kawamata, S., Go, M.J., Shinohara, C., Hata, K.I., Sawada, M., Yamamoto, M., Ohta, S., Ohara, Y., Yoshida, K., Kuwahara, J., Kitano, Y., Amano, N., Umekage, M., Kitaoka, F., Tanaka, A., Okada, C., Takasu, N., Ogawa, S., Yamanaka, S., and Takahashi, M. (2017). Autologous Induced Stem-Cell-Derived Retinal Cells for Macular Degeneration. N Engl J Med *376*, 1038-1046.

Mannu, G.S. (2014). Retinal phototransduction. Neurosciences (Riyadh) *19*, 275-280.

Maruotti, J., Sripathi, S.R., Bharti, K., Fuller, J., Wahlin, K.J., Ranganathan, V., Sluch, V.M., Berlinicke, C.A., Davis, J., Kim, C., Zhao, L., Wan, J., Qian, J., Corneo, B., Temple,

S., Dubey, R., Olenyuk, B.Z., Bhutto, I., Lutty, G.A., and Zack, D.J. (2015). Small-molecule-directed, efficient generation of retinal pigment epithelium from human pluripotent stem cells. Proc Natl Acad Sci U S A *112*, 10950-10955.

Maruotti, J., Wahlin, K., Gorrell, D., Bhutto, I., Lutty, G., and Zack, D.J. (2013). A simple and scalable process for the differentiation of retinal pigment epithelium from human pluripotent stem cells. Stem Cells Transl Med *2*, 341-354.

Mones, J., Leiva, M., Pena, T., Martinez, G., Biarnes, M., Garcia, M., Serrano, A., and Fernandez, E. (2016). A Swine Model of Selective Geographic Atrophy of Outer Retinal Layers Mimicking Atrophic AMD: A Phase I Escalating Dose of Subretinal Sodium Iodate. Invest Ophthalmol Vis Sci *57*, 3974-3983.

Mooney, I., and Lamotte, J. (2010). Emerging options for the management of age-related macular degeneration with stem cells. Stem Cells Cloning *4*, 1-10.

Murphy, S.P., Porrett, P.M., and Turka, L.A. (2011). Innate immunity in transplant tolerance and rejection. Immunol Rev *241*, 39-48.

Nakajima, F., Tokunaga, K., and Nakatsuji, N. (2007). Human leukocyte antigen matching estimations in a hypothetical bank of human embryonic stem cell lines in the Japanese population for use in cell transplantation therapy. Stem Cells *25*, 983-985.

Nazari, H., Zhang, L., Zhu, D., Chader, G.J., Falabella, P., Stefanini, F., Rowland, T., Clegg, D.O., Kashani, A.H., Hinton, D.R., and Humayun, M.S. (2015). Stem cell based therapies for age-related macular degeneration: The promises and the challenges. Prog Retin Eye Res *48*, 1-39.

Nork, T.M., Murphy, C.J., Kim, C.B., Ver Hoeve, J.N., Rasmussen, C.A., Miller, P.E., Wabers, H.D., Neider, M.W., Dubielzig, R.R., McCulloh, R.J., and Christian, B.J. (2012). Functional and anatomic consequences of subretinal dosing in the cynomolgus macaque. Arch Ophthalmol *130*, 65-75.

Osakada, F., Ikeda, H., Sasai, Y., and Takahashi, M. (2009a). Stepwise differentiation of pluripotent stem cells into retinal cells. Nat Protoc *4*, 811-824.

Osakada, F., Jin, Z.B., Hirami, Y., Ikeda, H., Danjyo, T., Watanabe, K., Sasai, Y., and Takahashi, M. (2009b). In vitro differentiation of retinal cells from human pluripotent stem cells by small-molecule induction. J Cell Sci *122*, 3169-3179.

Parinot, C., Rieu, Q., Chatagnon, J., Finnemann, S.C., and Nandrot, E.F. (2014). Large-scale purification of porcine or bovine photoreceptor outer segments for phagocytosis assays on retinal pigment epithelial cells. J Vis Exp.

Pasquet, L., Joffre, O., Santolaria, T., and van Meerwijk, J.P. (2011). Hematopoietic chimerism and transplantation tolerance: a role for regulatory T cells. Front Immunol *2*, 80.

Pennesi, M.E., Neuringer, M., and Courtney, R.J. (2012). Animal models of age related macular degeneration. Mol Aspects Med *33*, 487-509.

Pennington, B.O., Clegg, D.O., Melkoumian, Z.K., and Hikita, S.T. (2015). Defined culture of human embryonic stem cells and xeno-free derivation of retinal pigmented epithelial cells on a novel, synthetic substrate. Stem Cells Transl Med *4*, 165-177.

Phillips, S.J., Sadda, S.R., Tso, M.O., Humayan, M.S., de Juan, E., Jr., and Binder, S. (2003). Autologous transplantation of retinal pigment epithelium after mechanical debridement of Bruch's membrane. Curr Eye Res *26*, 81-88.

Pinilla, I., Cuenca, N., Martinez-Navarrete, G., Lund, R.D., and Sauve, Y. (2009). Intraretinal processing following photoreceptor rescue by non-retinal cells. Vision Res *49*, 2067-2077.

Plaza Reyes, A., Petrus-Reurer, S., Antonsson, L., Stenfelt, S., Bartuma, H., Panula, S., Mader, T., Douagi, I., Andre, H., Hovatta, O., Lanner, F., and Kvanta, A. (2016). Xeno-Free and Defined Human Embryonic Stem Cell-Derived Retinal Pigment Epithelial Cells Functionally Integrate in a Large-Eyed Preclinical Model. Stem Cell Reports *6*, 9-17.

Prince, J.H. (1964). The Rabbit in Eye Research (Springfield, IL: Charles Thomas).

Purves, D., G.J, A., Fitzpatrick, D., Hall, W.H., LaMantia, A.S., and McNamara, J.O. (2004). Neuroscience. 3rd Edition. (Sinauer Associates. Sunderland, Massachusetts, USA).

Radtke, N.D., Aramant, R.B., Petry, H.M., Green, P.T., Pidwell, D.J., and Seiler, M.J. (2008). Vision improvement in retinal degeneration patients by implantation of retina together with retinal pigment epithelium. Am J Ophthalmol *146*, 172-182.

Remtulla, S., and Hallett, P.E. (1985). A schematic eye for the mouse, and comparisons with the rat. Vision Res *25*, 21-31.

Riolobos, L., Hirata, R.K., Turtle, C.J., Wang, P.R., Gornalusse, G.G., Zavajlevski, M., Riddell, S.R., and Russell, D.W. (2013). HLA engineering of human pluripotent stem cells. Mol Ther *21*, 1232-1241.

Rodin, S., Antonsson, L., Hovatta, O., and Tryggvason, K. (2014a). Monolayer culturing and cloning of human pluripotent stem cells on laminin-521-based matrices under xeno-free and chemically defined conditions. Nat Protoc *9*, 2354-2368.

Rodin, S., Antonsson, L., Niaudet, C., Simonson, O.E., Salmela, E., Hansson, E.M., Domogatskaya, A., Xiao, Z., Damdimopoulou, P., Sheikhi, M., Inzunza, J., Nilsson, A.S., Baker, D., Kuiper, R., Sun, Y., Blennow, E., Nordenskjold, M., Grinnemo, K.H., Kere, J., Betsholtz, C., Hovatta, O., and Tryggvason, K. (2014b). Clonal culturing of human embryonic stem cells on laminin-521/E-cadherin matrix in defined and xeno-free environment. Nat Commun *5*, 3195.

Rowland, T.J., Blaschke, A.J., Buchholz, D.E., Hikita, S.T., Johnson, L.V., and Clegg, D.O. (2013). Differentiation of human pluripotent stem cells to retinal pigmented epithelium in defined conditions using purified extracellular matrix proteins. J Tissue Eng Regen Med *7*, 642-653.

Sakaguchi, S., Yamaguchi, T., Nomura, T., and Ono, M. (2008). Regulatory T cells and immune tolerance. Cell *133*, 775-787.

Schwartz, S.D., Hubschman, J.P., Heilwell, G., Franco-Cardenas, V., Pan, C.K., Ostrick, R.M., Mickunas, E., Gay, R., Klimanskaya, I., and Lanza, R. (2012). Embryonic stem cell trials for macular degeneration: a preliminary report. Lancet *379*, 713-720.

Schwartz, S.D., Regillo, C.D., Lam, B.L., Eliott, D., Rosenfeld, P.J., Gregori, N.Z., Hubschman, J.P., Davis, J.L., Heilwell, G., Spirn, M., Maguire, J., Gay, R., Bateman, J., Ostrick, R.M., Morris, D., Vincent, M., Anglade, E., Del Priore, L.V., and Lanza, R. (2015). Human embryonic stem cell-derived retinal pigment epithelium in patients

with age-related macular degeneration and Stargardt's macular dystrophy: follow-up of two open-label phase 1/2 studies. Lancet *385*, 509-516.

Schwartz, S.D., Tan, G., Hosseini, H., and Nagiel, A. (2016). Subretinal Transplantation of Embryonic Stem Cell-Derived Retinal Pigment Epithelium for the Treatment of Macular Degeneration: An Assessment at 4 Years. Invest Ophthalmol Vis Sci *57*, ORSFc1-9.

Sobrin, L., and Seddon, J.M. (2014). Nature and nurture- genes and environment- predict onset and progression of macular degeneration. Prog Retin Eye Res *40*, 1-15.

Song, W.K., Park, K.M., Kim, H.J., Lee, J.H., Choi, J., Chong, S.Y., Shim, S.H., Del Priore, L.V., and Lanza, R. (2015). Treatment of macular degeneration using embryonic stem cell-derived retinal pigment epithelium: preliminary results in Asian patients. Stem Cell Reports *4*, 860-872.

Stanzel, B.V., Liu, Z., Somboonthanakij, S., Wongsawad, W., Brinken, R., Eter, N., Corneo, B., Holz, F.G., Temple, S., Stern, J.H., and Blenkinsop, T.A. (2014). Human RPE stem cells grown into polarized RPE monolayers on a polyester matrix are maintained after grafting into rabbit subretinal space. Stem Cell Reports *2*, 64-77.

Stengel, K.F., Harden-Bowles, K., Yu, X., Rouge, L., Yin, J., Comps-Agrar, L., Wiesmann, C., Bazan, J.F., Eaton, D.L., and Grogan, J.L. (2012). Structure of TIGIT immunoreceptor bound to poliovirus receptor reveals a cell-cell adhesion and signaling mechanism that requires cis-trans receptor clustering. Proc Natl Acad Sci U S A *109*, 5399-5404.

Strauss, O. (2005). Introduction, I. The Retinal Pigment Epithelium in Visual Function. . Physiological Reviews *85*, 845–881.

Streilein, J.W., Ma, N., Wenkel, H., Ng, T.F., and Zamiri, P. (2002). Immunobiology and privilege of neuronal retina and pigment epithelium transplants. Vision Res *42*, 487-495.

Subrizi, A., Hiidenmaa, H., Ilmarinen, T., Nymark, S., Dubruel, P., Uusitalo, H., Yliperttula, M., Urtti, A., and Skottman, H. (2012). Generation of hESC-derived retinal pigment epithelium on biopolymer coated polyimide membranes. Biomaterials *33*, 8047-8054.

Sugino, I.K., Sun, Q., Wang, J., Nunes, C.F., Cheewatrakoolpong, N., Rapista, A., Johnson, A.C., Malcuit, C., Klimanskaya, I., Lanza, R., and Zarbin, M.A. (2011). Comparison of FRPE and human embryonic stem cell-derived RPE behavior on aged human Bruch's membrane. Invest Ophthalmol Vis Sci *52*, 4979-4997.

Sugita, S., Futagami, Y., Smith, S.B., Naggar, H., and Mochizuki, M. (2006). Retinal and ciliary body pigment epithelium suppress activation of T lymphocytes via transforming growth factor beta. Exp Eye Res *83*, 1459-1471.

Sugita, S., Horie, S., Nakamura, O., Futagami, Y., Takase, H., Keino, H., Aburatani, H., Katunuma, N., Ishidoh, K., Yamamoto, Y., and Mochizuki, M. (2008). Retinal pigment epithelium-derived CTLA-2alpha induces TGFbeta-producing T regulatory cells. J Immunol *181*, 7525-7536.

Sugita, S., Horie, S., Nakamura, O., Maruyama, K., Takase, H., Usui, Y., Takeuchi, M., Ishidoh, K., Koike, M., Uchiyama, Y., Peters, C., Yamamoto, Y., and Mochizuki, M. (2009a). Acquisition of T regulatory function in cathepsin L-inhibited T cells by eye-derived CTLA-2alpha during inflammatory conditions. J Immunol *183*, 5013-5022.

Sugita, S., Horie, S., Yamada, Y., and Mochizuki, M. (2010). Inhibition of B-cell activation by retinal pigment epithelium. Invest Ophthalmol Vis Sci *51*, 5783-5788.

Sugita, S., Makabe, K., Iwasaki, Y., Fujii, S., and Takahashi, M. (2018). Natural Killer Cell Inhibition by HLA-E Molecules on Induced Pluripotent Stem Cell-Derived Retinal Pigment Epithelial Cells. Invest Ophthalmol Vis Sci *59*, 1719-1731.

Sugita, S., Usui, Y., Horie, S., Futagami, Y., Aburatani, H., Okazaki, T., Honjo, T., Takeuchi, M., and Mochizuki, M. (2009b). T-cell suppression by programmed cell death 1 ligand 1 on retinal pigment epithelium during inflammatory conditions. Invest Ophthalmol Vis Sci *50*, 2862-2870.

Sunness, J.S. (1999). The natural history of geographic atrophy, the advanced atrophic form of age-related macular degeneration. Mol Vis *5*, 25.

Tahara-Hanaoka, S., Shibuya, K., Onoda, Y., Zhang, H., Yamazaki, S., Miyamoto, A., Honda, S., Lanier, L.L., and Shibuya, A. (2004). Functional characterization of DNAM-1 (CD226) interaction with its ligands PVR (CD155) and nectin-2 (PRR-2/CD112). Int Immunol *16*, 533-538.

Takahashi, K., and Yamanaka, S. (2006). Induction of pluripotent stem cells from mouse embryonic and adult fibroblast cultures by defined factors. Cell *126*, 663-676.

Tang, C., and Drukker, M. (2011). Potential barriers to therapeutics utilizing pluripotent cell derivatives: intrinsic immunogenicity of in vitro maintained and matured populations. Semin Immunopathol *33*, 563-572.

Tang, Q., and Bluestone, J.A. (2013). Regulatory T-cell therapy in transplantation: moving to the clinic. Cold Spring Harb Perspect Med *3*.

Tarallo, V., Hirano, Y., Gelfand, B.D., Dridi, S., Kerur, N., Kim, Y., Cho, W.G., Kaneko, H., Fowler, B.J., Bogdanovich, S., Albuquerque, R.J., Hauswirth, W.W., Chiodo, V.A., Kugel, J.F., Goodrich, J.A., Ponicsan, S.L., Chaudhuri, G., Murphy, M.P., Dunaief, J.L., Ambati, B.K., Ogura, Y., Yoo, J.W., Lee, D.K., Provost, P., Hinton, D.R., Nunez, G., Baffi, J.Z., Kleinman, M.E., and Ambati, J. (2012). DICER1 loss and Alu RNA induce age-related macular degeneration via the NLRP3 inflammasome and MyD88. Cell *149*, 847-859.

Taylor, C.J., Bolton, E.M., Pocock, S., Sharples, L.D., Pedersen, R.A., and Bradley, J.A. (2005). Banking on human embryonic stem cells: estimating the number of donor cell lines needed for HLA matching. Lancet *366*, 2019-2025.

Thomson, J.A., Itskovitz-Eldor, J., Shapiro, S.S., Waknitz, M.A., Swiergiel, J.J., Marshall, V.S., and Jones, J.M. (1998). Embryonic stem cell lines derived from human blastocysts. Science *282*, 1145-1147.

Torikai, H., Reik, A., Soldner, F., Warren, E.H., Yuen, C., Zhou, Y., Crossland, D.L., Huls, H., Littman, N., Zhang, Z., Tykodi, S.S., Kebriaei, P., Lee, D.A., Miller, J.C., Rebar, E.J., Holmes, M.C., Jaenisch, R., Champlin, R.E., Gregory, P.D., and Cooper, L.J. (2013). Toward eliminating HLA class I expression to generate universal cells from allogeneic donors. Blood *122*, 1341-1349.

Usui, Y., Okunuki, Y., Hattori, T., Kezuka, T., Keino, H., Ebihara, N., Sugita, S., Usui, M., Goto, H., and Takeuchi, M. (2008). Functional expression of B7H1 on retinal pigment epithelial cells. Exp Eye Res *86*, 52-59.

Vaajasaari, H., Ilmarinen, T., Juuti-Uusitalo, K., Rajala, K., Onnela, N., Narkilahti, S., Suuronen, R., Hyttinen, J., Uusitalo, H., and Skottman, H. (2011). Toward the defined and xeno-free differentiation of functional human pluripotent stem cell-derived retinal pigment epithelial cells. Mol Vis *17*, 558-575.

Valentino, T.L., Kaplan, H.J., Del Priore, L.V., Fang, S.R., Berger, A., and Silverman, M.S. (1995). Retinal pigment epithelial repopulation in monkeys after submacular surgery. Arch Ophthalmol *113*, 932-938.

van Velthoven, M.E., Faber, D.J., Verbraak, F.D., van Leeuwen, T.G., and de Smet, M.D. (2007). Recent developments in optical coherence tomography for imaging the retina. Prog Retin Eye Res *26*, 57-77.

Vessey, K.A., Greferath, U., Jobling, A.I., Phipps, J.A., Ho, T., Waugh, M., and Fletcher, E.L. (2012). Ccl2/Cx3cr1 knockout mice have inner retinal dysfunction but are not an accelerated model of AMD. Invest Ophthalmol Vis Sci *53*, 7833-7846.

Vugler, A., Carr, A.J., Lawrence, J., Chen, L.L., Burrell, K., Wright, A., Lundh, P., Semo, M., Ahmado, A., Gias, C., da Cruz, L., Moore, H., Andrews, P., Walsh, J., and Coffey, P. (2008). Elucidating the phenomenon of HESC-derived RPE: anatomy of cell genesis, expansion and retinal transplantation. Exp Neurol *214*, 347-361.

Wang, J., Iacovelli, J., Spencer, C., and Saint-Geniez, M. (2014). Direct effect of sodium iodate on neurosensory retina. Invest Ophthalmol Vis Sci *55*, 1941-1953.

Wenkel, H., and Streilein, J.W. (2000). Evidence that retinal pigment epithelium functions as an immune-privileged tissue. Invest Ophthalmol Vis Sci *41*, 3467-3473.

Wikler, K.C., and Rakic, P. (1990). Distribution of photoreceptor subtypes in the retina of diurnal and nocturnal primates. J Neurosci *10*, 3390-3401.

Wong, W.L., Su, X., Li, X., Cheung, C.M., Klein, R., Cheng, C.Y., and Wong, T.Y. (2014). Global prevalence of age-related macular degeneration and disease burden projection for 2020 and 2040: a systematic review and meta-analysis. Lancet Glob Health *2*, e106-116.

Wu, Z., Ayton, L.N., Luu, C.D., and Guymer, R.H. (2014). Relationship between retinal microstructures on optical coherence tomography and microperimetry in age-related macular degeneration. Ophthalmology *121*, 1445-1452.

Yang, Y., Ng, T.K., Ye, C., Yip, Y.W., Law, K., Chan, S.O., and Pang, C.P. (2014). Assessing sodium iodate-induced outer retinal changes in rats using confocal scanning laser ophthalmoscopy and optical coherence tomography. Invest Ophthalmol Vis Sci *55*, 1696-1705.

Yu, J., Vodyanik, M.A., Smuga-Otto, K., Antosiewicz-Bourget, J., Frane, J.L., Tian, S., Nie, J., Jonsdottir, G.A., Ruotti, V., Stewart, R., Slukvin, II, and Thomson, J.A. (2007). Induced pluripotent stem cell lines derived from human somatic cells. Science *318*, 1917-1920.

Zamiri, P., Masli, S., Kitaichi, N., Taylor, A.W., and Streilein, J.W. (2005). Thrombospondin plays a vital role in the immune privilege of the eye. Invest Ophthalmol Vis Sci *46*, 908-919.

Zamiri, P., Masli, S., Streilein, J.W., and Taylor, A.W. (2006). Pigment epithelial growth factor suppresses inflammation by modulating macrophage activation. Invest Ophthalmol Vis Sci *47*, 3912-3918.

Zeiss, C.J. (2010). Animals as models of age-related macular degeneration: an imperfect measure of the truth. Vet Pathol *47*, 396-413.

Zhang, X., and Bok, D. (1998). Transplantation of retinal pigment epithelial cells and immune response in the subretinal space. Invest Ophthalmol Vis Sci *39*, 1021-1027.

Zhao, J.J., Ouyang, H., Luo, J., Patel, S., Xue, Y., Quach, J., Sfeir, N., Zhang, M., Fu, X., Ding, S., Chen, S., and Zhang, K. (2014). Induction of retinal progenitors and neurons from mammalian Muller glia under defined conditions. J Biol Chem *289*, 11945-11951.

Zhu, D., Deng, X., Spee, C., Sonoda, S., Hsieh, C.L., Barron, E., Pera, M., and Hinton, D.R. (2011). Polarized secretion of PEDF from human embryonic stem cell-derived RPE promotes retinal progenitor cell survival. Invest Ophthalmol Vis Sci *52*, 1573-1585.

Zhu, Y., Carido, M., Meinhardt, A., Kurth, T., Karl, M.O., Ader, M., and Tanaka, E.M. (2013). Three-dimensional neuroepithelial culture from human embryonic stem cells and its use for quantitative conversion to retinal pigment epithelium. PLoS One *8*, e54552.